HARNESSING THE NUTRACEUTICAL PROPERTIES, MICROBIAL COMPOSITION OF SCARABAEOID BEETLE LARVAE AND ANTIBACTERIAL COMPOUNDS OF ITS ENDOZOIC FUNGUS (*Aspergillus welwitschia*)

SYLVIAH SYOMBUA MWANZA

A THESIS SUBMITTED IN PARTIAL FULFILLMENT OF THE REQUIREMENTS FOR THE AWARD OF THE DEGREE OF MASTER OF SCIENCE IN CHEMISTRY OF THE UNIVERSITY OF EMBU

AUGUST, 2024

DECLARATION

This thesis is my original work and has not been presented for examination in any learning institution.

Signature ……. Date …….

Sylviah Syombua Mwanza

B523/1372/2020

Department of Physical Sciences

University of Embu

This thesis has been submitted for examination with our approval as supervisors**.**

Signature ……. Date …….

Dr. Mark Kimani

Department of Physical Sciences

University of Embu

Signature ……. Date …….

Dr. Cynthia Mudalungu

Insects for Food, Feed and Other Uses Program

International Centre of Insect Physiology and Ecology, Duduville Campus, Nairobi

Signature ……. Date …….

Dr. Chrysantus Tanga

Insects for Food, Feed and Other Uses Program

International Centre of Insect Physiology and Ecology, Duduville Campus, Nairobi

DEDICATION

This thesis is dedicated to my family and many friends. I am particularly grateful to my loving parents; Mr. Sebastian Mwanza and Mrs. Beatrice Mwanza for their words of encouragement and their insistence on perseverance. My elder siblings; who have been constantly by my side and hold a very special place in my heart.

I extend this dedication to my friends and my church family: Team Nairobi Catholic Diocese of Kitui, whose support has been invaluable throughout this journey. All of you have been incredible supporters throughout my entire masters' program serving as my greatest cheerleaders.

ACKNOWLEDGMENTS

I would like to thank the Almighty God for the good health and grace that sustained me throughout this study. I am profoundly thankful to the University of Embu for the partial scholarship that enabled me to pursue my MSc studies. My heartfelt appreciation extends to my supervisors; Dr. Mark Kimani, Dr. Cynthia Mudalungu and Dr. Chrysantus Tanga for their diligent guidance, continuous support, insightful counsel and the extensive knowledge they shared with me during my research and thesis writing. I am deeply indebted to Dr. Cynthia Mudalungu for her steadfast interest, encouragement and invaluable guidance throughout the direction of this research. I am greatly thankful to the all donors for their financial support provided through the International Centre of Insect Physiology and Ecology (*icipe*). This research was financed by the Insects for Food and Feed (INSFEED) initiative spearheaded by Dr. Tanga.

I am also grateful to the Institute of Pharmaceutical Biology and Phytochemistry (IPBP), University of Münster, PharmaCampus Corrensstraße 48, D-48149 Münster, Germany, for conducting the NMR analysis of the isolated compounds. Special thanks go to Mr. Wanyama for his help in acquiring GC-MS and LC-MS data; and to the late Mr. Shem Ondiaka technical assistant at the Animal Rearing and Containment Unit in *icipe* for his valuable assistance in the larvae collection and rearing of the beetles.

Furthermore, I would like to extend my appreciation to the academic staff of the Department of Chemistry at the University of Embu led by Dr. Nyamato Simba, for their unwavering encouragement and insightful comments that significantly enhanced my knowledge and broadened the scope of my research to include various perspectives. My gratitude also extends to Mr. Hosea Mokaya and Mr James Kabii (Research Assistants, *icipe*), whose invaluable support and technical expertise were crucial during data acquisition and analysis.

My genuine gratitude goes to my family. Your belief in me even when I doubted myself made this achievement possible. I am also grateful to Dr. Blaise Kimbadi Lombe and Mr. Justus Mukavi for their immense mentorship and academic guidance. Finally, I extend my gratitude to my colleagues from the Behavioral and Chemical Ecology Unit (*icipe*), my course mates and all my friends for the unique roles each of you played during this Masters' study.

TABLE OF CONTENTS

LIST OF TABLES

LIST OF FIGURES

LIST OF APPENDICES

LIST OF ABBREVIATIONS AND ACRONYMS

1D and 2D NMR	One Dimensional and Two-Dimensional Nuclear Magnetic Resonance
ACE	Abundance-based coverage estimator
AMPs	Antimicrobial Peptides
AMR	Antimicrobial Resistance
ANOVA	Analysis of Variance
ASVs	Amplicon Sequence Variants
BHC	Benzene hexachloride
BSF	Black Soldier Fly
BTH	Butylated hydroxytoluene
CDC	Centers for Disease Control
$CDCl_3$	Deuterated chloroform
COI	Cytochrome c oxidase I
COSY	Correlation Spectroscopy
CTAB	Cetyltrimethylammonium Bromide
DADA2	Divisive Amplicon Denoising Algorithm
DDT	Dichlorodiphenyltrichloroethane
DM	Dry matter
DMSO	Dimethylsulphoxide
DPPH	2,2-diphenyl-1-picrylhydrazyl
EDTA	Ethyl Diamine Tetra Acetic Acid
EtOAc	Ethyl acetate
FSA	Fisheries Stock Assessment
GA	Gallic acid
Herg	Human Ether-à-go-go-Related Gene
HMBC	Heteronuclear Multiple-Bond Correlation
HPLC	High Performance Liquid Chromatography
HSQC	Heteronuclear Single Quantum Coherence
ICP-MS	Inductively Coupled Plasma Emission Mass Spectrometer
ITS	Internal Transcribed Spacer
KEGG	Kyoto Encyclopedia of Genes and Genomes
LC-MS	Liquid Chromatography Mass Spectrometer

LDL	Low-Density Lipoprotein
LMIC	Low and Middle-Income Countries
MCR-1	Mobilized Colistin Resistant gene
MDR	Multi Drug Resistant
MHA	Muller Hinton Agar
MIC	Minimum inhibitory concentration
MRSA	Methicillin-Resistant *Staphylococcus aureus*
MUFA	Mono-unsaturated fatty acids
NCBI	National Center for Biotechnology Information BLAST tool
NGS	Next Generation Sequencing
NOESY/NOE	Nuclear Overhauser Effect Spectroscopy
NPs	Natural Products
PAINS	Pan-Assay Interference Compounds
PCoA	Principal Component Analysis
PCR	Polymerase Chain Reaction
PDA	Potato Dextrose Agar
PERMANOVA	Permutational Multivariate Analysis of Variance
PICRUSt2	Phylogenetic Investigation of Communities by Reconstruction of Unobserved States, version 2
POPs	Persistent Organic Pollutants
PUFA	Poly-unsaturated fatty acids
PVP	Polyvinylpyrrolidone
QE	Quercetin
RDA	Recommended Dietary Levels
Rrna	ribosomal Ribonucleic Acid
RSA	Radical Scavenging Activity
SDGs	Sustainable Development Goals
SFA	Saturated fatty acids
SMILES	Simplified Molecular Input Line Entry System
SNK	Student-Newman-keuls
STAMP	sTatistical Analysis of Metagenomic Profiles
TCA	Tricarboxylic acid
TFC	Total flavonoids content

TLC	Thin Layer Chromatography
TPC	Total phenol content
UN SDGs	United Nations Sustainable Development Goals
UTIs	Urinary Tract Infections
VRE	Vancomycin-Resistant *Enterococcus Faecium*

ABSTRACT

The systematic development of antibiotic resistance poses huge worldwide health challenges, specifically in low- and middle- income countries (LMICs) increasing the treatment costs. There is heightened need to broaden the search for new antibiotic sources such as exploration of insects beyond soil microorganisms. Insects harbor symbiotic microbes in their guts which can be utilized in developing effective antimicrobial agents. However, entomophagy is the main activity associated with edible insects leaving a paucity of knowledge on their therapeutic benefits. Further, very few researches have been done to understand the microbial composition of comestible insects. This research focused on exploring novel functional properties and characterizing the associated microbiota from the gut of two scarabaeoid larvae collected from Embu, Murang'a and Nairobi counties. Further, the culturable fungal organisms were investigated for their antibacterial potency. The larvae were dissected to obtain the gut portions then pooled and divided into two proportions. One part was used for culturing the fungal isolates and the other was used to obtain DNA for metagenomics analysis. The degutted body remains were used for nutritional profiling. Bioassay-guided isolation was carried out to obtain the bio-active compounds whose structures were elucidated using spectroscopic techniques. The most bioactive fungus was identified using Sanger sequencing targeting the Internal Transcribed Spacer (ITS) gene. The larvae were identified using morphological features and molecular tools as *Cetonia aurata* and *Oryctes rhinoceros*. They were also found to be excellent sources of both macro [44% for *O. rhinoceros* and 63% for *C. aurata*] and micronutrients calcium (20.42–22.65 mg/g) and zinc minerals (0.28–0.3 mg/g). The dominant bacterial communities in their gut were Firmicutes (42.10%) and Bacteroidota (32.50%) for *C. aurata*, while *O. rhinoceros* was dominated by Proteobacteria (35.00%), Actinobacteriota (11.40%), and Desulfobacterota (7.40%). The fungal community was represented by the class Lecanoromycetes (92.60%) in *O. rhinoceros,* whereas Saccharomycetes (92.60%) prevailed in *C. aurata*. This work uncovered possible microbiota functions to include the generation of biosynthetic intermediates necessary for anabolic and catabolic activities, adaptive metabolism and energy production. The screening antibacterial results revealed that the most active mixed fungal extract originated from dung beetle larvae in Murang'a. Sub-culturing yielded to the 15 axenic strains. Antibacterial assays identified the most active strain to be *Aspergillus welwitschia,* with ethyl acetate fraction displaying the highest activity against the tested bacterial strains. Rubasperone B and rubrofusarin B were successfully isolated from this fraction and linked to the observed antibacterial activity. These findings indicate that the Scarabaeoid beetle larvae are endowed with macronutrients and entomochemicals that could find application in fortifying food and feed substances. Additionally, the predicted functions of the gut microbiota provide a theoretical framework for biotechnological uses in waste management and bio-functional foods. In pharmacology, the characterized compounds are significant in the development of new medications to help combat the impacts of Multi-Drug Resistant (MDR) bacteria and contribute to the accomplishment of the UN Sustainable Development Goals (SDGs) chiefly SDG 3 on well-being and good health.

CHAPTER ONE

INTRODUCTION

1.1 Background Information

Treatment of many diseases has always been done using natural products (Oliveira *et al*., 2009). Since penicillin discovery in 1929 by Flemming, many antibacterial drugs have been successfully developed and impacted on human health and the mortality rates differently (Obakiro *et al*., 2021). Antibacterial resistance occurs when the multi-drug resistant (MDR) bacteria evade the effect of the drug using different mechanisms leaving humanity with no choice but look for new treatment options (Church & McKillip, 2021).The UK Government-commissioned O'Neill report predicted that this antimicrobial resistance (AMR) infections could claim lives of 10 million people per year. The cost of treating these infections has been estimated as US$ 100 trillion worldwide if no urgent action is taken by 2050 (Brogan & Mossialos, 2016; Chandler, 2019). The UN in 2015, declared AMR as a risk to the global sustainability and progress efforts in resolving our world 2030 Agenda which includes the sustainable development goals (SDGs). SDG 3 states that living a healthy life and welfare for people of all ages should be ensured and promoted. However, due to lack of effective antibiotics, this UN goal will not be achievable (Jonathan & Stoltenberg, 2012). New antimicrobial innovations should be greatly promoted not only to help in reviving the declining drug discovery pipeline but also to achieve the UN SDGs (Jasovský *et al*., 2016).

Insect-microbe interactions serve as an example of a new microbial natural products (NPs) source and have increased interest over the last 20 years due to production of biotechnologically and pharmaceutically active molecules (Menegatti *et al.*, 2020). For instance, the insect's intestinal tract microbiota has been identified as a source of antibacterial substances against humanoid bacteria according to a study by Heise *et al.* (2019). These antibacterial substances have been classified as antimicrobial peptides (AMPs) which are positively charged and composed of peptides with 5 – 100 amino acids. These compounds exhibit antibacterial activities across the board. They are a component of the insect's natural system and have a low risk of resistance, making them ideal candidates for new antimicrobial development (Teixeira *et al*., 2020).

Insects dwell in great numbers and their offsprings are often threatened by invading species. As a result, the insects are colonized by symbionts which occupy 10% of the

insect's biomass and provide mutual benefits to the host insect leading to insect host–microbial relationship (Eggleton, 2020). The gut microbiota comprises of bacterial protagonists and fungi symbionts (Barcoto *et al*., 2020). AMPs have been widely discovered but very little attention has been given to those from fungal gut microbiota of edible insects (Mudalungu *et al.*, 2021). Filamentous fungi (*Aspergillus*) are known to produce metabolites with antibiotic properties (Blackwell *et al*., 2007). The origin of the fungi dictates the kind of metabolites produced. Fungal endophytes have proven to be a source of different novel and biological active scaffolds (Huang *et al.*, 2010). The beetle gut system is associated with robust selection pressures on the microbial communities; therefore, isolating fungi from such environments produces more potent biomolecules than those typically produced under more stable conditions (Blackwell *et al*., 2007). Nevertheless, the antibacterial activity of these molecules from fungal gut microbiota of edible dung beetle larvae remains unexplored.

The *Scarabaeidae* family comprises many edible beetles, however, only dung beetles have been found to have diverse gut microbial communities (Ebert *et al*., 2021). Despite the fact that much research on beetles has been done, they have only focused on the transmission of the microbes between larvae and adults (Mabhegedhe, 2017) with limiting information about their variation with geographical site and lignin/nitrogen-degrading metabolic pathways associated with them. In addition, the novel bio-functional properties of dung beetle larvae remain unknown, limiting their possible use as functional ingredients in food fortification. This research aimed at investigating the antibacterial efficacy of the isolated and identified active culturable fungal gut symbionts of dung beetle larvae. The associated fungal microbiota was cultured, followed by bioassay-guided isolation and structural elucidation of the target bioactive compounds. Further, the pharmacokinetics of the isolated compounds were assessed to validate their use as potential drug targets.

1.2 Statement of the Problem

The world population is projected to reach 9.2 billion by the year 2050, with most of the unprecedented demographic dynamism reportedly occurring in low-income countries (Bongaarts, 2009). This presents a challenge to food supply chain disruption and nutrition security, as was intensified by the recent pandemic of Covid -19. The number of deaths triggered by the multidrug-resistant germs could increase by a million

every year (Provenzani *et al*., 2020).Worse yet the infections that are unresponsive to first line drugs have raised leading to lack of safe, efficacious, quality and affordable therapeutic agents (Chandler, 2019). Since bacterial pathogens are acquiring resistance at a quicker rate, the number of novel scaffolds in the drug development pipeline is rapidly decreasing (Mwangi *et al*., 2019). The increased drug resistance is as a result of biological mechanisms such as gene transfer and mutations which cause genetic changes in microorganisms as they adapt to their environment, allowing them to thrive even in the presence of antimicrobials (Rodríguez-Beltrán *et al.,* 2021). Several biologically active scaffolds have been isolated from the microbiota associated with different kinds of insects and found to inhibit bacterial strains of clinical importance using novel mechanism of action. However, only 29% of the small molecules are from beetles (Mudalungu *et al.*, 2021). Moreover, fungi symbionts from the dung beetles remain unexplored. Therefore, this research was designed to provide information about the nutritional composition, microbial composition and antibacterial efficacy of culturable fungal symbionts from edible dung beetle larvae.

1.3 Justification

During covid19 pandemic, it became evident that adequate nutrition plays a fundamental role in strengthening the immune system, thereby reducing mortality rates. Ensuring food security by providing nutrient-rich foods is of utmost concern due to the increased prevalence of lifestyle disorders such as obesity, cognitive disorders and cases of malnutrition. Insects are sustainable and nutritious, thereby they can be used to improve global health and nutrition. Moreover, effective antibiotics shortage in the medicinal field to help curb the effects of MDR continues to motivate the quest for new natural molecules (Santoro *et al*., 2020). Microorganisms such as fungi are acknowledged to produce of biologically active natural products which are of pharmacological importance. They are phylogenetically, morphologically, ecologically and metabolically diverse (Raja *et al.,* 2017). Most of the antibiotics have been obtained from NPs (Maglangit *et al.,* 2021). Edible insects have the potential of harboring antibacterial molecules like beneficial sterols and flavonoids which have demonstrated activity against common nosocomial pathogens (Mudalungu *et al*., 2023).

Further, current studies have shown that insect – microbes' interactions in combination with analytical dereplication procedures are a rich source of novel compounds

(Bhowmick, 2021). Previous screening of bacterial protagonists from buffalo dung beetles gave on to the discovery of lenzimycins A (**1**) and B (**2**), which had a minimum inhibitory concentration (MIC) value range of 8.0 to 16.0 µg/mL against *Enterococcus faecalis* and *E. faecium.* Also, they have been found to have MIC value of 0.5 to 1.0 µg/mL against *E. Faecalis* and *E. Faecium.* These bacteria are known to be vancomycin resistant (An *et al.*, 2020). Despite the act of entomophagy being encouraged, the bio-functional composition of edible scarabaeoid beetle larvae remains underexplored. Further, the antibacterial molecules from their gut remain untapped and understudied (Mudalungu *et al.*, 2021; Molloy & Hertweck, 2017). During the larval developmental stage, the insects are prone to pathogen manifestations hence they synthesize a lot of metabolites (Joosten *et al*., 2020) which can be exploited as potential antibacterial sources. These results of this study will significantly contribute to the achievement of achievement of SDGs vision 2030.

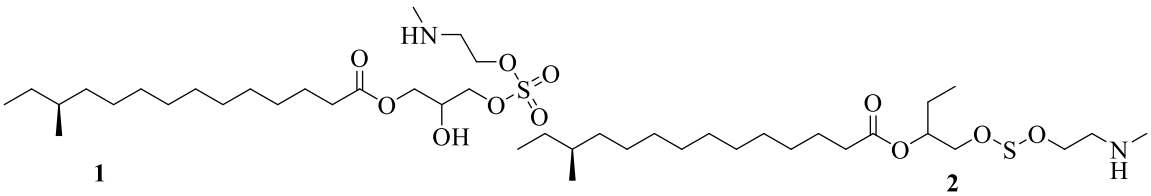

Figure 1:1: Structures of compounds isolated from *Brevibacillus* sp. PTH23, a bacterial symbiont associated with the dung beetle; *Onthophagus lenzii*

1.4 Hypotheses

I. The dung beetle larvae will have similar nutritional profiles.
II. The gut microbiota from scarab beetle larvae will not vary depending on geographical location.
III. The extracts and compounds from the microbiota of the scarab beetle larvae will not exhibit antibacterial properties.
IV. The spectroscopic data of the isolated antibacterial compounds will not be sufficient for their structure elucidation.

1.5 Objectives

1.5.1 General Objective

To investigate the nutritional, microbial composition and antibacterial properties of extracts and compounds from microbiota associated with the digestive tract of edible scarab beetle larvae.

1.5.2 Specific Objectives

I. To determine the nutritional and antioxidant properties of edible scarab beetle larvae.
II. To characterize the microbiota from the gut of scarab beetle larvae.
III. To isolate secondary metabolites from the associated fungal gut microbiota in a bioassay-guided manner.
IV. To elucidate the structures of the isolated antibacterial compounds using various spectroscopic techniques and prediction of their pharmacokinetics.

1.6 Scope and Limitations

The study has potential limitations;

I. Sampling was conducted in three sites per location, but this might have failed to capture the full diversity and variability of nutritional and gut microbiota in the whole region due to varying environmental conditions and climatic patterns. The samples also were obtained during the off-rainy season; therefore, a well-designed sampling strategy covering all seasons is necessary for a more comprehensive conclusion.
II. Metagenomics analyses might have failed to capture the entire community due to the high diversity and uneven abundance of microbial members, leading to the rarer ones being overshadowed by the most abundant ones.
III. Screening for optimum media conditions for metabolite production in the lab may not accurately replicate natural environments, leading to potential discrepancies in metabolite yield and activity.

CHAPTER TWO

LITERATURE REVIEW

2.1 The Desperate Quest for Antibiotics

Infectious diseases such as urinary tract infections (UTIs), brucellosis, pneumonia, leprosy and tuberculosis pose a great threat to human health in developing countries due to increased antibiotic resistance (Chakraborti *et al.*, 2019). Research done in Kenya indicated that these infectious diseases are burden to individuals in both urban and rural settings hindering their development (Feikin *et al.*, 2011). Recently, the Centers for Disease Control (CDC) published the antimicrobial resistance threats in the US indicating that more than 35000 deaths result from these Multi-Drug Resistant (MRD) pathogens (Hunter, 2020). These infections are commonly treated using antibiotics which were first discovered in the 1930s leading to decline of serum therapy which required prior knowledge about the bacteria responsible for the since the therapy was antibody based (Casadevall *et al.*, 2004).

The microbes are developing resistance towards these therapeutics leading to a reduction in their efficiency and failure of treatment leading to an increased number of hospitalized patients (Mwangi *et al.*, 2019). Worse yet, there has been a drop in discovery of effective and new antimicrobials due to lack of sufficient provision from the government, straitened returns from the investment, increased costs and monitoring huddlers. Even pharmacological companies have deserted the antibacterial field and focused on developing drugs that will solve the chronic crisis and benefit economically leading to an urgent need to develop novel drugs (Martens & Demain, 2017). As a result, strict measures are required to stop the spread of resilient bacteria, which pose a threat to community health in the fight against microbial infections (Lupei *et al.*, 2010; Lombardi *et al.*, 2019).

The antibiotics were mostly obtained from natural products which include fungi (Cephalosporins), soil bacteria especially the actinomycetes (neomycin and streptomycin active against *Mycobacterium tuberculosis*) and other bacterial natural products (Monolactams) (Hutchings *et al.*, 2019). However, in the earlier decades, natural products use in the pharmaceutical industries has declined although they present the most successful drug discoveries (Atanasov *et al.*, 2021). Their elimination is as a

result of their diminishing returns leading to increased focus on combinative chemistry to develop unique scaffolds with novel mode of action and help curb drug resistance. The latter case has failed to counteract the decline of new antibiotics in the drug discovery pipeline and the urge to discover is on the rise to help curb global and societal challenges which include the increased deaths associated with multi drug resistant pathogens (Merrikh & Kohli, 2020).

2.2 The SDGs and Antibacterial Resistance

AMR is a major civic health threat and pose an enormous fiscal load on worldwide healthcare. The increased AMR cases continue to threaten the attainment of many SDGs. For example, Goal 1 is to ensure that there is no poverty, and Goal 2 is to ensure that there is no hunger. The production rate of food is projected to raise from 50 to 70% to cater for the growing population worldwide by 2030. Antimicrobial usage in food production will likewise rise by a similar amount (Marshall & Levy, 2011). The MDR will continue to jeopardize long-term food security, causing farmers' economic forecasts to fail. Having food security threatened, increased hunger levels globally will be experienced and products from the farms will not be marketable. People looking for decent job opportunities and their performance at work place will be adversely affected by the effects of these MDR. This will make Goal 8 – decent jobs and economic progress unachievable (Gajdács *et al.*, 2021).

People living in LMICs have less developed health infrastructures hence they are more vulnerable to these MDR infections. They cannot access the right medication since it is expensive hence opt for self-medication (Ateshim *et al*., 2019). For this case, AMR will directly worsen community inequalities limiting the achievement of Goal 1 and Goal 11: to reduce inequalities (Alvarez-Uria *et al*., 2016; Ateshim *et al*., 2019). In order to achieve these SDGs, government stakeholders and other unions should have guidelines for fighting the AMR in their national agendas (WHO, 2017). The WHO has established priority lists of MDR microbes that poses major threats to public health in order to combat this. Carbapenem-resistant *Pseudomonas aeruginosa,* methicillin-resistant *Staphylococcus aureus* (MRSA), extended-spectrum -lactamases; *Escherichia coli* and vancomycin-resistant *enterococci* (VRE); *Acinetobacter baumannii* and *Klebsiella pneumoniae* (Tillotson, 2018; Tacconelli *et al.*, 2018; Mwangi *et al*., 2019; Dhingra *et al*., 2020).

Natural selection is an intrinsic mechanism in evolution that confers features for enhanced environmental adaptability and survival on organisms (Sharma, 2003). The extensive use of medications, organo-pesticides and the release of the unutilized antibiotics into the environment from human waste has resulted in the identification of several strains of bacteria with MDR features or genes over time (Fuzi *et al.*, 2020). Current studies have indicated several cases that MDR bacteria has become resistant to nearly all clinically available antibiotics (Cheah *et al*., 2016; Luo *et al*., 2020; Ara *et al*., 2021). Due to the rise in drug resistance against traditional antibiotics, developing and designing new and distinct molecules could help mitigate the effects associated with drug resistance.

Recently, the antimicrobial drug discovery sector seems to be reviving slowly after several decades due to a lot of research which is aimed to combat the effects of MDR. Many of the conventional therapeutics use these common modes of mechanisms and their structures are similar; once the bacteria become resistant to one then the other one also becomes ineffective. As a result of effects of these MDR pathogens, scientists continue to look for ways to inhibit their growth such as use of nano-formulations, *β*-lactamases, phytochemicals discovery, RNA silencing, AMPs, and, their mixtures with antimicrobials, however, the methods have limitations (Fatima *et al.,* 2021). However, AMPs have numerous advantages over these strategies. They include having a wide range of spectrum activity against microbial strains and have many sources in nature including insects (Lei *et al.*, 2019). Another strategy is drug repurposing whereby new useful bioactivities of old medications are branded by screening against relevant infectious targets. For instance, *ent*-kaurane diterpenoids discovered sometimes ago, have recently been repurposed based on their ability to exhibit diverse pharmacological activities (Kibet *et al*., 2024). Insects due to their innate nature can be potential sources of these lead molecules.

2.3 Insects as Potential Antimicrobial Sources

Several researches have shown that to increase chances of eliminating the antimicrobial resistance, natural products research should not only focus on products from soil bacteria. They should also shift to other natural sources that could have antimicrobials with novel mechanism of action such as the insects especially their guts' microbiota (Challinor & Bode, 2015; Mudalungu *et al*., 2021). Insects presents the most plentiful

and also diverse animals on the world based on the fact that they can survive under hostile surroundings (Van Moll *et al.*, 2021). During the larval development stage, the insects adapt mechanisms that aid in combating growth of dependent microbes in their environment.

The insects' bacterial defensive mechanisms have been widely studied; For example, research done on *Acromyrmex rugosus* (attine ants) and their mutualists show that they inhibit the growth of *Escovopsis* by producing a combination of antifungal compounds (Ortega *et al.*, 2019). These secretions (antimicrobial peptides) are specific towards a certain pathogen and rapidly produced from the body of the insect (Manniello *et al*., 2021). Different molecules have been successfully isolated from the insect's microbiota and found to have different biological activities.

2.3.1 Biological Activities of Compounds Isolated from Insects

Cecropins are linear and helical, while defensins are typically beta-sheet peptides stabilized by disulfide bonds. These molecules form part of the innate immune system of an organism and possess antimicrobial properties. Contrastingly, defensins have been found to kill Gram positive bacteria whereas cecropins kill both Gram negative and Gram positive bacteria (Buonocore *et al*., 2021). Termites have been found to harbor *Streptomyces* strains which have been widely explored, leading to discovery of thylamino-8-dimethyl-D-riboflavin (**3**) and roseoflavin (**4**). Roseoflavin had MIC values < 4 µg/mL against *S. aureus* and *B. subtilis*, but did not inhibit the growth of Gram-negative *S. typhimurim* and *E.coli* at a maximum dose of 25 µg/mL (Zhou *et al*., 2021). Polyketide-derived tetramate macrolactams have been discovered using a *Streptomyces* strain. For example, frontalamides A (**5**) and B (**6**) were found to have anticancer and antimalarial activities (Liu *et al*., 2019; Mudalungu *et al.*, 2021).

The polyketide class has been widely researched leading to isolation of various active compounds from insect symbionts (Badwaik *et al.*, 2018). Unfortunately, many of the small molecules are not obtained from edible insects but the art of entomophagy is being encouraged to meet the increased demand for animal proteins (Jantzen *et al*., 2020).

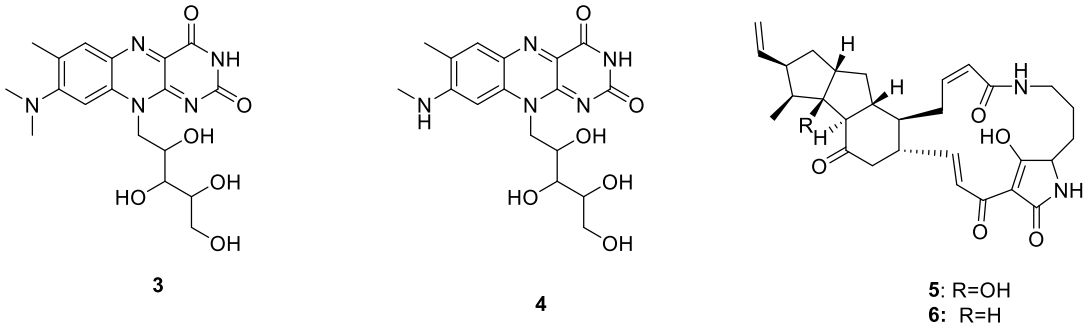

Figure 2:1: Structures of bioactive compounds from different insects' microbiota

2.4 Edible Insects

Entomophagy serves as a sustainable substitute to conventional sources of food or feed benefiting the environment, health, and livelihoods (Van Huis *et al*., 2013). Insects have served as sources of food and medicine since ancient times (Laureati *et al*., 2016). These insects are highly diverse, abundantly present in nature for sustainable harvesting, and are endowed with several therapeutic and functional food properties (Mudalungu *et al*., 2021; Rumpold & Schlüter, 2013). Apart from the ecological benefits, insects such as beetles are known to contain high protein content with excellent essential amino acids, micronutrients, antinutrients, fat-soluble tocopherols and bioactive molecules which are essential in combating metabolic disorders (Omotoso, 2018; Anaduaka *et al*., 2021; Mudalungu *et al*., 2021). For instance, adult *Holotrichia parallela* Motschulsky is known to be a good source of protein (70.27%), minerals (3.61%) especially potassium (2851 mg/kg) and low crude fat (10.36%) (Qiao-ru *et al*., 2010).

Additionally, the larval stage of *Protaetia brevitarsis* Lewis, traditionally used as medicine in Asia, is documented as an excellent source of bioactive components with excellent antioxidant activities (Suh *et al*., 2011). Insects also have better protein digestibility compared with conventional sources of protein such as soya beans and milk protein casein (Akinnawo & Ketiku, 2000). The coconut rhinoceros beetle (*Oryctes rhinoceros* L.) and the green rose chafer (*Cetonia aurata* L.) are known delicacies worldwide (Félix, 2019; Van Huis, 2021). Although, some documented information exists on the nutritional composition of *O. rhinoceros*, no similar knowledge on *C. aurata* has been reported. This information bridges the scarce knowledge gap on the medicinal properties and nutrient profiles of these beetles, highlighting their possible use as functional ingredients in food fortification.

Insects are also responsible for low emissions of greenhouse gases, avoid deforestation since they require little portions of land and have high nutritional content values (Mishyna *et al*., 2020). They also have the possibility to meet healthy, pleasant, accessible and sustainable principles (Jantzen *et al*., 2020). Africa has many insects that can be eaten. They include the genera *Hymenoptera, Isoptera, Odonata, Coleoptera*, among others and each order has been associated with fungi and other microorganisms (Mutungi *et al*., 2019). Several beetles have been associated with the three fungal phyla namely *Ascomycota*, *Zygomycota* and *Basidiomycota* (Ziganshina *et al*., 2018).

The comestible insects are good sources of AMPs that have antibacterial potent activities. A research done by Correa *et al.* (2019) on Black soldier fly (BSF) fungal microbiota led to the discovery of six α – pyrone derivatives (**7 - 12**) and one diketopiperazine (**13**). Among these compounds, only compound (**10**) showed greatest bioactivity against MRSA with MIC value of 62.5 µg/mL and IC_{50} of 11.4 ± 0.7 µg/mL.

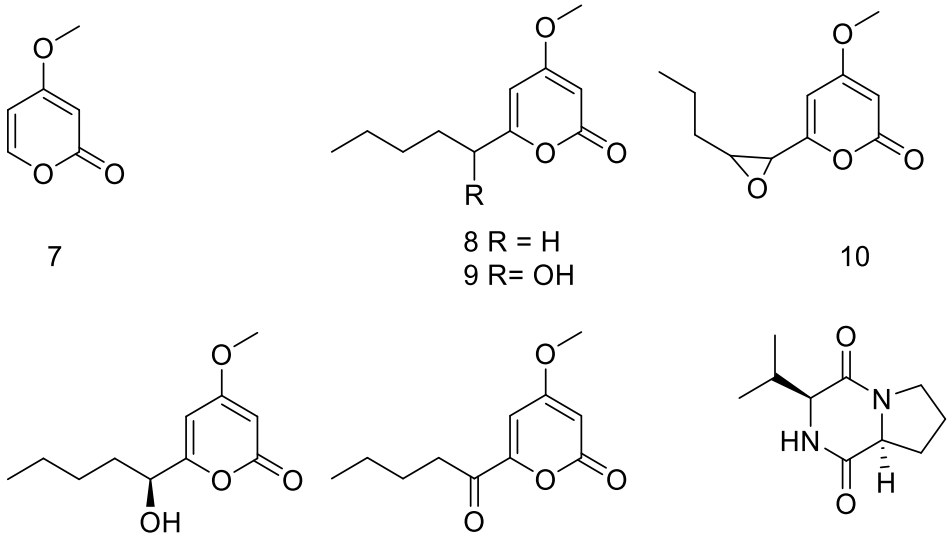

Figure 2:2: Compounds structures of molecules isolated from *Chrysosporium multifidum* extract obtained from BSF fungal microbiota

2.4.1 The Scarab Family (Coleoptera: Scarabaeidae)

The family Scarabaeidae represents the most consumed worldwide insects since it contains 40% of all known insects (Reátegui *et al*., 2018). Beetles are known to grow fungus underground or on woods as a source of food and habitat which they provide with organic matter. These gardens with a lot of nutrients are prone to infestations by nematodes and opportunistic insects forcing the insects to evolve and develop defensive

mechanisms to protect them (Li *et al.*, 2021). The antagonists compete for nutrients and habitat with the host. For example, *Dendroctonus frontalis,* (the southern pine beetle), grows the fungus *Entomocorticium* sp. which is threatened by hostile fungus *Ophiostoma minus*, but they produce Mycangimycin (**14**) which they carry with their exoskeleton to protect the fungus, which has been isolated from the *Streptomyces thermosacchari* strain (Human *et al*., 2017).

2.4.1.1 Dung Beetles

Dung beetles are holometabolic diverse insects with four stages of development; egg, larva, pupa and adult. Each stage has a unique morphology and feeds on herbivorous mammal dung. It has been found that these beetles grow on nutrient limited meals, such as dung by making brood balls for larvae development and require the association of microbes for nutrient synthesis, especially cellulose degradation and utilization (Hammer & Moran, 2019). Through this they play important roles in cellulose biodegradation, increasing bioturbation and suppressing gut parasites in their environs (Brown *et al*., 2010). Their involvement in the breakdown of lignocellulosic material presents a sustainable and environmentally friendly approach to waste management, potentially attributable to microbial fermentation, given their lack of active endogenous cellulase enzymes (Han *et al*., 2024).

Despite the increased interest and numerous studies in insect gut microbial composition (Engel & Moran, 2013), the ecological functions offered by dung beetles and the biodiversity of their gut microbiota remain largely understudied. Moreover, researchers have focused on culturable plant cell wall degrading microbes associated with root-feeding pests, such as scarab beetles or the transfer of gut microbes from female adults to larvae in beetle species (Estes *et al.*, 2013; Sari *et al.*, 2016; Shelomi and Chen, 2020) leaving a paucity of information about variations in their gut microbial communities and the lignin/nitrogen-degrading metabolic pathways associated with them.

The dung beetles' larvae; *C. aurata* and *O. rhinoceros* belong to the family of Scarabaeidae and live in similar environs. They show high species diversity ranging from their body masses, size and their outside morphology (Pacheco & Vaz-de-Mello, 2019). The Scarabaeidae are often stated in literature for their medicinal value. In China, the crude of *Holotrichia diomphalia* larvae is used to treat edema, furuncle, liver

cirrhosis and apoplexy. In northern India, the dung beetle paste, *Catharsius* sp., is also taken orally to treat diarrhea (Chakravorty *et al.*, 2011; Dong *et al*., 2011).

2.4.2 Biological Activities of Natural Products Isolated from Fungal Microbiota of Edible Insects

Fungi are eukaryotic and depend on endosymbionts especially invertebrates for supply of nutrients (Ruess & Müller-Navarra, 2019). These cross kingdom interactions between insects and fungi have promoted development of different antimicrobial, antimalarial and immunosuppressive drugs (Zhou *et al*., 2021). An example of a fungus that is resident reliant on is *Pseudallescheria boydii* which belongs to the phylum *Ascomycota* and can be found in different hosts (Cortez *et al*., 2008). Research done on fungi isolated from the intestinal tract of *Holotrichia parallela* larva led to isolation of different secondary metabolites which include the two novel sesquiterpene boydenes (**19** and **20**) and four epipolythiodioxopiperazines named as boydines (**15 - 19**). Boydine (**16**) was found to have a MIC value ranging between 0.2 to 0.8 µM against many active anaerobic bacteria (Wu *et al.*, 2014).

Other compounds that have been isolated are the three natalenamides (**21 - 23**) from a culture broth of termite which has been associated with *Actinomadura* sp. and grows fungus. Compounds (**21**) and (**22**) showed weak cytotoxic activities against Hela/A549 and HepG2 cells. As for compound (**23**), it exhibited inhibitory effects just like the kojic acid, (a skin-whitening cosmetic) on IBMX – melanin mediated synthesis in a dose-dependent way (Lee *et al.*, 2018). Although, different compounds have been isolated from insects, little is known about fungal microbiota associated with dung beetles' larvae. This research therefore, focused on investigation of bioactive fungal symbionts associated with edible scarab beetle larvae.

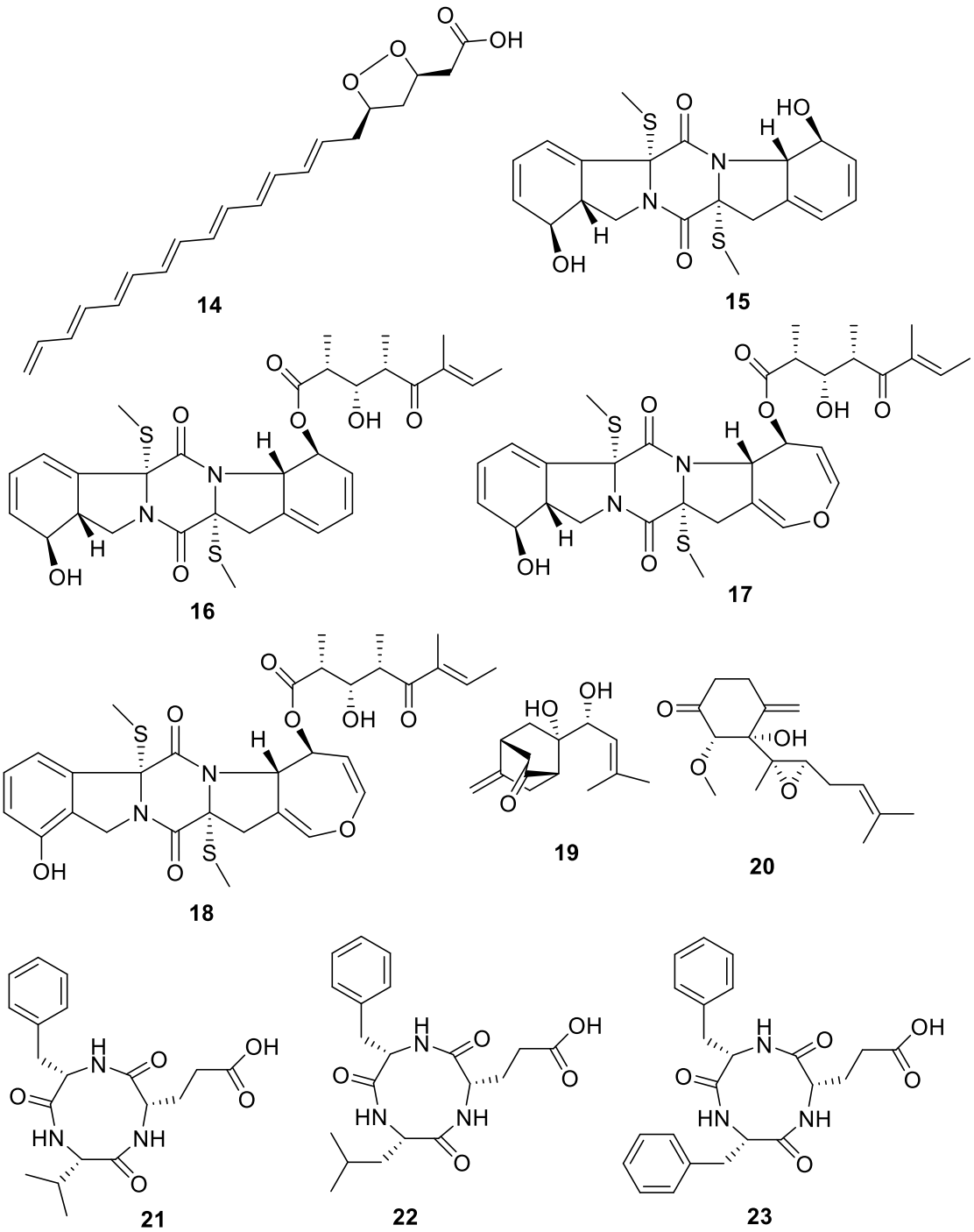

Figure 2.4: Compound structures identified from the fungal microbiome of edible insects

CHAPTER THREE

MATERIALS AND METHODS

3.1 Study Area

The study area involved collecting two beetle larvae species from Embu, Murang'a and Nairobi Counties in Kenya. These three counties were chosen based on their agricultural activities and diversity of organic waste suitable as food substrates for beetle larvae. Three sites were sampled in each county: Embu County [Nthangaiya (S00˚27’58.9”, E037˚33’58.6”), University of Embu (S00˚30’41.3”, E037˚27’29.5”) and Gachururiri (S00˚42’25.6”, E037˚28’58.7”)]; Murang’a County [Kiunyu (S00˚57’21.8”, E037˚1’9.2”), Njoguini (S00˚43’17.7”, E037˚7’38.2”) and Kairi (S00˚36’48.3”, E037˚0’44.3”)] and Nairobi County [Mwiki (S01˚13’47.2”, E036˚57’1.0”), Ruai (S01˚17’27.7”, E037˚0’29.6”) and Kangemi (S01˚15’53.9”, E036˚44’37.5”)][**Figure 3.1**]. The larvae were identified and distinguished morphologically using taxonomic keys described by Bedford (1974) and CABI (2023) [**Figure 3.2**].

3.2 Sample Collection

About 500–600 larvae were collected at each site (Murang’a and Nairobi) and 250-300 were found in Embu. Those from the same area were merged for further processing. The collected larvae samples were then transported in perforated plastic containers with wet substrate within 24 hours to the Animal Rearing and Containment Unit (ARCU) at the International Centre of Insect Physiology and Ecology (icipe), Nairobi, Kenya for further processing and analysis.

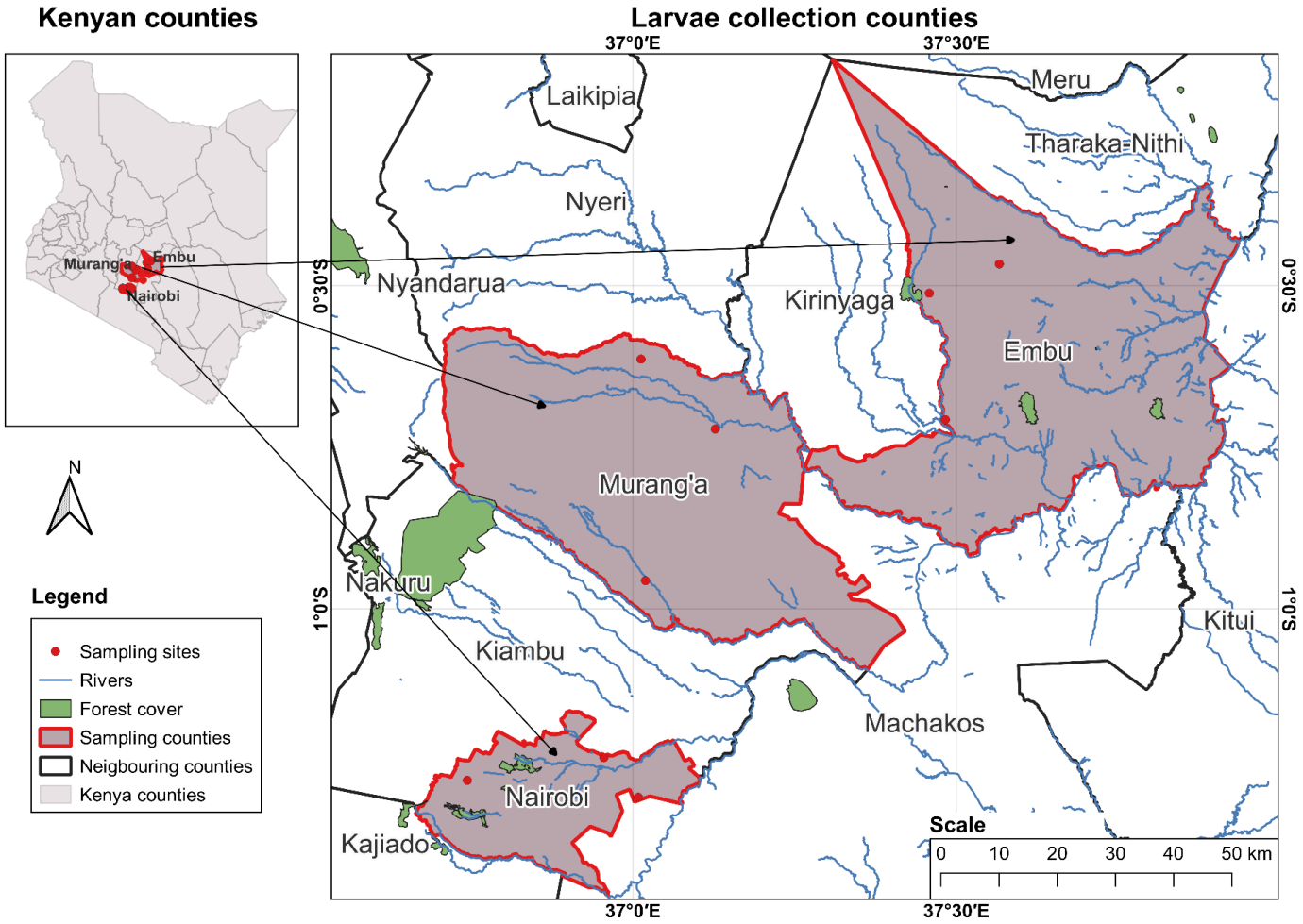

Figure 3:1: Kenyan map (drawn using QGIS software) showing the three countries in which the larvae collection was done. The red dots in each county represent the exact location in which the larvae were obtained.

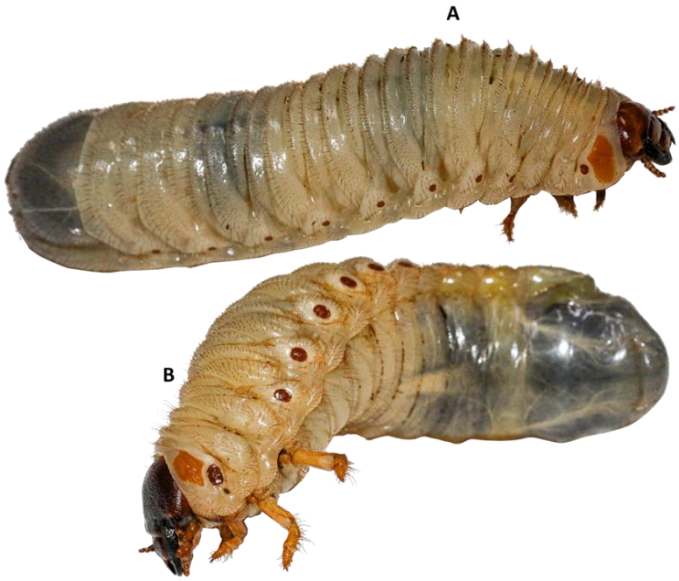

Figure 3:2: Morphologically distinct Scarab larvae; *C. aurata* (**A,** under 1.9x magnification) and *O. rhinoceros* (**B**). At the third instar, the larvae of *C. aurata* has a length of 55 mm, a diameter of 35 mm and three pairs of limbs, while *O. rhinoceros* has a length of 85mm, a diameter of 45 mm and also three pairs of limbs. (Photos taken by Brian Mwashi- *icipe*)

3.3 Sample Preparation

The captured larvae were housed in plastic containers and provided with fresh organic material until processing to minimize differences in gut microbiota composition as a result of diet changes until dissection (Franzini *et al.*, 2016). Larvae dissection was done according to the protocol described by Mabhegedhe (2017). The entire guts of five larvae per site were dissected and collected from all live individual samples within 24 hours of capture. Dissections were performed in sterile glassware using micro-scissors and forceps that were surface disinfected with 40% bleach and 70% ethanol, ensuring that all procedures were conducted with thoroughly cleaned tools. The larvae were briefly anesthetized for 15 minutes in -20℃ freezer to immobilize them and upon removal, they were thoroughly rinsed with tap water before placing them on sterile preparation dishes. They were then surface-sterilized with 70% ethyl alcohol for 50 seconds and then rinsed in six successive changes of germ-free distilled water. The cuticle was then sliced along the lines allowing the ring-shaped muscles to be removed. The head was removed and a circular cut performed on the anus to allow the gut to be

extracted. The whole guts were stored in sterile 15 mL falcon tubes at -20℃ until DNA extraction. The dissected guts were then homogenized using a QIAGEN Tissue Lyser II to obtain 15 homogenates to represent the different sites. The homogenates were split into two parts: the DNA for the metagenomics study was extracted from one part and the other was utilized for growing the fungal isolates. The degutted body remains of 200- 600 larvae were used for nutritional profiling.

3.4 Molecular Identification of the Beetle Larvae from the Various Target Sites

Molecular tools employed included DNA extraction from individual legs of the beetle larvae collected from the various sites using Isolate II Genomic Kit (Bio line), following the guidelines provided by the manufacturer. Subsequently, the amplified DNA was subjected to polymerase chain reaction (PCR) using two primers (one for each insect) due to the lack of universality of a single primer to target the COI mitochondrial gene in the *O. rhinoceros* beetle and 28S ribosomal RNA in the *C. aurata*. The COI gene section was targeted using LCO 1490 (forward, 5′-GGTCAACAAATCATAAAGATATTGG-3′) and HCO 2198 (reverse, 5′-TAAACTTCAGGGTGACCAAAAAATCA-3′) primers (Wilson, 2012). The mixture for PCR reaction contained 4 μL of *O. rhinoceros* DNA, 6 μL 5x HOT FIREPOL® Master Mix, 20.8 μL RNA free water, 0.6 μL forward primer and 0.6 μL of reverse primer (10 mM). The temperature for the PCR program was set for 15 mins at 95℃, followed by 40 cycles for 45 seconds 95℃, 1 minute at 53℃, 72℃ for 10 minutes and final extension for 5 minutes at 72℃. Conversely, 28s rRNA primers were Lep D 2 forward (5′ - AGTCGTGTTGCTTGATAGTGCAG-3′) and Lep - D2 reverse (5′-TTGGTCCGTGTTTCAAGACGGG - 3′). 2 μL of *C. aurata* DNA, 6 μL 5x HOT FIREPOL® Master Mix, 11 μL PCR water, 0.5 μL forward (10 mM) and 0.5 μL reverse primer (10 mM) were added to the PCR mixture for this reaction. The PCR technique was carried out for 15 minutes at 95℃, followed by 40 cycles of 30 seconds at 95℃, 30 seconds at 58.8℃, 1 minute at 72℃ and 10 minutes at 72℃. The resulting PCR amplicons were confirmed using gel electrophoresis (2% agarose), which was viewed using Kodak Gel Logic 200 Imaging System (SPW Industrial, Laguna Hills, CA, USA) under ultraviolet light. After being cleaned using ExoSAP-IT (Affymetrix, Santa Clara, CA, USA), the remaining PCR amplicons were sequenced by Macrogen Inc. (Amsterdam, The Netherlands). A BLAST tool (Sonnhammer & Durbin, 1995) was used to reveal the identity by querying the obtained sequences against the known

sequences in NCBI Gene bank nr (https://www.ncbi.nlm.nih.gov/tools/primer-blast/). The MAFFT plugin in Geneious Prime software version 2020.2.2 was used for alignment whereby the obtained sequences were aligned with available beetle related sequences sourced from Gene bank nr Database (Kearse *et al.,* 2012). PhyML 3.0 was used to create maximum-likelihood phylogenies with automated selected model utilizing the Akaike information criteria (Guindon *et al.,* 2010).

3.5 Nutritional Profiling

3.5.1 Beetle Larvae Sample Preparation for Proximate Analysis

The degutted body remains were dried using oven (WTB binder, Tuttlingen, Germany) for 24 hours at 60℃. The dried samples were then pulverized using a GRT-750A(K) grinder (Zhejiang, China). The Association of Official Analytical Chemists guidelines were followed in order to estimate the proximate parameters, which included crude protein, moisture content, dry matter, fiber and ash (Helrich, 1990). By oven-drying the material for two hours at 135℃, the moisture and dry-matter content were measured. 1 g of the samples was ignited at 550℃ in a muffle furnace (Heraeus-Kundendienst, Düsseldorf, Germany) to determine the ash content. Kjeldhal technique was used for the determination of crude protein content. A conversion factor (K_p) of 4.76 was considered for nitrogen to protein conversion in the whole larvae to avoid overestimation due to presence of nonprotein nitrogen content as reported in the darkling beetle; *Alphitobius diaperinus* and the yellow mealworm; *Tenebrio molitor* by Janssen *et al*., (2017). The fiber content was determined by acid and base digestion in a fiber analyzer SA30520200 (FIWE, Velp Scientifica, Europe).

3.5.2 Entomochemicals and Radical Scavenging Activity

3.5.2.1 Total Flavonoids Content (TFC)

The TFC was determined using aluminum chloride colorimetric assay following the protocol outlined by Mokaya *et al*. (2022) with minor adjustments. To 50 mg of each sample, 1 mL 50% methanol was added, vortexed using Vortex-Genie 2 then spun for 10 mins at 4200 rpm. Next, 500 µL of the supernatant was mixed with 3.2 mL of 50% methanol and 0.15 mL of 5% sodium nitrate was added. Following a 5 minutes incubation period at room temperature, 0.15 mL of 10% aluminum chloride was added, allowed to settle for 1 minute and then 1M sodium hydroxide was added. Using an Evolution™ Pro UV-Vis Spectrophotometer (Thermo-fisher scientific, Maddison, USA), the absorbance was measured at 510 nm, in relation to a blank consisting of all

the components of the assay minus sample. The UV-Vis Spectrophotometer was used to assess the authentic standard quercetin (QE) (20 – 250 µg/mL) in order to create a calibration curve for external quantification of the TFC, which was expressed in mg of QE equivalent per 100g.

3.5.2.2 Total Phenols Content (TPC)

The TPC was measured in consonance with procedure previously outlined by Mokaya *et al*. (2022). For every sample, 50 mg of the larvae powder was weighed and dissolved in 50% methanol, vortexed briefly and centrifuged for 10 mins at 4200 rpm. Upon centrifugation, 500 µL of the supernatant was picked and mixed with of 0.2 N Folin-Ciocalteu (2.5 mL) then left to stand for 5 mins. After incubation, addition of 2 mL of a 75g/L Na_2CO_3 solution was done and left to stand for 2 hours. At 760 nm, absorbance readings were obtained using Evolution™ Pro UV-Vis Spectrophotometer (Thermo-scientific, Maddison, USA) against a blank made with all other reagents without the sample. Authentic standard gallic acid (GA) (20–250 µg/mL) was also analyzed by the UV-Vis Spectrophotometer to generate a standardization curve for external quantification of the TPC, quantified in mg of GA equivalent per 100g.

3.5.2.3 Radical Scavenging Activity (RSA)

Assessment of RSA was done using 2,2-diphenyl-1-picrylhydrazyl (DPPH) assay according to methods reported by Mokaya *et al*. (2022). Every sample (2.5 mg) was dissolved in 1 mL of 50% methanol vortexed for 1 min. This was followed by spinning at 4200 rpm for 10 mins. After combining 0.75 mL of the upper layer with 1.5 mL of 5 mg/100 mL methanol DPPH. The mixture was allowed to remain at 24℃ for 5 minutes. The control consisted of 0.75 mL of methanol mixed with 1.5 mL of DPPH solution, whereas the blank contained 0.75 mL of extract solution mixed with 1.5 mL of methanol. The absorbance was read at 517 nanometers using the Evolution™ Pro UV-Vis Spectrophotometer (Thermo-scientific, Maddison, USA). The same procedure was repeated using extract dissolved in 50% hexane with a resultant concentration of 30 mg/mL. Hexane (50%) and methanol (50%) were chosen based on their extractabilities for entomochemicals and lipids, respectively. The percent inhibition was obtained using;

$$\% \text{ Inhibition} = \left(\frac{\text{Control absorbance} - \text{Sample absorbance}}{\text{Control absorbance} * 100}\right) * 100$$

3.5.3 Amino Acids Determination

Amino acids profile of the beetle larvae was done following previous methods stated by Murugu *et al.* (2021). Ground larvae (100 mg each) were hydrolyzation of 100 mg of each sample was done using 2 mL of 6 N Hydrochloric acid at 110℃ for 1 day beneath nitrogen gas. Afterward, the resultants were concentrated under vacuum and using 1 mL of 0.01% formic acid and 95% acetonitrile, the residues were reconstituted. These mixtures were then thoroughly mixed for 30 secs, sonicated for 30 mins and finally spanned at 14000 rpm for 15 mins. The upper layer was evaluated on an Agilent single quadrupole LC-MS 1200 series (Agilent Technologies, Inc., Santa Clara, CA, USA). In order to accomplish the chromatographic separation, a Zorbax RX-C18, 4.6 × 250mm, 5 μm column was used operating at 40℃. The mobile phase comprised of water (A) and acetonitrile (B) all supplemented with formic acid (0.01%). The following gradient elution was used: 0 to 6 minutes, 10% B; 6 to 7.5 minutes, 10% to 80% B; 7.5 to 10.5 minutes, 80% B; 10.5 to 13 minutes, 80% to 100% B; 13 to 18 minutes, 100% B; 18 to 20 minutes, 100% to 10% B; 20 to 25 minutes, 10% B. The rate of flow was programmed as follows: 0 – 13 min; 0.25 mL/min, 13 – 25; 0.5 mL/min and the injection capacity was set at 5 µL. The mass spectrometer was run in API-positive mode with mass range of m/z 50 to 600. An authentic standard of amino acids (Sigma–Aldrich, St. Louis, MO, USA) was also analysed by LC-MS and used to externally quantify the amino acids. All the analyses were performed in triplicates.

3.5.4 Fatty Acids Determination

The extraction of total lipids and methylation to fatty acids methyl esters was conducted using a protocol outlined by Ochieng *et al.* (2022). Folch-based extraction method, involving extraction of 1 g of each sample with butylated hydroxytoluene (BHT) (0.05 mg/mL) in a 10 mL, mixture of 2 volumes of dichloromethane to one volume of methanol was applied. Upon centrifugation for 15 mins at 4200 rpm, the supernatants were vacuum evaporated to remove the solvents and recover fats of ~ 250 mg. Subsequently, 100 mg of fat extracts were methylated by addition 1 mL of 100 mg/mL sodium methoxide, 1 min for vortexing, 10 min for sonicating and incubation for 1 hour in a 70℃-water bath. After addition of 100 µL of distilled water and further vortexing for a minute, the reaction was quenched. The methyl esters of the fatty acids were extracted using 1 mL of GC-grade hexane. After drying the supernatant on anhydrous sodium sulfate, the resultant was spun at 14000 rpm for 15 mins. The dry supernatant

(1.0 μL) was analyzed using GC–MS on a 7890A GC (Agilent Technologies Inc., Santa Clara, CA, USA) coupled with a 5975C mass selective detector (Agilent Technologies Inc., Santa Clara, CA, USA). The column fitted on the GC was (5%-phenyl)-methylpolysiloxane (HP5 MS) low bleed capillary column (30 m × 0.25 mm i.d., 0.25 µm; J&W, Folsom, CA, USA). Helium was the carrier gas utilized, and it flowed at a rate of 1.25 mL/min.

The initial temperature was set to increase by 10℃ every minute starting at 35℃ and ending at 285℃. Starting and final temperatures were held for 5 and 20.4 minutes respectively. The mass selecting detector and ion source were upheld at 180℃ and 230℃ temperatures respectively. Using electron impact at an acceleration energy of 70 electron-volts, spectral masses and fragment ions in the range of 40–550 m/z were obtained using full-scan mode. The filament was set to operate at a delay period of 3.3 minutes. Using the equation; $\mathrm{Y} = 5\mathrm{E} + 0.7\mathrm{X} + 2\mathrm{E} + 07$ a linear quantification curve (peak area vs. concentration) was created. Serial dilutions of pure methyl octadecenoate standard (0.2 – 125 ng/L) were made from octadecanoic acid (Sigma-Aldrich, St. Louis, MO) and examined in full-scan mode using GC-MS. The resulting standardization curve was used to analyze the several fatty acids in the processed samples and had its coefficient of determination value was 0.9997. The data acquisition was done using ChemStation B.02.02 software where the integration values were set with initial threshold of 3, initial peak width of 0.01. By comparing the retention durations and mass spectral data with that of standard as well as from the published MS- libraries by the National Institute of Standards and Technology the fatty acids were identified.

3.5.5 Minerals Determination

The mineral composition was determined as per the protocol previously outlined by Tanga *et al.,* (2023). The samples were processed by dry ashing in muffle furnace (Heraeus-Kundendienst, Düsseldorf, Germany) at a temperature of 550℃ for 3 hours. Upon cooling, 5 mL of 6N nitric acid was put in 1 g of each sample and subjected to microwave-assisted digestion for 20 mins. The hydrolysates were tested for calcium, magnesium, iron, sodium, manganese, zinc and potassium using inductively coupled plasma emission mass spectrometer (Agilent 7900 ICP-MS, Inc., Santa Clara, CA, USA).

3.6 Gut Microbial Communities Profiling

3.6.1 Genomic DNA Extraction from Gut Samples

DNA was extracted from every sample using CTAB – phenol- chloroform process as outlined by Ausubel *et al*. (1992). First, individual thawed gut samples were homogenized using Qiagen TissueLyser II. To the 250 µL of the homogenate from each sample, an equivalent quantity of pre-chilled CTAB buffer was added. The mixture was then filled up with warmed CTAB buffer and digestion enzyme (25 µL of proteinase K) then incubated at 65℃ for 15 minutes with continuous shaking every 5 minutes. The supernatant was spanned at 15000 x g and then transferred to a clean 2 µL Eppendorf micro-centrifuge tube. To the supernatant, one volume of chloroform-isoamyl alcohol (24:1) was added. The tubes were inverted severally to minimize protein contamination. This was followed by centrifugation at 1500 rpm and subsequent transfer of supernatant to a sterile1.5 µL Eppendorf micro-centrifuges tubes. To precipitate the DNA, addition of 0.7x isopropanol to the supernatant was done and inverted severally.

The resultant was centrifugated at 1500 rpm for 8 mins to create a pellet and the upper layer carefully discarded. The pellet was rinsed twice with 250 mL of ethanol (70%) followed by one wash with 100% ice cold ethanol and centrifugation steps of 1500 rpm per wash. After air-drying, the pellets were dissolved in EB elution buffer (Meridian Bioscience). The phenolic compounds were removed from DNA using agarose gel electrophoresis (1%) modified with 1% polyvinylpyrrolidone (PVP). The addition of PVP helps in retarding the electrophoretic mobility of fulvic and humic acids, preventing comigration with the non-degraded DNA (Young *et al*., 1993). DNA was extracted from the gels and measured using NanoDropTM 2000 UV-Vis spectrophotometer (Thermo Fischer Scientific, Wilmington, USA). For 16S rDNA (bacteria) and 18S rDNA (protists), DNA samples with high quality ranging from 1.7 to 2.1 based on A260/A280 nm were chosen and kept at - 80℃ until processing. Afterward, approximately 80 µL of the DNA obtained was sent to Macrogen Inc (Netherlands) for Illumina next-generation 439 sequencing (NGS).

3.6.2 Bioinformatics

FASTQC (v.0.11.6) was utilized to evaluate the raw sequence read quality (Wingett & Andrews, 2018). Pre-processing of the raw reads was done using the Divisive Amplicon Denoising Algorithm (DADA2) (v 1.28.0). This workflow was proposed by (Callahan

et al., 2016) done in R v4.3.0 using the R Studio v2023.06.0 interface (R Core Team, 2023). Cutadapt (v4.6) was used to trim, dereplicate and perform error rate reading at 0.2 from our raw sequences (Martin, 2011). Trimming and filtering out of 16s and 18s sequence reads were performed with the following custom parameters: forward reads at 250 base pairs, reverse at 160 base pairs, maxN= 0, maxEE= (2,5) and truncQ= 2. Low-quality reads were then eliminated to increase the merging chances and the accuracy of error learning in DADA2. Demultiplexing was carried out using the "derepFastq" function then the 'Remove Bimera Denovo' function was employed to eliminate spurilous and chimeric reads to ensure only high-quality sequence reads were inferred into their associated amplicon sequence variants (ASVs). Phylogeny was assigned against pretrained databases; SILVA (16s) (Quast *et al*., 2012) and Protist Ribosomal Reference (18s) (Guillou *et al*., 2012) based on pairwise identification using the 'assign Taxonomy' function. The DECIPHER package v2.28.0's "AlignSeqs" function was used to align multiple sequences (Wright, 2016). Further analyses, manipulation and data visualization were performed using phyloseq v1.44.0 (McMurdie & Holmes, 2013), Tidyverse package v2.0.0 (Wickham *et al*., 2019), metagMisc v0.5.0 (Kyritsi *et al*., 2023) and Janitor package v2.2.0 (Firke, 2021).

Two phyloseq objects for both bacteria and protists were created followed by eliminating all ASVs corresponding to undesired sequences such as chloroplast, mitochondria and archaea using the "subset_taxa" function of phyloseq. Subsequent taxa were then further filtered to ensure that only all the most abundant taxa were retained. The metadata, ASVs and taxonomy tables were combined to create a phyloseq (McMurdie & Holmes, 2013) object to aid in visualization. Using the thirty most prevalent readings, a stacked bar plots were made to show the composition of the gut microbial communities at genus level. The mean ASV richness for each sample was obtained by rarefying to a sampling depth of 6500 reads using 'rarefy_even_depth' function and 'vegan' package (Oksanen *et al*., 2018) to reduce the effects of unequal sequence reads between the samples. Alpha diversity was determined using the Microbiota process v1.9.3 based on sample ASV outlines from a rarefied phyloseq object using; "Chao1," "abundance-based coverage estimator (ACE)," "Pielou's Evenness," "Simpson Evenness" and "Shannon" diversity predictors. The resultant before being visualized the indices were first put through the Shapiro-Wilk test to determine their normalcy using the "ggpubr" package v0.6.0 (Kassambara, 2018).

Effects of beetle larvae genus and geographical location on the alpha diversity were then assessed using Kruskal-wallis pairwise comparisons. Beta-diversity (β-diversity) was computed using the Weighted UniFrac distance to assess the bacterial community clustering pattern using the "phyloseq::ordinate" function. This was visualized using principal-coordinate analysis (PCoA) biplots using the 'vegan' package v2.6.4 in R (Oksanen *et al*., 2018). Defining core microbiota was done by making detailed comparisons of bacterial species determined down to the genus level to describe the number of shared ASVs. For this, Venn diagrams were produced by utilizing the 'Venn Diagram' package v1.7.3 (Chen & Boutros, 2011) to illustrate the core shared bacterial genera, which were classified as those that had a 30% prevalence in both larvae species. Permutational multivariate analysis of variance with Betadisper was used to detect variations within the gut microbiota between the larvae sampled from different locations using the "Adonis" function of "vegan" package (v2.6.4) package in R (Oksanen *et al*., 2018).

3.6.4 Functional Prediction of the Detritivores Bacterial Gut Microbiota

The phylogenetic Investigation of Communities by Reconstruction of Unobserved counts per sample (PICRUSt2, version 2, (Douglas *et al*., 2019)) used in order to forecast the functional analysis of the bacterial gut microbiota. The predicted gene family-counts per sample were tabulated using DC reads abundance, orthologous groups and identifiers constructed with Kyoto Encyclopedia of Genes and Genomes (KEGG). The categories unconnected to the physiology and metabolism of bacteria were removed after level 3 classification of KEGG identifiers. Results from level 3 categories were visualized by generating a heatmap using STatistical Analysis of Metagenomic Profiles (STAMP) software (Parks & Beiko, 2010). Box plots in STAMP were utilized to identify pathways with significant differences between the two saprophagous larvae.

3.7 Biomolecules Extraction and Characterization

3.7.1 Culturing and Extraction

The homogenates culturing was done on solid media plates supplemented with 2 mL of 25 mg/mL chloramphenicol prepared by autoclaving 10 g of monohydrate dextrose, 50 g of potato dextrose agar, 3 g of yeast and 5 g of mycological peptone dissolved in 1 L of distilled water to obtain mixed fungal isolates. The culturing process was done on

two plates for each of the 15 homogenates to obtain mixed fungal isolates for four days. The plates were inspected daily for hyphae emerging. One plate from every site was used for sub-culturing of pure fungal isolates. The other plate was soaked in 30 mL methanol for 24 hours. Filtration using Whatman filter papers was done to separate mycelium and the aqueous phase after which the excess solvent was reduced in vacuo to obtain dry powder extracts.

3.7.2 Preliminary Screening for Antibacterial Activity

The crude extracts of the mixed fungal cultures from the 15 sites were screened for antibacterial activity using the disc-diffusion method as described by Duraipandiyan & Ignacimuthu, (2009) with slight modifications. The bacteria suspensions of *S. aureus, E. coli, B. subtilis and P. aeruginosa* obtained from the lab were made from overnight cultures in Muller Hinton Agar (MHA) media plates (MHA plates prepared by dissolving 38 g of MHA media in 1 L of deionized water then autoclaved) by resuspending them in double-distilled water. The turbidity of the suspension was adjusted using UV spectrophotometer to match that of 0.5 m McFarland standard. 100 µL of the adjusted bacteria suspension was added to the MHA plates. Sterile beads were used to evenly distribute the bacteria over the MHA media and allowed to dry for few minutes. Six discs (6 mm) were then placed on the seeded plates and loaded with different crude extracts each 20 µl. 20 µl of streptomycin served as the positive control while 10% DMSO was the negative control. Incubation of the plates were done at 37℃ for1 day and the zones of inhibition measured around each 6 mm disc to record the antibacterial activity of the fungal crude extracts. The means of the zones of inhibition were obtained, tabulated and the most bioactive mixed fungal culture was identified. The bioactive mixed fungal culture was used for sub-culturing to obtain 15 axenic cultures which were then subjected to the preliminary antibacterial screening described above. After obtaining the means of the zones of inhibition, the most bioactive fungus against the gram-negative bacteria was selected for identification and mass cultivation to extract metabolites.

3.7.3 Identification of the Bioactive Fungus

The bioactive fungus was recognized using both morphological and internal transcribed spacer (ITS) gene sequence analysis. Morphological characteristics of the fungus were assessed according to method described by Raper & Fennell (1965). The extraction of

DNA from the fungi was done as per the assay as described by Orwa *et al*. (2020) with insignificant modifications. In a 2 mL tube, a weighed amount of mycelium, extraction buffer (Tris-HCl, EDTA, NaCl and CTAB), and sterile beads were mixed. After lysing, the mycelium for 30 seconds, 25 µL of Proteinase K was added to the conduit and briefly vortexed. Proteinase K is a proteolytic enzyme that was used to break down proteins including the ones present in nucleus and cell membrane. The mixture was then spanned at 14000 rpm for 10 mins after adding chloroform and isoamyl alcohol. The upper layer was combined with a little amount of CTAB and chloroform before undergoing centrifugation for 10 minutes at 14000 rpm. After that, the supernatant was poured into a sterile 1.5 mL tube. An equivalent volume of icy isopropanol was added followed by overnight incubation at 20°C before undergoing spans for 10 mins at 14000 rpm. The particle was washed with 80% ethanol at 4ºC, spanned for 10 minutes at 14000 rpm and then dried for 10 minutes.

Conventional PCR was used to magnify zones of fungal DNA: ITS1-2 rRNA was amplified using common primers ITS1 (TCCGTAGGTGAACCTGCGGG) and ITS4 (TCCTCCGCTTATTGATGGC. PCR reactions were made as per the methods described in section 3.6.1. On a thermocycler, DNA amplification occurred using the following conditions: 95℃ for 15 mins, then 35 amplification cycles of 94℃ for 30 seconds, 58.5℃ for 30 seconds and 72℃ for 45 seconds), followed final extension of 72℃ for 10 minutes. The PCR product was viewed using a 1.5 percent agarose gel electrophoresis. The amplified DNA was sent to Macrogen for sanger sequencing followed by identification of the fungus.

3.7.4 Solid Culture and Liquid Fermentation

A culture of the bioactive fungus was cultivated on alterant PDA medium consisting of potato dextrose agar (50 g), peptone (5 g), glucose (10 g), yeast (3 g) per liter and to prevent bacterial growth 1 mg/mL of streptomycin in 120 petri dishes at 25℃ for 42 days until fully grown. During the 8th day, three to four agar plugs (0.4 cm by 0.4 cm) from two petri dishes containing seed culture were added to five 1000 mL flasks containing 500 mL of alterant Czapek's medium consisting of Sucrose (30 g), yeast (50 g), potassium nitrate (3 g), potassium chloride (2 g), dipotassium phosphate (1 g), magnesium sulfate heptahydrate (0.5 g), potassium fluoride (1 g), iron sulfate (0.1 g), zinc sulphate (0.5 g) and copper sulphate (0.5 g) per 1 liter. This was done under aseptic

conditions and incubated in the dark for about 40 days with weekly hand shaking before harvest.

3.7.5 Bioassay-Guided Fractionation and Isolation of Target Secondary Metabolites

Solid cultures of the fully grown fungus mycelia were collected and extracted three times using 80% acetone at 23℃ for 24 hours. This acetone extract was concentrated *in vacuo* at 40℃ on a rotatory evaporator to afford a blackish liquid residue (300 mL). Liquid-liquid partitioning was done on this blackish extract using ethyl acetate to yield two fractions which were also concentrated to yield 814.1 mg (EtOAc fraction) and 9.8 g for the aqueous fraction. The fractions were subjected to antibacterial screening to determine the most active fraction.

For the liquid cultures, centrifugation and filtration were used to remove the mycelium from the broth. Fractionation of the liquid crude extract was done as defined by Mudalungu *et al*. (2016) with insignificant modifications. The acquired wet mycelia was soaked in 80% acetone and left overnight to ensure better recovery of the metabolites from the mycelia. This followed five times extraction under room temperature for 30 minutes, then filtered and evaporated *in vacuo* to yield (990.9 mg). To get the crude substance from aqueous phase, the extract was adsorbed on a reverse-phase solid-phase amberlite mesh, eluted with methanol and concentrated to yield 7.8 g. The two crude extracts were mixed and liquid–liquid fractionation described above was repeated. The fractions were subjected to preliminary antibacterial activity tests as described above to determine their antibacterial potency. Dose-dependent assay was also conducted for the ethyl acetate fraction at final concentrations ranging from 100 to 13 mg/mL (prepared from twofold serial dilutions).

3.7.6 Isolation of Pure Compounds

Several chromatographic methods were used to isolate and purify the secondary metabolites found in the EtOAc extract. Silica gel G 60 column (60 mm mesh, E. Merck Darmstadt, Germany) was used to chromatograph the crude extract (1800 mg), which was then eluted with hexane: Ethyl acetate: Methanol to yield five fractions (v/v, 100:0:0, 50:50:0, 0:100:0, 0:50:50, 0:0:100, respectively). The fractions profile was observed using thin-layer chromatography (TLC) done on precoated silica gel 60 F_{254} aluminum sheets (E. Merck Darmstadt, Germany) and visualized using an overhead

UV lamp. Briefly, components of limited interest were exposed by fraction 1 eluted with 100% hexane. Fractions 2 and 3 were pooled together based on their similar TLC profiles to yield 110 mg which was further subjected to preparative reverse phase HPLC 1100 series LCMS (Agilent Technologies, Inc., Santa Clara, CA, USA) eluted using acidified acetonitrile – water solvent system for 55 minutes. Water and acetonitrile used in HPLC system were of analytical grade and all other reagent were analytical grade. The separation was done using Zorbax RX-C18, 4.6 × 250mm column operated at 40℃. Chromatograms were obtained at wavelengths of 220, 254, and 270 nm. The flow proportion was set at 2.5 mL/min. Mobile phases consisted of solvent A (0.01% formic acid in LCMS grade water (v/v)) and solvent B (0.01% formic acid in acetonitrile (v/v)). The gradient started from 0.01% to 5% in 2 min, 5% to 15% in 5 min, 15% to 45% in 5 min, 45% to 60% in 15 min, 60% to 75% in 15 min, isocratic at 75% in 5 min, 75% to 100% in 5 min, 100% (isocratic) in 2 min and 100% to 5% B in 2 min. The purified compounds were used for further structural analysis. The retention times and masses for compound 1 was 47.3 mins, 4.1 mg, while for compound 2 was 50.0 mins, 1.7 mg.

3.7.8 Characterization of Pure Compounds from Bioactive Fractions

3.7.8.1 Single Quadrupole LCMS Profiling

The identification was performed on Agilent 1200 series LCMS (Agilent Technologies, Inc., Santa Clara, CA, USA) fitted with an autosampler, a degasser, quaternary pump system, a photodiode array detector, an MSD trap with an atmospheric pressure electrospray ion source. The single quadrupole mass spectrometer was under positive mode with scan range from *m/z* 100 to 1500. The needle voltage was 3.5 kV, while the nebulizer gas (nitrogen), had a flowrate of 12 L/min and the capillary temperature was set at 350℃. The separation was done using Zorbax RX-C18, 4.6 × 250mm, 5 μm column operated at 40℃. The flow rate was set at 1.0 mL/min. Mobile phases consisted of LCMS grade water (solvent A) and acetonitrile (solvent B) acidified with 0.01% formic acid. The gradient started from 5% to 10% in 10 min, 10% to 30% in 30 min, 30% to 60% in 1 min, 60% to 75% in 10 min, isocratic at 75% in 3 min, 75% to 90% in 5 min, 90% to 100% in 2 min, isocratic at 100% in to min, and from 100% to 5% B in 2 min. To identify the molecules, HP Chemstation software and Data Analysis 4.2 was used.

3.7.8.2 NMR Processing

NMR spectra (1D-Proton, 13-Carbon, COSY, NOESY, HSQC, and HMBC) were acquired using an Agilent DD2 (600 MHz) spectrometer at a temperature of 24.85℃ in deuterated chloroform. Reference signals from the deuterated chloroform solvent (proton shifts at 7.260 ppm and carbon-13 shifts at 77.000 ppm) were employed to calibrate the obtained spectra. The spectra were processed and analyzed using MestreNOVA v. 11 software (Mestrelab Research, Chemistry Software Solutions, Santiago de Compostela, Spain).

3.7.9 Physiochemical, ADME Properties and *in vitro* Antibacterial Efficacy of Isolated Compounds

The SwissADME tool, available for free online at http://www.swissadme.ch/ (accessed on 20 March 2024), was utilized to predict the physicochemical properties and lipophilicity, pharmacokinetic, water solubility and drug-likeness properties of the isolated molecules as described by Kibet *et al*., (2024). The SMILES codes for the compounds were entered into the designated input box on the SwissADME webpage. After initiating the analysis by clicking the "Run!" button, the process was completed, and the data were subsequently downloaded as Excel files in CSV format. Hepatotoxicity AMES toxicity, hERG I and II inhibition and skin sensitization toxicities were predicted using the pKCSM web server, available at https://biosig.lab.uq.edu.au/pkcsm/ (accessed on 21st March 2024). Within pKCSM, the SMILES codes for each molecule were individually submitted for toxicity prediction, and the outcomes were systematically documented. The compounds were also subjected to antibacterial screening according to the procedures described above.

3.8 Statistical Data Analysis

All statistical analyses were achieved using R-core team (2017). The Shapiro–Wilk test was employed to establish the suitability of data sets for subsequent analyses. Data sets from any of the assays that violated the Shapiro Wilks test hypothesis of normal distribution were subjected to Kruskal-Wallis's test and means compared using Dunns' test using Agricole package (De Mendiburu & Simon, 2015). Conversely, data sets that were normally distributed were subjected to one-way ANOVA and mean separated using Student-Newman-keuls (SNK) test with the aid of Fisheries Stock Assessment

(FSA) (Ogle & Ogle, 2017) and Agricole packages (De Mendiburu & Simon, 2015). All the assays were performed in triplicates.

CHAPTER FOUR

RESULTS AND DISCUSSION

4.1 Morphological/Molecular Identification and Phylogenetic Analysis of the Collected Larvae

The similar characteristics of the larvae were creamy-white, with a soft, grub-like body. Their soft skin was covered in many setae (hair-like structures that perform sensory functions). They possessed three bodily parts: the head, the thorax, and an enlarged dark abdomen housing the hindgut. They also featured three pairs of short functioning legs on the thoracic segment and large mandibles designed to devour decaying organic materials. *Cetonia aurata* larvae measured 55-60 mm long, 35-40 mm in diameter, and had a brown head capsule that was 5.2-6.0 mm wide. On the other hand, *O. rhinoceros* larvae measured 85-96 mm in length, 45-50 mm in diameter, and had a brown head capsule that was 10.7-11.1 mm broad.

The BLAST analyses of the sequences of the two beetle larvae revealed 97% and 96.30% match with *C. aurata* and *O. rhinoceros*, respectively [**Figure 4.1**]. These sequences obtained from *C. aurata* and *O. rhinoceros* have been banked in the GenBank nr database with the accession numbers OQ925397.1 and OR115609.1 respectively. The morphological characteristics of the larvae were comparable to those described in literature (Bedford, 1974; CABI, 2023). The two major species identified included *C. aurata* and *O. rhinoceros*, which is consistent to that identified by Mckenna *et al.* (2015) and Marshall *et al.* (2017) in USA and Australia, respectively.

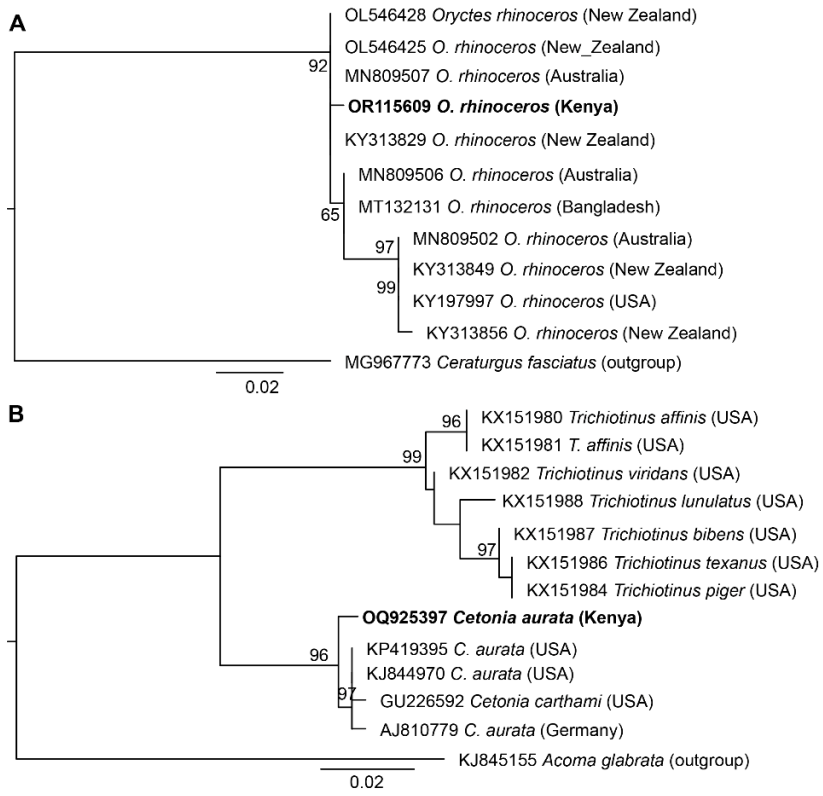

Figure 4:1: A-Maximum likelihood phylogenetic trees of cytochrome oxidase subunit 1 (COI) gene sequences from *O. rhinoceros* larvae and **B**-28s rRNA sequences from *C. aurata* beetle larvae (tree B). Sequences of *O. rhinoceros* and *C. aurata* in this study is indicated in bold. Between 1000 bootstrap repetitions, the bootstrap values represent the % agreement. Substitutions per site are indicated by branch length. The outgroup sequence at the bottom of each tree was used for rooting

4.2 Nutritional Profiling

4.2.1 Radical Scavenging Activities

The RSA of methanolic extracts of *C. aurata* larvae ranged between 91.1–92.7%, while that of *O. rhinoceros* ranged between 55–60% (**Figure 4.2 A**). The RSA of *O. rhinoceros* was considerably (p=0.0184) lower than that of *C. aurata* larvae. The RSA of the two beetle larvae did not vary significantly across the various locations but differed significantly (F=16.02, df=5, *P*<0.05) between the species (**Table 1**). The RSA for hexane extracts of *C. aurata* and *O. rhinoceros* ranged between 33.83–88.60% and 71.60–86.70%, respectively (**Table 4.1**). Unlike the methanolic extracts, the RSA from the hexane extracts of *C. aurata*, varied significantly (F=10.60, df=5, p-value=0.000408) across the sampling locations with no discernible species effects (**Figure 4.2 B** and **Table 4.1**). The larvae of *C. aurata* larvae exhibited high RSA activities, which could be due to the presence of high bioactive peptides, particularly with lysine (L) in their sequences which has been found to have high antioxidant

activity as identified from GWLK peptide obtained from *Zizyphus jujuba* derived protein hydrolysates (Memarpoor-Yazdi *et al.,* 2013; Lange & Nakamura, 2021). Other reports have also shown that proteins might contribute significantly to the RSA (Suh *et al.,* 2011; Mokaya *et al.,* 2022).

The RSA from *C. aurata* larvae are comparable to that reported for *Protaetia brevitarsis* (92%) and *Allomyrina dichotoma* (81.5%), respectively), but slightly lesser than that reported by Suh *et al.* (2010; 2011). The similarity of RSA in the hexane extracts from *C. aurata* and *O. rhinoceros* signifies equal solubility of the compounds present (Di Mattia *et al*., 2019). Nevertheless, the RSA of hexane from *C. aurata* and *O. rhinoceros* was higher than the 7.8% activity previously reported in *Allomyrina dichotoma* (Suh *et al*., 2010), but identical to values stated by Mokaya *et al.* (2022). The outstanding bioactive components and RSA identified in this study have significant health implications. Therefore, the consumption of *C. aurata* and *O. rhinoceros* should be widely promoted as alternative food sources with reduced ecological impact (Fiebelkorn *et al*., 2020).

4.2.2 Total Flavonoids and Total Phenols Content

The total flavonoids content (TFC) values for *C. aurata* ranged between 17.78–34.90 mg QE /100 g, while that for *O. rhinoceros* ranged between 28.64–35.02 mg of QE per 100 g [**Figure 4.2 C**]. The total phenols content (TPC) of *O. rhinoceros* and *C. aurata* ranged between 44.10–50.82 and 50.19–54.60 mg GAE/100 g, respectively [**Figure 4.2 D**]. There was no influence of TPC and TFC across the species and target location, therefore null hypothesis was accepted [**Table 4.1**]. This study unravels that the entomochemical compounds (flavonoids and phenols) of these beetle species, are known to be responsible for the prominent radical scavenging activities (Lange & Nakamura, 2021). The total phenols contents recorded in two beetle species superseded 38.3 mg GAE/100g and 3.65 mg/100g reported in other beetle species (*Rhynchophorus phoenicis* and *Oryctes owariensis*, respectively). However, the phenol levels are lower than the values (541 mg GAE /100g) reported in silk moth (*Samia cynthia ricini*) and in flower beetle; *Protaetia brevitarsis* Lewis 73.53 mg GA g−1 extract (Suh & Kang, 2012; Ukoroije & Bobmanuel, 2019b; Botella-Martínez *et al*., 2021; Mokaya *et al*., 2022). The TFC levels in *C. aurata* and *O. rhinoceros* were comparably lower than 93 -231 mg/g range previously reported in the wild silk moths: *Anaphe panda, Gonometa*

postica and *Argema mimosae* (Mokaya *et al.,* 2022). The differences in the chemical composition described among the insect species can be attributed to the bioactive component levels present in the dietary sources, which explains why insects foraging exclusively on vegetarian diets have higher bioaccumulants than the organic waste feeders (Di Mattia *et al*., 2019). The polyphenolic compounds identified in the two scarab beetles have been previously reported to counteract aliments associated with old age and others affecting the locomotor system (Del Carmen Villegas-Aguilar *et al*., 2023) through their radical scavenging potentials.

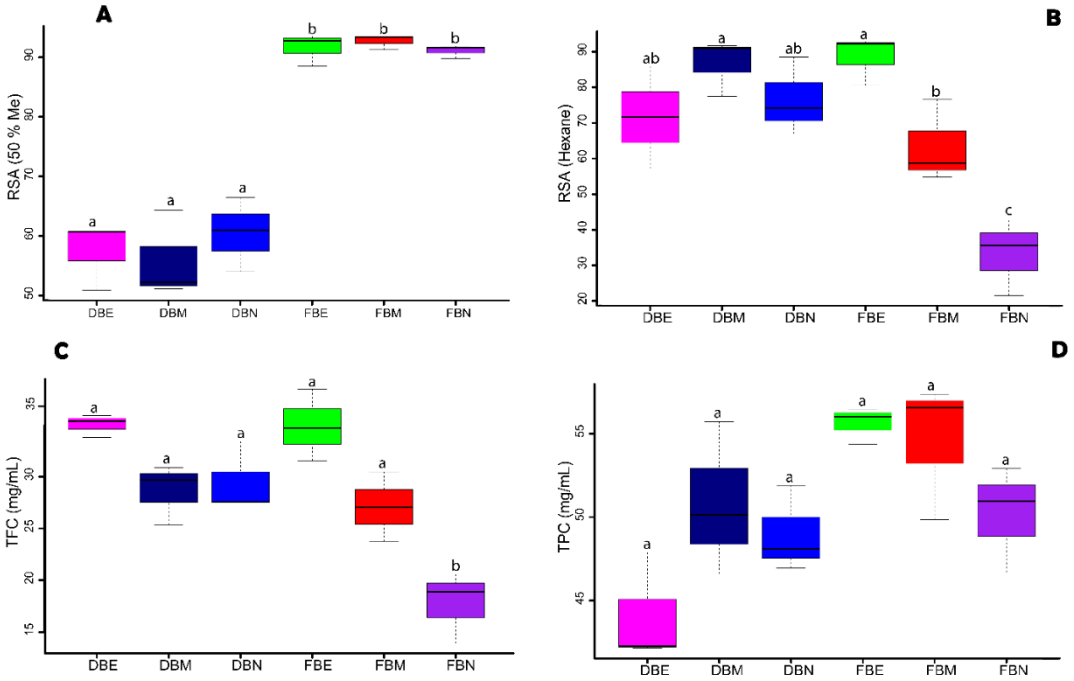

Figure 4:2: Box plots showing variations in radical scavenging activity (RSA); A - in 50% methanol, B - hexane and bio functional compounds; C - total flavonoids and D-total phenols content; FB - represents *C. aurata* larvae while DB- is *O. rhinoceros* larvae. The last letter at end of FB or DB represents the site of collection. *C. aurata* from Nairobi (FBN), Murang'a (FBM), Embu (FBE), *O. rhinoceros* from Nairobi (DBN), Murang'a (DBM) and Embu (DBE). Boxplots with distinct letters at the top exhibit considerable differences at p<0

Table 4.1: The Antioxidant activities and entomochemical contents of beetle larvae in three different Counties

Sampling location	Larvae	Total Flavonoids (mg QE/100 g)	Total phenols (mg GAE/100 g)	RSA in He (50%)	RSA of 50% Me (%)
Murang'a	*C. aurata*	27.08 ±1.94^{a}	54.60±2.38^{a}	63.40±6.70^{b}	92.73±0.74^{b}
	O. rhinoceros	28.64 ±1.68^{a}	50.82±2.65^{a}	86.70±4.61^{a}	55.89±4.22^{a}
Nairobi	*C. aurata*	17.78 ±1.99^{b}	50.19±1.83^{a}	33.83±6.20^{c}	91.10±0.64^{b}
	O. rhinoceros	29.48 ±1.96^{a}	48.98±1.49^{a}	76.60±6.35^{ab}	60.48±3.60^{a}
Embu	*C. aurata*	34.90 ±1.99^{a}	55.62 ±0.64^{a}	88.60±4.00^{a}	91.62±1.57^{b}
	O. rhinoceros	35.02 ± 0.64^{a}	44.10±1.89^{a}	71.60±8.26^{ab}	57.45±3.27^{a}

P Value	0.00018	0.298	0.000408	0.0184
F value	12.84	1.384	16.02	10.60
Df	5	5	5	5

QE- quercetin equivalent, Me – Methanol, He - Hexane, RSA- radical scavenging activity, GAE- gallic acid equivalent, df – degrees of freedom. Means are expressed as mean plus standard error. The means in each column that have the same letters do not differ substantially at $p<0.05$

4.2.3 Proximate Composition

The proximate components of the two beetle larvae species from the three collection sites are presented in **Table 4.2**. The ash (P=0.02253), crude fiber (P=0.008885) and crude protein content (P=0.01605) of the larvae varied significantly across the sampled locations and species type hence null hypothesis was rejected. The fiber content of *O. rhinoceros* in Murang'a and Embu was significantly higher, while the ash content of *C. aurata* (8.35%) was higher in Embu only. Food susceptibility to microbial spoilage is determined by its moisture content with lower levels known to correspond to longer shelf-life (Banjo *et al*., 2006). The two larvae of *C. aurata* and *O. rhinoceros* investigated had similar moisture content, which were inconsistent to that reported on longhorn beetle (*Analeptes trifasciata*) and *Oryctes boas* (rhinoceros beetle) air-dried at 50℃ for 2 days (Yang *et al*., 2014).

The ash content mirrors the micronutrients levels in the insect biomass and the value found in this study are comparable to that stated for most insects (Verkerk *et al*., 2007). Fiber content in edible insects is chiefly comprised of the chitinous exoskeleton (Ozimek *et al.,* 1985; Zhang *et al.,* 2000; Qiao-ru *et al.,* 2010) and may vary reliant on the species and the physiological needs. The fiber content of *O. rhinoceros* and *C. aurata* varied across the species and collection sites. The fiber content recorded for *C. aurata* and *O. rhinoceros* differed from that of *H. parallela* (Yang *et al*., 2014) and *Rhynchophorus phoenicis f.* (Omotoso & Adedire, 2007). *Cetonia aurata* from Murang'a and Nairobi recorded significantly higher protein levels than *O. rhinoceros* in Murang'a and Embu. The results for crude protein reported in this study falls within the protein range (21 – 70 g/100 g of DM) estimated for many coleopteran beetles (Bukkens, 1997; Verkerk *et al*., 2007; Qiao-ru *et al*., 2010). Crude protein analysis was based on K_p of 4.76 to avoid overestimation from non-protein sources while using K_p of 6.25 (Janssen *et al*., 2017).

Considerable variation of crude protein in insects across different locations have previously been reported by several authors (Qiao-ru *et al*., 2010) particularly for *H. parallela.* These large variations in protein content between the two larvae might be due to differences in growth conditions, and the differences in diet (organic waste) conversion efficiency to appreciable proportion of protein content (Thomas, 2018; Da Silva Lucas *et al*., 2020). Interestingly, the protein content of *C. aurata* and *O. rhinoceros* larvae compared favorably with 40–75 g/100 g of DM to conventional protein bases such as beef, fish, soya bean and pork thereby valorizing the larvae of these beetle species as nutritious diets with potential to significantly contribute to over 85% of protein RDA. The larvae pose as a sustainable protein source with health benefits to young babies, elderly, pregnant and lactating women with malnourished conditions.

Table 4.2: Proximate composition (expressed in % of DM) of the two larvae collected from Murang'a, Embu and Nairobi counties.

Sampling Location	Larvae	Dry matter	Moisture	Ash	Crude fiber	Protein
Murang'a	*C. aurata*	94.00±1^{a}	6.00±1.00^{a}	7.57±0.53^{ab}	4.74±0.03^{d}	63.37±0.73^{a}
	O. rhinoceros	93.67±0.33^{a}	6.33±0.33^{a}	7.22±0.36^{ab}	7.71±0.01^{a}	44.43±0.24^{b}
Embu	*C. aurata*	93.67±0.67^{a}	6.33±0.67^{a}	8.35±0.26^{a}	-	-
	O. rhinoceros	90.33±3^{a}	10.00±3.00^{a}	6.13± 0.41^{bc}	7.57±0.02^{b}	44.40±0.427^{b}
Nairobi	*C. aurata*	92.00±0.57^{a}	8.00±0.58^{a}	7.88±0.41^{a}	4.13±0.01^{e}	63.01±0.73^{a}
	O. rhinoceros	93.33±0.33^{a}	6.67±0.33^{a}	4.98±0.40^{c}	6.06±0.01^{c}	44.60±0.83^{b}
	Df	5	5	5	4	4
	χ^2	7.3667	7.7651	13.093	13.548	12.182
	P value	0.1948	0.2558	0.02253	0.008885	0.01605

The values are displayed as the mean plus standard error. (-) denotes not done. The means in each column show a considerate difference at $p<0.05$, denoted by distinct superscript letters

4.2.3.1 Amino Acids Profile

Twelve amino acids were detected from *C. aurata* and *O. rhinoceros* [**Table 4.3**]. Methionine and lysine varied significantly between the species except across locations. Glutamic acid, isoleucine, leucine, tyrosine and phenylalanine were the main prevalent amino acids in the two beetle larvae species [**Figure 4.3**]. The green color in **Figure 5** that the concentrations of the amino acids were comparable in the two larvae species. The concentration of histidine was lowest in the samples from the target locations [**Table 4.3**].

Table 4.3: Amino acid profile (mg/g) of *C. aurata* and *O. rhinoceros* sampled from three counties; Embu, Murang'a and Nairobi

		Murang'a		**Embu**		**Nairobi**				
	Amino acids	*C. aurata*	*O. rhinoceros*	*O. rhinoceros*	*C. aurata*	*O. rhinoceros*	*C. aurata*	**P value**	**Df**	**χ^2**
Essential amino acids	Valine (V)	14.37±0.53^a	9.22±4.37^a	13.73±0.30^a	13.15±0.23^a	14.31±0.41^a	14.20±0.89^a	0.2901	5	6.1696
	Threonine (T)	5.56±0.38^a	4.67±2.34^a	7.08±0.17^a	6.00±0.06^a	7.32±0.12^a	6.35±0.42^a	0.06232	5	10.497
	Phenylalanine (F)	18.17±0.99^a	10.66±5.27^a	16.94±0.91^a	15.57±0.27^a	16.60±0.23^a	17.21±1.98^a	0.2989	5	6.076
	Methionine (M)	5.36±0.23^a	1.64±1.10^b	3.99±0.11^a	5.01±0.11^a	2.78±1.14^a	5.62±0.25^a	0.0135	5	14.357
	Lysine (K)	10.96±0.34^a	5.40±2.47^b	8.23±0.35^a	9.64±0.27^a	8.01±0.27^a	9.95±0.26^a	0.01103	5	14.848
	Isoleucine (I)	19.53±1.31^a	12.22±5.92^a	18.35±0.34^a	16.85±0.27^a	19.21±0.60^a	13.39±5.86^a	0.3056	5	6.0058
	Leucine (L)	12.27±0.59^a	8.70±4.14^a	14.87±1.06^a	12.02±1.06^a	13.28±1.47^a	13.44±0.31^a	0.25881	5	6.521
	Histidine (H)	3.69±0.23^a	2.29±0.78^a	2.96±0.16^a	3.70±0.55^a	2.86±0.06^a	3.54±0.27^a	0.1001	5	9.2339
Non-essential amino acids	Glutamic acid (E)	17.50±0.96^a	12.63±5.33^a	18.12±0.46^a	17.26±0.57^a	18.37±0.76^a	19.07±0.40^a	0.2549	5	6.5673
	Proline (P)	15.09±0.39^a	12.60±4.48^a	16.49±1.05^a	15.18±0.41^a	18.52±0.22^a	15.39±0.67^a	0.1325	5	8.462
	Serine (S)	9.15±0.07^a	6.71±3.00^a	9.47±0.31^a	9.84±0.26^a	9.96±0.29^a	9.58±0.10^a	0.4074	5	5.0702
	Tyrosine (Y)	16.88±0.43^a	11.01±5.18^a	17.04±0.05^a	15.47±0.61^a	16.57±0.11^a	16.43±1.13^a	0.09022	5	9.5146

The means in each column that have distinct superscript letters differ considerably at $p < 0.05$

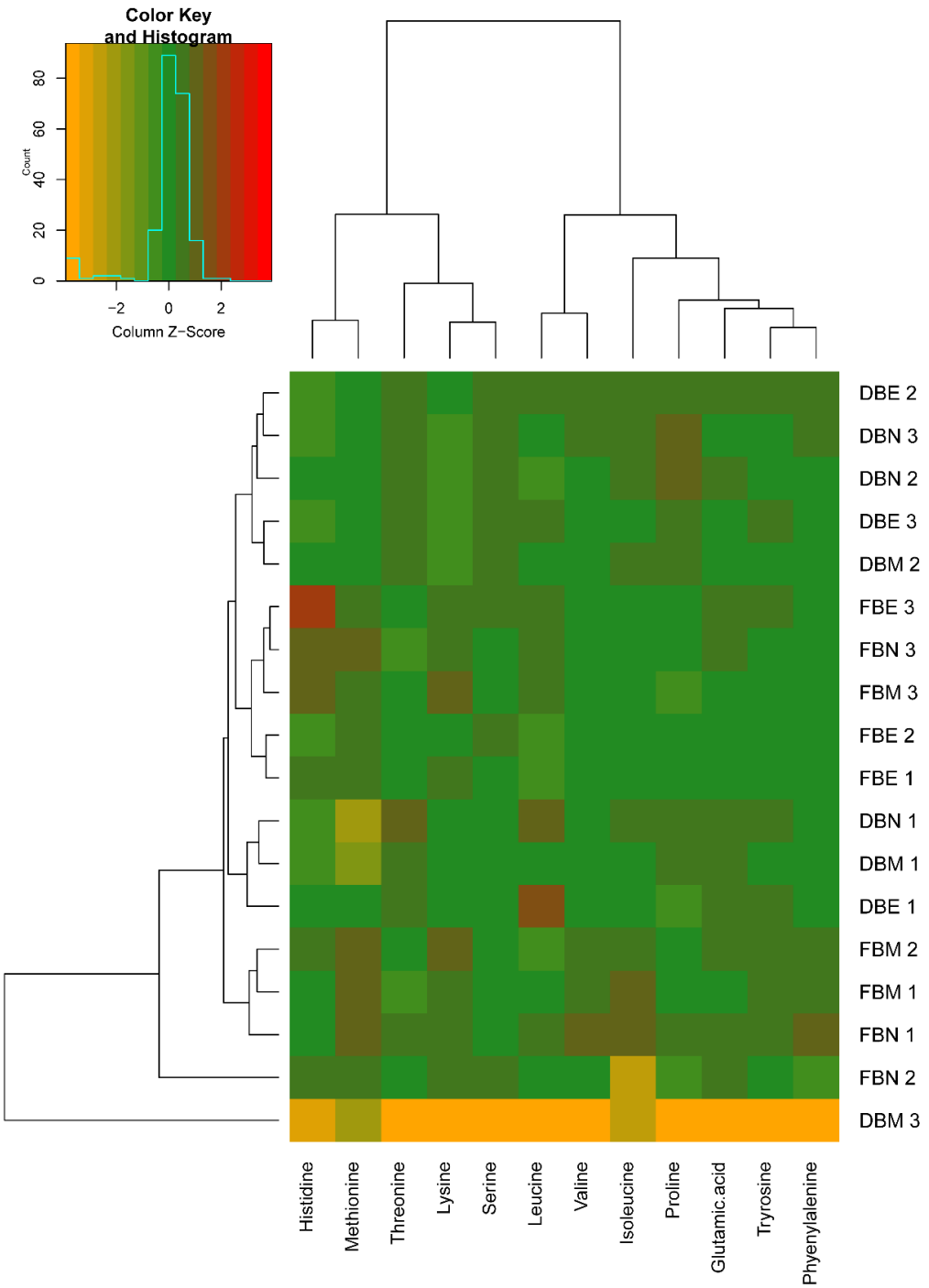

Figure 4:3: Heatmap showing concentrations of amino acids in *C. aurata* and *O. rhinoceros*. Dark-brown color shows the highest concentration while orange and red color represents the lowest concentration. The samples had comparable amounts since green color was the most prevalent color. The acronym FB - represents *C. aurata* larvae while DB- is *O. rhinoceros* larvae. The last letter at end of FB or DB represents the site of collection. The larvae of *C. aurata* from Nairobi (FBN), Murang'a (FBM), Embu (FBE), *O. rhinoceros* from Nairobi (DBN), Murang'a (DBM) and Embu (DBE)

The characterization of amino acids profiles of novel food sources such as insects is paramount for making nutritionally informed decisions akin to combating malnutrition.

The unravelling of isoleucine, phenylalanine, valine and lysine as the predominating essential amino acids in the two larvae corroborates findings by earlier studies on *O. rhinoceros* larvae (Okaraonye & Ikewuchi, 2008) and *H. parallela* (Qiao-ru *et al*., 2010). These amino acids (isoleucine, phenylalanine and valine) comprise a list of hydrophobic amino acids which offer bioactive remedial cushions against some health risks (Atowa *et al*., 2021). Lysine is a precious amino acid with deficient levels widely documented in cereal and plant-based products (Qiao-ru *et al*., 2010). Its detection in appreciable levels indicates that *C. aurata* and *O. rhinoceros* larvae are nutritional resources that can be utilized to enrich commonly consumed plant-based food products with imbalanced nutrient profiles.

Lysine is precursor in the synthesis of carnitine, which is instrumental in fat metabolism and also plays an important role in the hormone creation, enzymes and antibodies. Amino acids containing Sulphur with thio- ether linkages such as methionine was the only detected from *C. aurata* than in *O. rhinoceros* larvae. Methionine are actively involved in the detoxification mechanisms and production of other metabolically important compounds such as choline (Ademola *et al*., 2017; Fogang Mba *et al*., 2017). The detection of glutamic acid as the most prevalent non-essential amino acid concords to findings reported in other Coleopteran beetles (Qiao-ru *et al*., 2010; Oriolowo *et al*., 2020). Glutamic acid is an important savory amino acid, whose deficiency in food leads to glutamate formiminotransferase disorder. Based on the amino acids' profiles of the two beetle species larvae, it is admissible that such novel insects can be part of dietary diversification aimed at supplementing conventional low quality plant diets to alleviate malnutrition.

4.2.3.2 Fatty Acids Profile

A total of 19 FAs were identified with 6 monounsaturated fatty acids (MUFA), 5 polyunsaturated fatty acids (PUFA) and 8 saturated fatty acids (SFA) [**Table 4.4**]. Stearic acid, margaric and palmitic acids of the SFAs, oleic acid and palmitoleic acid of the MUFAs and arachidonic and linoleic acids of the PUFAs were the most abundant fatty acids detected. Linoleic and arachidonic acids (PUFAs) were not detected from larvae sampled from Murang'a. The ω-6/ω-3 ratio was 3.44 and 6.64 for *C. aurata* and *O. rhinoceros* from Embu, respectively. Comparative total fatty acid values of *C. aurata*

and *O. rhinoceros* to that of other animal-based sources and veal are shown in **Figure 4.4**.

Table 4.4: Fatty acid composition (in mg/g of DM) of beetle larvae obtained from Embu, Murang'a and Nairobi counties

		Murang'a		Nairobi	Embu				
FAME	**Common Name**	***C. aurata***	***O. rhinocerous***	***C. aurata***	***C. aurata***	***O. rhinocerous***	**P value**	**Df**	**χ^2**
Methyl dodecanoate	Lauric acid	9.42±0.26^{c}	-	14.24±1.55^{bc}	29.68±3.80^{a}	22.64±1.75^{ab}	0.018785	3	9.9744
Methyl tetradecanoate	Myristic acid	-	1.39±0.13^{c}	16.83±3.82^{bc}	39.97±1.33^{a}	38.34±1.09^{a}	0.02162	3	9.6667
Methyl 8-heptadecenoate	Margaric acid	-	-	-	113.66±4.04	-	-	-	-
Methyl undecanoate	Undecanoic acid	-	-	-	36.66±3.22	-	-	-	-
11-Methyl octadecanoate	Stearic acid	91.53±4.00^{b}	21.8±1.18^{d}	87.21±1.47^{bc}	37.20±3.25^{cd}	102.64±4.37^{a}	0.012	4	12.856
Methyl 10*Z*-nonadecenoate	Nonadecanoic acid	-	-	14.88±1.19^{a}	-	28.52±2.25^{b}	0.04953	1	3.8571
Methyl hexadecanoate	Palmitic acid	1.29±0.05^{a}	28.37±1.41^{b}	107.11±1.70^{c}	35.64±2.96^{b}	52.43±3.32^{d}	0.009074	4	13.5
Methyl eicosanoate	Arachidic acid	-	-	-	-	46.53±4.67	-	-	-
	Σ SFA	102.24	51.56	240.27	292.81	291.1	-	-	-
Methyl-5*Z*,8,11*Z*,14*Z*-eicosatetraenoate	Arachidonic acid	-	-	22.21±1.76^{b}	96.40±5.75^{a}	69.91±4.67^{c}	0.02732	2	7.2
Methyl 9*Z*,12*Z*-octadecadienoate	Linoleic acid	-	-	24.52±1.86^{b}	34.90±3.53^{a}	12.70±0.64^{c}	0.02732	2	7.2
Methyl 9*Z*,12*E*-octadecadienoate	Conjugated linoleic acid	10.62± 0.29	-	-	-	-	-	-	-
Methyl- 8*Z*,11*Z*,14*Z*-eicosatrienoate	Dihomo - gamma linolenic acid (DGLA)	-	-	-	32.30±12.99	-	-	-	-
5,14,23-Octadecatrien-14,15-diol	14,15-Dihydroxylinolenic acid	-	-	-	47.62±14.49^{a}	12.44±0.42^{b}	0.01672	1	10.001
	Σ PUFA	10.62	-	46.73	211.22	95.05	-	-	-
Methyl-9*Z*-hexadecenoate	Palmitoleic acid	85.39±2.84^{a}	2.07±0.75^{d}	38.43±1.38^{c}	9.11±0.53^{b}	94.04±2.89^{e}	0.009074	4	13.5
13-Methyltetradec-9-enoate	*Myristoleic acid*	-	-	-	4.04±0.18	-	-	-	-
Methyl- 9E-octadecenoate	Ricinoleic acid	-	-	-	-	12.75±0.53	-	-	-
Methyl- 9*Z*-octadecenoate	Oleic Acid	120.84±2.89^{a}	9.74±0.27^{c}	54.92±2.31^{b}	-	20.00±2.48^{d}	0.01556	3	10.385

Methyl-11*Z*-eicosenoate	Gondoic acid	-	-	-	-	26.20±5.03	-	-	-
Methyl 6-octadecenoate	Petroselinic acid	-	12.86±0.53	-	-	-	-	-	
	Σ MUFA	206.23	24.67	93.35	13.15	152.99	-	-	-
	ΣFAs	319.09	-	380.35	517.18	539.14			
	% SFA	32.04	-	63.17	56.62	53.99			
	% PUFA	3.32	-	12.29	40.84	17.62			
	% MUFA	64.63	-	24.54	2.54	28.38			
	ω-6/ω-3 ratio	-	-	-	3.44	6.64			

Each row's means that share the same letter do not differ much, - means not detected

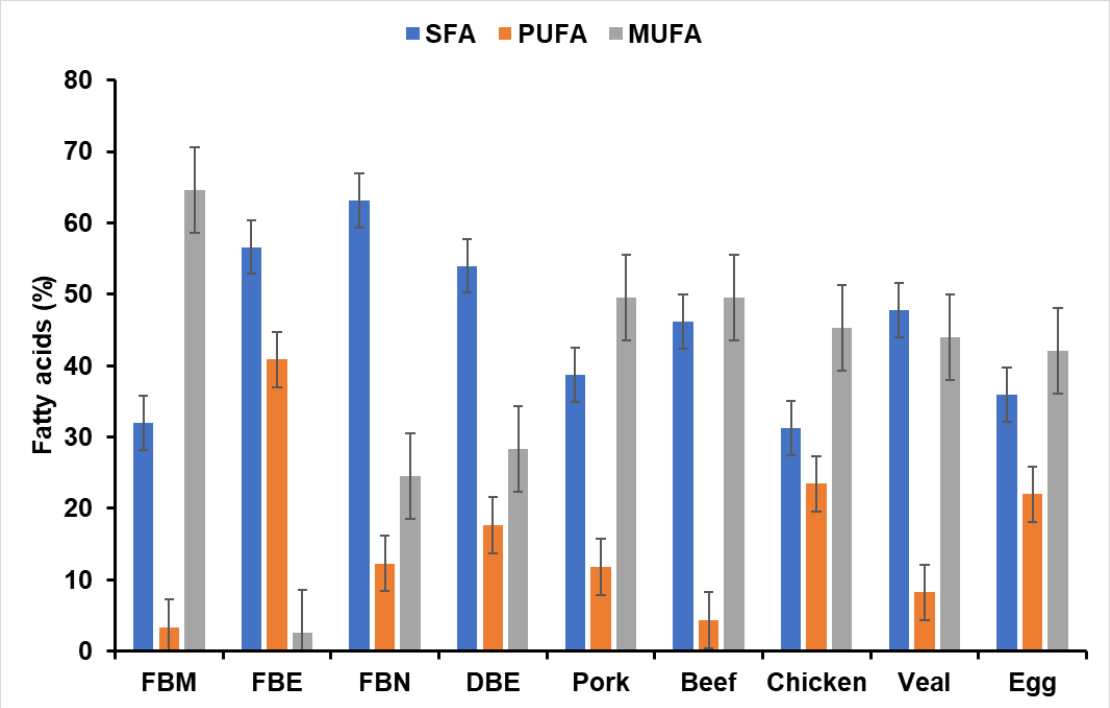

Figure 4:4: Bar chart showing comparative values of fatty acids found in beetle larvae (*C. aurata* and *O. rhinoceros*) to that of other animal and vegetable based sources (on a dry matter basis, or DM).Source: FAO/GoK (Ghosh *et al*., 2017). FB - represents *C. aurata* larvae while DB- is *O. rhinoceros* larvae. The last letter at end of FB or DB represents the site collected. The larvae of *C. aurata* from Murang'a (FBM), Embu (FBE), Nairobi (FBN) and *O. rhinoceros* from Embu (DBE). SFA – saturated fatty acids, PUFA – polyunsaturated fatty acids, MUFA – Monounsaturated fatty acids

The ratio of total fatty acids, SFA: MUFA: PUFA mirrors the patterns previously reported in *Protaetia brevitarsis* larvae (Yeo *et al*., 2013) and *O. rhinoceros* larvae (Okaraonye & Ikewuchi, 2008). Further, the detection of stearic and palmitic acids of the SFA, palmitoleic and oleic acids of the MUFAs as the abundant fatty acids ratifies similar findings from previous reports on edible beetles; *Apomecyna parumpunctata*, *O. monoceros*, *O. boas* (Thomas & Kiin-Kabari, 2022). Oleic acid is a common MUFA in living systems and is known to counteract risks of cancer, heart attack, atherosclerosis and dementia (Yeo *et al*., 2013). Stearic and palmitic acids are important ingredients in the food industry for texture and tenderness modification of products. Higher palmitic acid levels, especially in *C. aurata* from Nairobi, portends high atherogenicity due to their propensity to increase low-density lipoprotein (LDL)

cholesterol (Womeni *et al*., 2009). Despite the negative health perceptions associated with saturated fatty acids, their coexistence with unsaturated fatty acids is paramount for a synchronous complementary functionality (Akpossan *et al*., 2015).

The threshold ratio of ω-6/ω-3 ratio fatty acids were recorded for *C. aurata* and *O. rhinoceros,* which implies that the larvae could be considered as targets of optimal health benefits (Fogang Mba *et al*., 2017). However, these ratios were dependent on the detectable fatty acids from each larval species sampled from the three sites. Similar results have been reported from edible adult dung beetles like *Onthophagus seniculus*, *Copris nevinsoni*, and *Liatongus rhadamitus* (Bophimai & Siri, 2010). Disparities in the fat amounts of edible insects are dependent on many factors including dietary sources, species, location, temperature and intra-tissue differences within an organism (Manditsera *et al*., 2019; Jantzen *et al*., 2020; Thomas & Kiin-Kabari, 2022).

4.2.3.3 Mineral Composition

A total of eight minerals were detected from the two beetle larvae collected from the three sites [**Table 4.5**]. Apart from zinc, the concentrations of all minerals varied significantly (p<0.05) between the species and target location, thereby alternative hypothesis was accepted. Calcium (15.75–22.65 mg/g) and potassium (13.62–22.88 mg/g) were the most abundant mineral elements recorded in the larvae of the two beetle species. The larvae of *O. rhinoceros* from Nairobi and Murang'a exhibited considerably (p>0.05) higher values of calcium (20.42–22.65 mg/g) and zinc minerals (0.28–0.3 mg/g).

Table 4.5: Mineral composition (in mg/g of DM) of *C. aurata* and *O. rhinoceros*

Sampling Location	Larvae	Na	Mg	K	Ca	Mn	Fe	Cu	Zn
Nairobi	*C. aurata*	2.45±0.01^{c}	3.15±0.04^{d}	16.25±0.23^{c}	17.95±0.26^{bcd}	0.05±0.01^{c}	0.55±0.01^{c}	0.12±0.01^{a}	0.27±0.01^{a}
	O. rhinoceros	6.11±0.03^{a}	5.04±0.09^{a}	17.97±0.06^{b}	22.65±1.75^{a}	0.09±0.01^{a}	0.74±0.01^{a}	0.05±0.01^{b}	0.30±0.01^{a}
Murang'a	*C. aurata*	2.33±0.01^{c}	3.33±0.01^{d}	17.27±0.13^{bc}	18.83±0.19^{bc}	0.05±0.01^{c}	0.59±0.01^{b}	0.11±0.01^{a}	0.28±0.01^{a}
	O. rhinoceros	6.05±0.30^{a}	4.59±0.18^{b}	17.38±0.89^{bc}	20.42±0.83^{b}	0.07±0.01^{b}	0.74±0.02^{a}	0.04±0.01^{b}	0.28±0.02^{a}
Embu	*C. aurata*	2.50±0.12^{c}	3.29±0.04^{d}	22.88±0.26^{a}	17.43±0.36^{cd}	0.05±0.01^{c}	0.53±0.01^{c}	0.11±0.01^{a}	0.28±0.01^{a}
	O. rhinoceros	4.90±0.04^{b}	3.57±0.02^{c}	13.62±0.02^{d}	15.75±0.19^{d}	0.06±0.01^{c}	0.54±0.01^{c}	0.02±0.01^{d}	0.22±0.01^{a}
	P value	2.07e^{-07}	2.64e^{-06}	6.63e^{-06}	0.00161	0.000244	0.000244	3.7e^{-07}	0.1219845
	F value	378.4	160.8	117.9	17.51	34.3	34.3	311.2	8.69
	Df	5	5	5	5	5	5	5	5

Means are expressed as mean ±SE. Each row's means that share the similar letters do n ot differ much at p<0.05

Edible insects are reportedly credible sources of micro-nutrients (Joint & WHO, 2002; Van Huis *et al.,* 2021). The minerals found in this study had been previously detected from *Oryctes owariensis*, *H. parallela* and *Rhynchophorus phoenicis f.* (Omotoso & Adedire, 2007; Yang *et al*., 2014; Ukoroije & Bobmanuel, 2019a). The variabilities in the concentration of individual minerals detected from the larvae species may be as a result of dietary sources, age and ecotype (Paiko *et al*., 2014; Atowa *et al*., 2021). Most researchers have reported low calcium content of edible insects while alluding to their lack of mineralized skeleton (Kim *et al*., 2019), however, in this study, calcium was an abundant mineral. The high calcium content maybe attributed to their detritus nature of devouring decaying organic matter and in the process, may sequestrate calcium from the soil (Banjo *et al*., 2006). Abundance of calcium over other minerals has also been reported from larvae of long-horned beetle, *A. parumpunctata* Chev. (Thomas, 2018). In fact, the levels of calcium, iron and zinc found in this study supersedes the levels of 4.5, 1.8 and 4.6 mg/100g respectively, reported by Williams (2007) in beef.

Owing to their cheap and sustainable accessibility, beetle larvae can be better sources of micro-nutrients than conventional sources of protein. The integration of larvae meal or powder or flour in food formulations would likely contributes to 68.88%, 50.5% and 18% of the RDA for iron, zinc and calcium, respectively. Hence, these larvae can be rich candidates for combating micro-nutrient deficiency common majority of the modern populace, especially children. Iron and zinc deficiencies are the leading causes of anemia and cognitive disorders in under five years old children. These cases are rampant in areas associated with over-reliance on cereals as staple food and minimal intake of animal products (Roohani *et al*., 2013). Integrating sustainable protein sources such as the beetle larvae reported herein into cereal based staple products may be a great step towards alleviation of micro-nutrient related disorders among the undernourished population.

4.3 Gut Microbial Communities Profiling

4.3.1 Classification of Gut Microbial Communities of the Scarab Beetles

Gut microbiota represents a complex and diversified system in which thousands of microbial species dwell. These microbes particularly in dung beetles, evolve with the host and serve a significant role in the digestive systems of the insects since they rely on rigid food sources or limited nutrients (Wang *et al*., 2020; Tafesh-Edwards & Eleftherianos, 2023). For this objective, the microbial communities of two closely

related saprophagous beetle larvae were characterized to determine whether geographical location and host phylogeny had an influence on the microbial composition. Their gut microbiomes obtained from different geographical sites were determined using 16S/18S rRNA gene amplicon sequencing. After deletion of chimeras, 7969 bacterial and 703 fungal sequences remained with mean lengths of 400 base pairs. The number of bacterial sequences considerably varied between different samples, ranging from 6044 to 18978 for *C. aurata* and 10170 to 17976 for *O. rhinoceros* (**Table 4.6**). Regarding the fungal species, *O. rhinoceros* had the shortest number of the sequences (151–27564), but *C. aurata* had much longer ones (3577–100236), (**Table 4.6**). ACE (**Table 4.6**) and rarefaction curves (**Appendix 7.1)** indicated that the bacterial gut communities were adequate for a reliable comparison of the bacterial gut communities.

Table 4.6: Total number of rarified bacterial sequences and species richness of bacterial communities in both Scarabaeoid beetle larvae

Species	Collection locality	Total no. of rarefied bacterial sequences	Total no. of rarefied fungal sequences	ACE	Chao1	Shannon	Pielou
Oryctes rhinoceros	Murang'a	10170	151	300.50	300.75	5.48	0.96
O. rhinoceros	Embu	14766	5444	391.06	392.53	5.55	0.93
O. rhinoceros	Murang'a	15169	-	218.59	222.24	4.38	0.82
O. rhinoceros	Embu	17976	-	369.41	369.62	5.67	0.96
O. rhinoceros	Embu	17162	-	502.59	504.15	5.69	0.92
O. rhinoceros	Murang'a	25404	-	400.00	400.00	5.75	0.96
O. rhinoceros	Nairobi	12720	11211	418.57	418.55	5.77	0.96
Cetonia aurata	Embu	10656	25692	305.46	305.60	5.41	0.95
C. aurata	Murang'a	10690	23518	588.30	594.22	5.62	0.89
C. aurata	Embu	6044	-	302.70	303.20	5.52	0.97
C. aurata	Murang'a	30205	-	252.00	252.00	5.29	0.96
C. aurata	Nairobi	18978	100436	436.73	440.53	5.51	0.91
Geographical site effect		χ^2			7.87	2.90	7.10
		Pr(< or >F)			0.04	0.08	0.03
		Df			2	2	2
Host phylogeny		χ^2			0.33	3.30	0.56
		Pr >F			0.56	0.07	0.45
		Df			1	1	1

The total count of rarefied sequences identified in each species is provided. The ACE and Chao1 values serve as indicators of species richness. Kruskal-Wallis tests revealed significant differences in species evenness across the board. Evenness values ranging from 0 to 1 suggest that the bacterial communities are distributed evenly

Across the samples collected from the different sites, about 3871 genera level taxa were identified, representing 5 taxa of Archean and 3866 taxa of bacteria. The larvae from *C. aurata* and *O. rhinoceros* were predominated by similar phyla and genera of bacteria,

however, the relative proportions of the communities were different among the two beetle species. Among the 14 phyla found; the Firmicutes (42.10%) and Bacteroidota (32.50%) were the most prevalent in *C. aurata*, whereas Proteobacteria (35.00%), Actinobacteriota (11.40%) and Desulfobacterota (7.40%) were prominent in *O. rhinoceros* (**Table 4.7**). Unlike the host phylogeny, sampling site affected the gut microbiome relative abundance hence null hypothesis was rejected at $P<0.05$.

Table 4.7: Percentage abundance of the bacterial ASVs at the Phylum level for both species

Phylum	**(% of ASVs) *O. rhinoceros***	**(% of ASVs) *C. aurata***
Firmicutes	25.30	42.10
Bacteroidota	15.30	32.50
Proteobacteria	35.00	10.20
Actinobacteriota	11.40	9.60
Desulfobacterota	7.40	2.60
Patescibacteria	0.80	0.90
Planctomycetota	2.20	0.70
Deferribacterota	0.50	0.40
Myxococcota	0.10	0.30
Acidobacteriota	0.30	0.20
Deinococcota	0.40	0.20
Verrucomicrobiota	0.80	0.20

There were 23 classes found in the ASVs, with Alphaproteobacteria (29.60%) and Actinobacteria (8.60%) being the most common in *O. rhinoceros* compared to *C. aurata*, which had Bacteroidia (32.50%), Bacilli (22.40%) and Clostridia (19.20%) (**Table 4.8**).

Table 4.8: Percentage abundance of the bacterial ASVs at the Class level for both species

Class	***O. rhinoceros* (% of ASVs)**	***C. aurata* (% of ASVs)**
Alphaproteobacteria	29.60	4.50
Clostridia	17.50	19.20
Bacteroidia	15.30	32.50
Actinobacteria	8.60	8.40
Bacilli	7.40	22.40
Desulfovibrionia	7.40	2.60
Gammaproteobacteria	5.40	5.70
Planctomycetes	2.20	0.70
Acidimicrobiia	2.00	0.60
Saccharimonadia	0.80	0.90
Verrucomicrobiae	0.80	0.20
Coriobacteriia	0.50	0.40
Deferribacteres	0.50	0.40
Deinococci	0.40	0.20

Thermoleophilia	0.40	0.30
Desulfitobacteriia	0.20	0.00
Acidobacteriae	0.10	0.10
Blastocatellia	0.10	0.00
Desulfotomaculia	0.10	0.30
Endomicrobia	0.10	0.00
Syntrophomonadia	0.10	0.10
Vicinamibacteria	0.10	0.10

In terms of genera, *Paracoccus* > *Proteiniphilum* > *Christensenellaceae* R-7 group > *Desulfovibrio* > *Ensifer* had the highest relative abundances in *O. rhinoceros*. On the other hand, *C. aurata* had *Alistipes* > *Christensenellaceae* R-7 group > and *Bacillus* > *Enterococcus* as the most abundant groups (**Figure 4.5**). The main bacterial phyla; firmicutes, protobacteria and Bacteroidetes found in the gut tract of many insects are also present in the two beetle larvae. This agrees with the results reported from the scarab beetle larvae as the most prevalent phyla groups in their gut microbiota (Tagliavia *et al*., 2014; El-Sayed & Ibrahim, 2015).

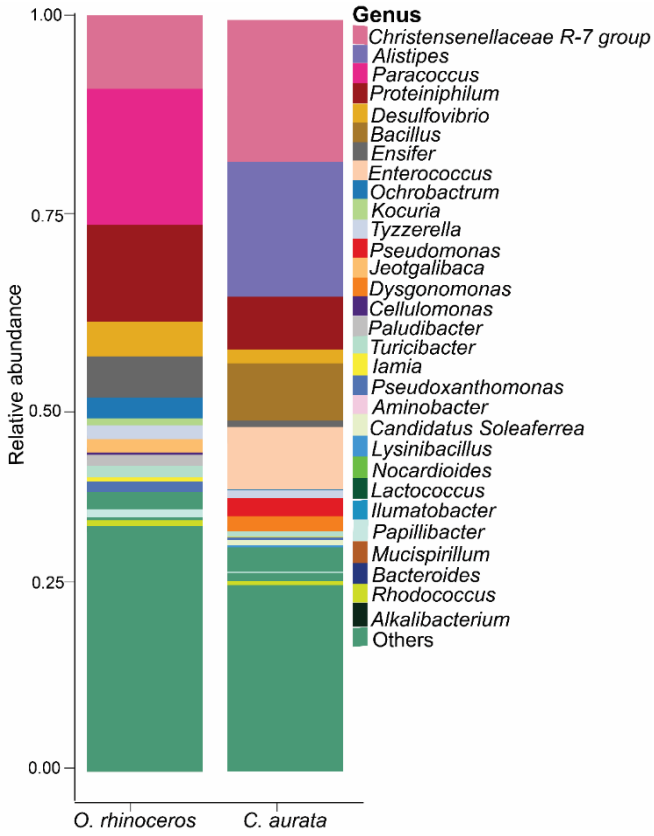

Figure 4:5: Taxonomic classification of microbial communities found in the gut of scarab beetle larvae. Bar plots representing the relative abundance of the predominant

bacterial ASVs at the genus level between the *O. rhinoceros* and *C. aurata* larvae. "Others" refers to all ASVs with an initial relative abundance below 1%

Besides the previously listed species, the presence of distinct bacterial communities was noted in sites like Nairobi that were more prevalent than the rest of the areas: *Bacillus* (36.5%) in *C. aurata*, *Turicibacter* (1.3%) and *Desulfovibrio* species (14.8%) in *O. rhinoceros*. *Dysgonomonas* (4.0%), *Candidatus Saccharimonas* (1.6%) and *Blastococcus* (2.10%) were the most prevalent in Murang'a *C. aurata* larvae (**Figure 4.6**). The larval samples from Nairobi, unlike those in the other regions, live in marshy compost piles prone to human pollution and harbored many unique bacterial species. These larvae could have evolved ontogenetically and host the many unique microbes to help them in defense, digestion or metabolic processes while in their adverse environs.

In Embu, it was *Nocardioides* (1.8%), *Ensifer* (10.2%) from *C. aurata* and *Iamia* (1.7%) from *O. rhinoceros* (**Figure 4.6**). For these allopatric sites (**Figure 4.6**) relative abundances drove the main difference instead of the existence or lack of certain microorganisms. Although previous studies suggest that there is correlation between bacterial diversity with diet, complex environs and the beetle phylogeny (Franzini *et al*., 2016; Ebert *et al*., 2021; Jácome-Hernández *et al*., 2023), differences were observed in the relative abundance of the microbes. Other insects have also reported similar outcomes like the burying dung beetles - *Euoniticellus* species (Shukla *et al*., 2016), *Heliconius erato* (butterfly) (Hammer *et al*., 2014) and dung Beetle *Copris incertus* (Suárez-Moo *et al*., 2020).

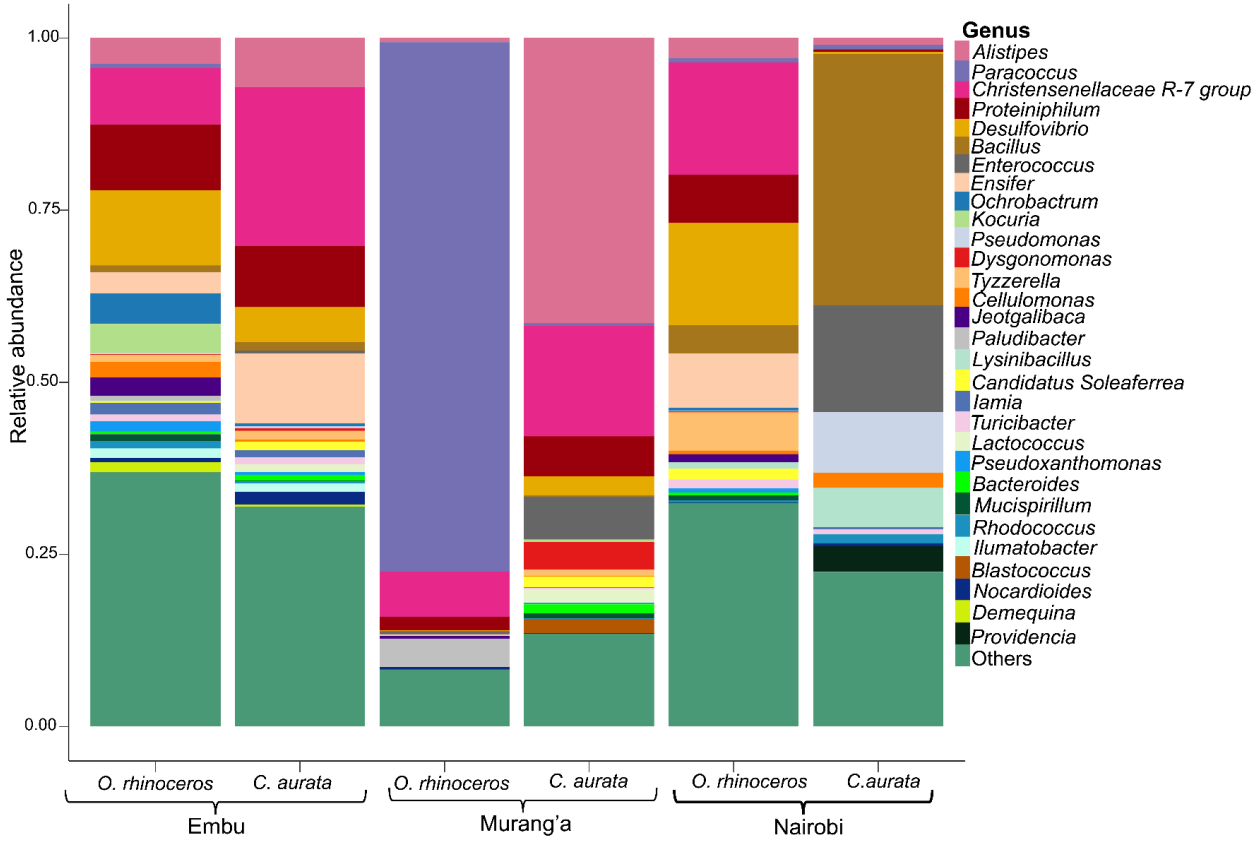

Figure 4:6: Stacked bar plots displaying the taxonomic profiles of the thirty most prevalent bacterial communities found within the guts of *O. rhinoceros* and *C. aurata* collected from the same region. Bacteria that could not be classified at the genera level were grouped under 'Others

According to the scatter dot plot (**Appendix 7.2**), the most common bacterial species in *C. aurata* were *Alistipes inops* and *Alistipes ssp*, whereas *Paracoccus denitrificans* and *Christensenellaceae R-7 group spp*. were found in *O. rhinoceros*. Although these primers were only designed to identify bacterial 16S rDNA, Archaeal rDNA had 0.001% of reads in both species with *Methanobrevibacter arboriphilus* species being the only methanogen microorganisms detected. Methanogenic archaea have been found in other beetles, millipedes, termites and cockroaches (Šustr *et al*., 2014; Tinker & Ottesen, 2016).

The fungal microbiota from the larvae were characterized from six samples by amplifying the 18S gene. A total of 94 taxa were identified, with the phylum Ascomycota accounting for nearly 99% of the total sequence reads. The phyla Basidiomycota, Chytridiomycota, and Rozellomycota accounted for the remaining sequence reads (1%) (**Table 4.9**).

Table 4.9: Percentage abundance of the fungal ASVs at the Phylum level for both species

Phylum	***O. rhinoceros* (% of ASVs)**	***C. aurata* (% of ASVs)**
Ascomycota	99.10	99.80
Basidiomycota	0.50	0.10
Chytridiomycota	0.00	0.20
Rozellomycota	0.50	0.00

The class Lecanoromycetes (92.60%) exhibited greater dominance in *O. rhinoceros* larvae, whereas class Saccharomycetes (92.60%) was more prominent in *C. aurata* larvae (**Table 4.10**).

Table 4.10: Percentage abundance of the fungal ASVs at the Class level for both species

Class	***O. rhinoceros* (% of ASVs)**	***C. aurata* (% of ASVs)**
Sordariomycetes	0.00	0.30
Saccharomycetes	6.40	92.60
Rozellomycota_cls_Incertae_sedis	0.50	0.00
Malasseziomycetes	0.50	0.00
Lecanoromycetes	92.40	4.50
Eurotiomycetes	0.20	2.30
Cladochytriomycetes	0.00	0.10
Chytridiomycetes	0.00	0.10

The most dominant Ascomycetes in *O. rhinoceros* were from the genera *Pertusaria* and *Phlyctis*, while in *C. aurata*, it was from *Spathaspora* (**Figure 4.7**).

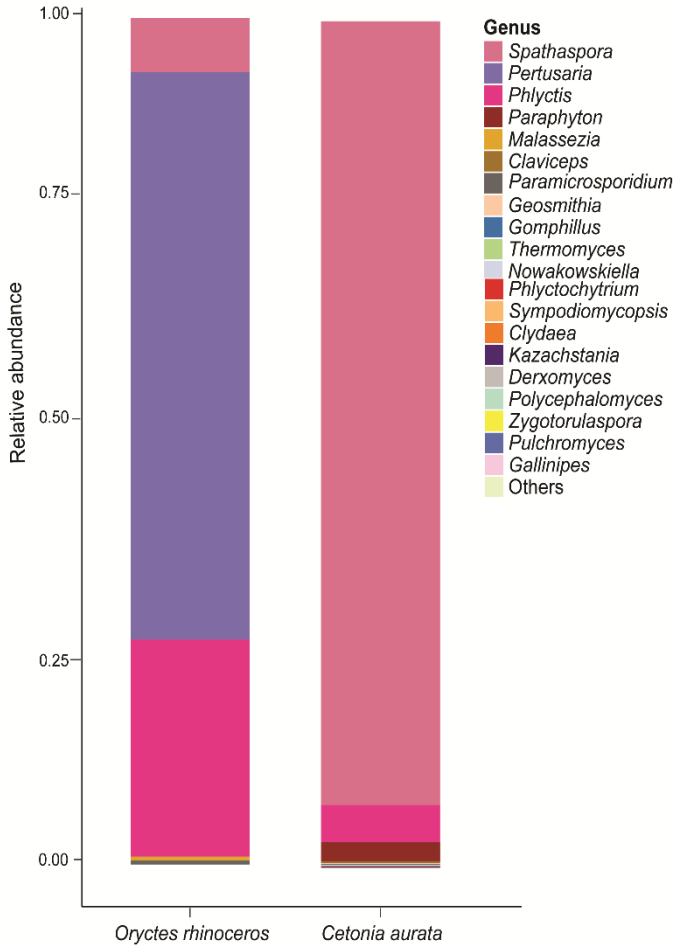

Figure 4:7: Fungal communities found within the Scarab beetle larvae gut. Plots of relative abundances of the most prevalent ASVs at the genus level for *O. rhinoceros* and *C. aurata*. The "Others" group contained fungi that could not be classified at the genus level

Similar to bacterial communities, variations in the relative richness of fungal communities at the genera level were detected at allopatric sites. The genus *Paraphyton* dominated the gut microbiota of *C. aurata* beetle larvae from Embu and Murang'a, accounting for more than 16% of the total. *Phlyctis*, a lichenized fungus dominated the Murang'a *O. rhinoceros* larvae (**Figure 4.8**). At species level, *Spathaspora boniae* dominated in *C. aurata* with 92.6% prevalence, while *Pertusaria obruta* was dominant in *O. rhinoceros* with 67%. Despite the differences in the relative abundances across the larval species, the specific shared gut microbes among the larvae were congruent.

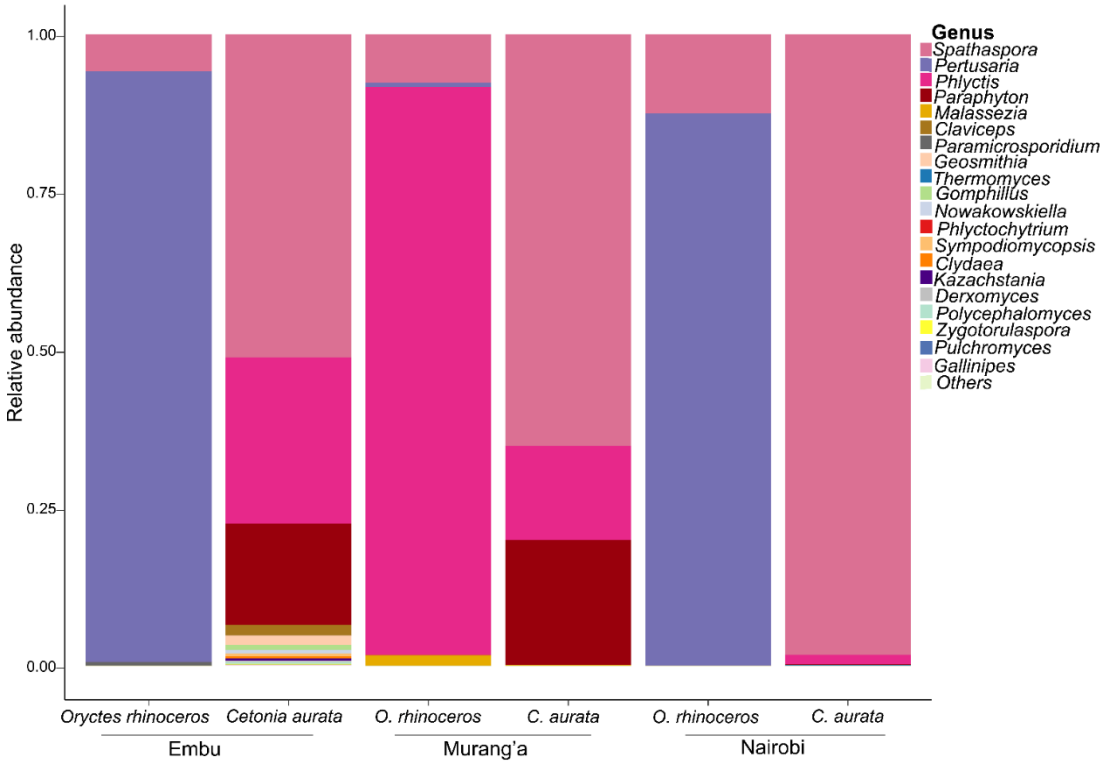

Figure 4:8: The comparative analysis of the fungal taxa groups associated with *O. rhinoceros* and *C. aurata* from the same region conducted at the genus level. The abundant fungal ASVs were displayed using stacked bar plots for each beetle species. Fungi that could not be classified at the genus level were categorized under "Others"

Few or no fungal species identified in this current study have also been a similar case in the gut microbiomes of other beetles such as the Pachysoma MacLeay desert dung beetles (Franzini, 2017). The fungi (Chytridiomycota) and yeast (Spathaspora) microbes from the insect gut microbiota break the lignin-cellulose linkages (Hou, 2012; Comeau *et al*., 2016). Yeasts and some actinomycetes also aid in the degradation of hydrolysable tannins, phenolic polymer produced by higher plants (Vega & Blackwell, 2005). Pathways involved in carbon assimilation include Leloir pathway: which involves galactose sugar degradation to biomass and energy in the presence of yeast strains such as *Candida albicans* and baker's yeast *Saccharomyces cerevisiae* (Harrison *et al*., 2022). Contrary to our results, the two strains were not present implying that other Saccharomycetes yeasts like *Spathaspora boniae* present may perform similar roles.

4.3.2 Unraveling the Diversity of Bacterial Communities

Beetle larval phylogeny had no significant effects on species richness or evenness; P>0.05, (**Table 4.6**). Analysis of *O. rhinoceros* larvae from Murang'a had a low number of observed OTUs (206), whereas those from other sites ranged from 301–545. Further, *C. aurata* (562.8) from Murang'a had a higher Chao1 value than the others, with *O. rhinoceros* (202.5) from the same region having the lowest. The samples collected from Nairobi and Embu exhibited similar species richness as compared to Murang'a ones (chi-squared=7.87, df = 2, p-value = 0.04). The Shannon index estimations yielded a range of 4.3-5.7, with no significant variations across the groups (chi-squared=6.90, df = 2, p-value=0.07). Simpson evenness scores in both species ranged from 0.8 to 0.9. Additionally, samples from Nairobi and Embu exhibited comparable species evenness but varied significantly from the Murang'a: χ^2= 8.12, degrees of freedom = 2, P = 0.03 (**Figure 4.9**, **Table 4.6**).

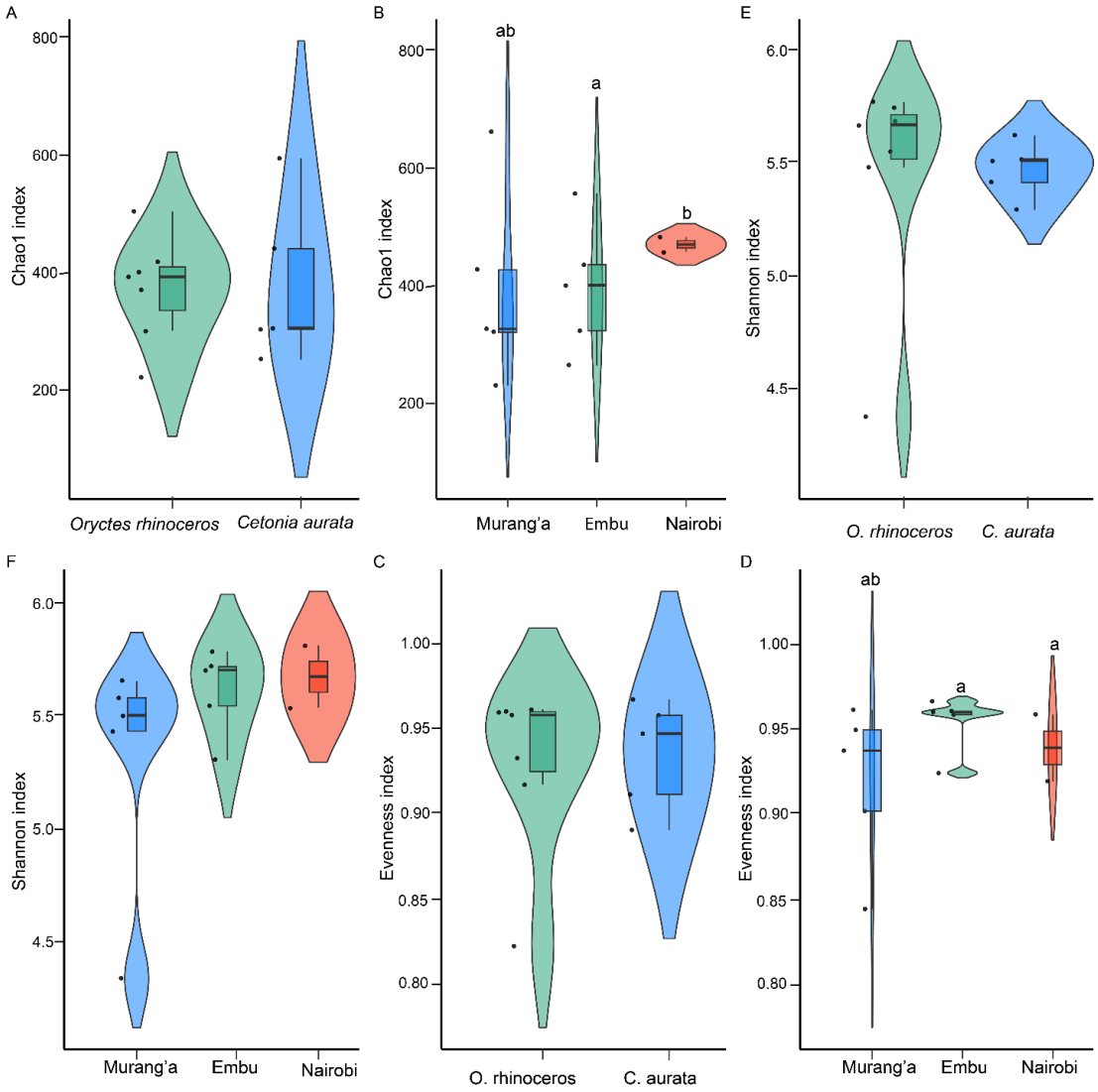

Figure 4:9: Alpha diversity in bacterial gut communities in scarab beetles collected from different sites. Chao1 richness index estimates (**4.9A, 4.9 B**), Shannon diversity index estimates (**4.9A C, 4.9A D**), and Evenness estimates (**4.9A E, 4.9 F**) for gut bacteria. Raincloud plots without letters on top are not significantly different. Raincloud plots combine an illustration of how the data is distributed (cloud) with rain which represents the jittered raw data and Boxplots

The variation in the allopatric larvae might be attributed to differences in abiotic conditions within the host geographical location, which could directly influence host phenotype. For instance, aspects of host diet such as fiber content (Friedman *et al*., 2017), salinity (Hallali *et al*., 2018) and prey diversity (Peiman & Robinson, 2012) might vary spatially by giving certain microorganisms preference over others in microbial communities. Further, temperature and humidity changes are competitive

dynamics among the gut microbes by modifying the proportions of microbial communities (Winfrey & Sheldon, 2021). Moreover, gut-specialized microbes frequently have lower thermal tolerances than their hosts or may confer distinct selection benefits to the host dependent on the temperature. Thus, these differences in the relative abundances of microbiome in the allopatric two scarab beetle larvae could be attributed to variations in vegetation cover across the three counties, which influence the composition of the dung.

4.3.3 Interspecific Variation and Geographical Site Effect on Scarab Gut Microbial Communities

Weighted UniFrac measures of diversity were used to compare the gut bacterial communities of detritivores beetle larvae, which account for the occurrence or non-existence of a specific ASV, its evolution relationship to other microbial ASVs, and the abundance of the ASVs. To illustrate comparisons of the bacterial population between the two species and in relation to geographical collection location, a PCoA based on weighted UniFrac distances was utilized. The PCoA distances, using unweighted UniFrac distances, indicated that Axis 1 contributed 22.1% of the variation, whereas Axis 2 contributed 15.4% (**Figure 4.10 A** and **Figure 4.10 B**). Here, *O. rhinoceros* had a subtle separation from *C. aurata* along axis 1 (**Figure 4.10 A**) with Nairobi and Embu having a higher degree of intra-group clustering than Murang'a resulting from the differences in their relative abundances (**Figure 4.10 B**). Furthermore, the geographic and host phylogeny effects, validated by pairwise PERMANOVA, considering Bray-Curtis distances, revealed that they did not influence the presence of the specific microbes (R^2= 0.11, P =0.05) and (R^2 =0.16, P =0.98), respectively.

Comparisons of the gut microbial community's core bacteria were done at the genus level by identifying bacterial communities with over 30% abundance at the genus level across the two larvae species. The larvae had a consistent core microbe of 21 species regardless of species (**Figure 4.10 C**). Regarding the location effect, only 16 bacterial genera were shared across all the sampling sites (**Figure 4.10 D**). The samples from Nairobi harbored 531 unique bacterial genera followed by Embu with 21 (**Figure 4.10 D**). It was revealed that a large portion of the shared taxa were anerobic, sulfate degrading bacteria from Desulfobacterota family (Desulfovibrionaceae), Alphaproteobacteria and fermentative bacteria Bacteroidetes (Dysgonomonadaceae). The presence of core bacteria between the larvae might be attributed to the fact that the

bacteria were acquired from their surroundings at sometime during their existence, regardless of whether the transmission from one generation of hosts to the next was vertical or horizontal (S˘ ípek *et al*., 2008). Moreover, the host phylogeny did not influence the gut microbiota composition.

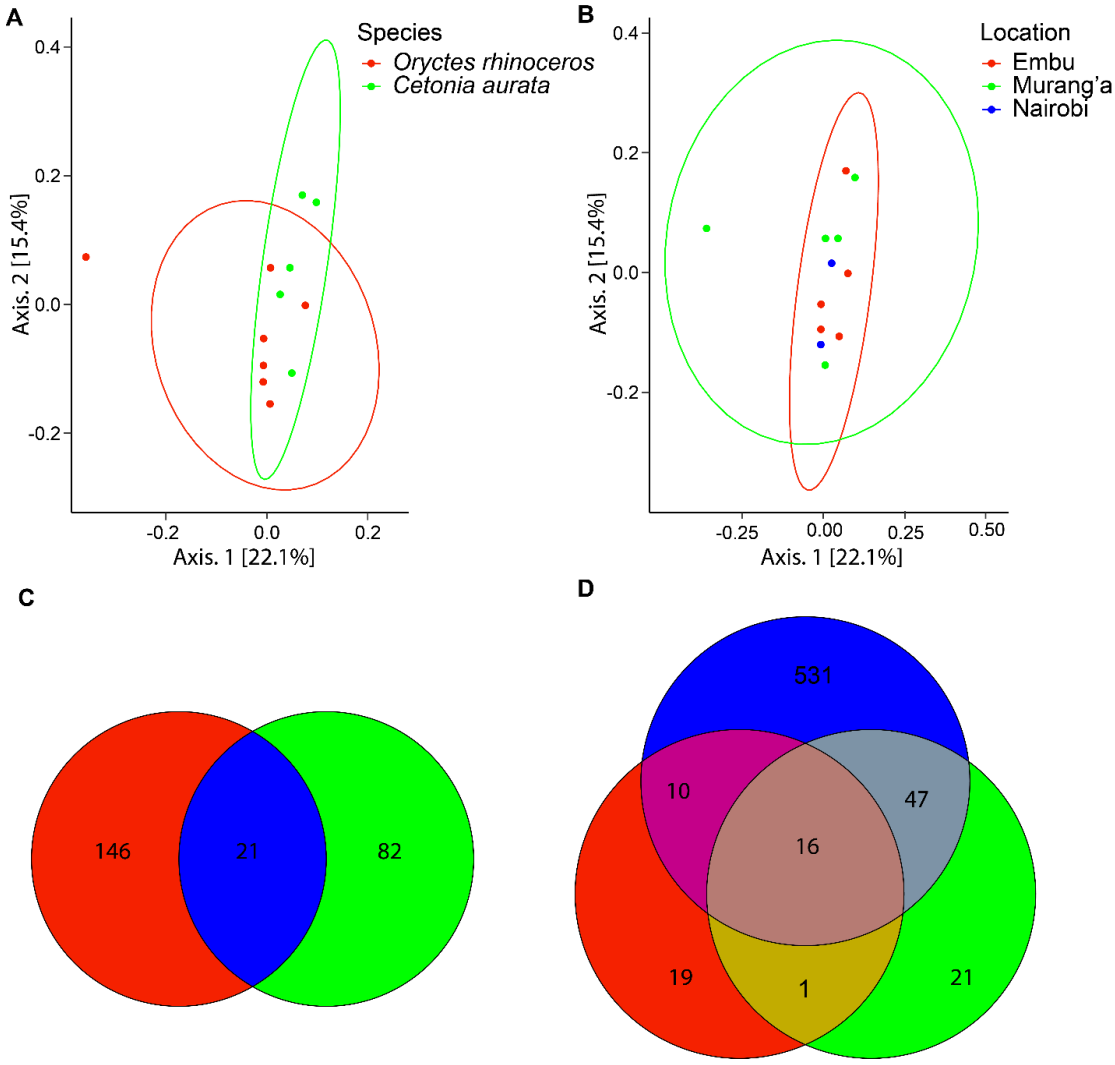

Figure 4:10: Unweighted UniFrac distance measurements in coprophagous beetle larvae between species (**Figure 4.10 A**) and with regard to location (**Figure 4.10 B**) derived from bacterial gut communities. Comparisons of the detritivores beetle larvae (**Figure 4.10 C**) and location-wise (**Figure 4.10 D**) using a Venn diagram to reveal the shared bacterial gut diversity. Values inside the Venn Diagrams indicate shared ASVs between the species and location wise

4.3.4 Functional Analyses of the Classified Microbes

4.3.4.1 Functional Role in Waste Management and Bioremediation

From the predicted PICRUSt2 results, the functional analysis of the gut microbiota revealed more abundant pathways at primary levels like; generation of precursor metabolites, biosynthesis, assimilation/degradation/utilization and energy. Carbon and energy pathways that were highly expressed included protocatechuate degradation, lactose degradation, fermentation of pyruvate and the phosphate pentose along with processes such as fermentation, glycolysis, and the tricarboxylic acid (TCA) cycle.

The variety and complexity of insect-bacteria interactions provide significant possibilities for biotechnological applications. Functional analyses of the dung beetle larvae in this study showed that the identified microbial communities had various metabolic functions valuable to the host. For instance, the prevalent presence of cellulase-producing strains within families like Bacillaceae, Bacteroidetes, Clostridiaceae, Christensenellaceae and Pseudomonadaceae underscores their crucial contribution to breaking down lignocellulosic biomass (Chouaia *et al*., 2019). This is chiefly relevant in the setting of rapid urbanization and population growth, alongside inadequate domestic waste management, which leads to uncontrolled waste generation and accumulation, increased greenhouse gas emissions and accumulation, especially in low-income countries (Ferronato & Torretta, 2019). The prevailing waste management strategies are neither environmentally eco-friendly nor economically sustainable (Zhang *et al*., 2022). However, beetle gut microbes perform complex metabolic processes on lignocellulosic material offer a glimmer of hope. *Bacillus* species, *Pseudomonas mosselii* and the putative symbiont *Proteiniphilum* have known lignocellulosic biodegradation activities as previously reported in other insects (Mabhegedhe *et al*., 2016; Shelomi *et al*., 2019; Shelomi & Chen, 2020; Ali *et al*., 2023). Notably, the TCA and protocatechuate degradation pathways were more expressed in the beetle larvae from Nairobi County that actively feed on green composting trash, highlighting their utility as bioreactors for lignocellulose degradation in domestic waste.

Regarding the nitrogen fixation process, metabolic pathways associated with amino acid uptake in bacteria such as aspartate and asparagine biosynthesis, glutamate and glutamine biosynthesis, lysine biosynthesis, threonine metabolism, and glycine betaine degradation pathways, were identified. Other pathways that aid in nitrogen fixation

include myo-inositol degradation, formaldehyde assimilation, and purine and pyrimidine pathways. Fatty acid metabolism pathways such as lipid biosynthesis also play a significant role in supplying precursors known for symbiotic nitrogen fixation.

Super pathways such as demethylmenaquinol-6 biosynthesis II, Entner-Doudoroff pathway among others were also observed. All these categories were distributed among the saprophagous beetle larvae (**Appendix 7.3**). A considarable difference (P<0.05) was found in the following KEGG pathways; *C. aurata* microbiota had a higher abundance in LACTOSECAT-PWY, PWY-2941, PWY-6470 while *O. rhinoceros* was more enriched in P184-PWY, PWY-5505 andPWY-7090 (**Figure 4.11**).

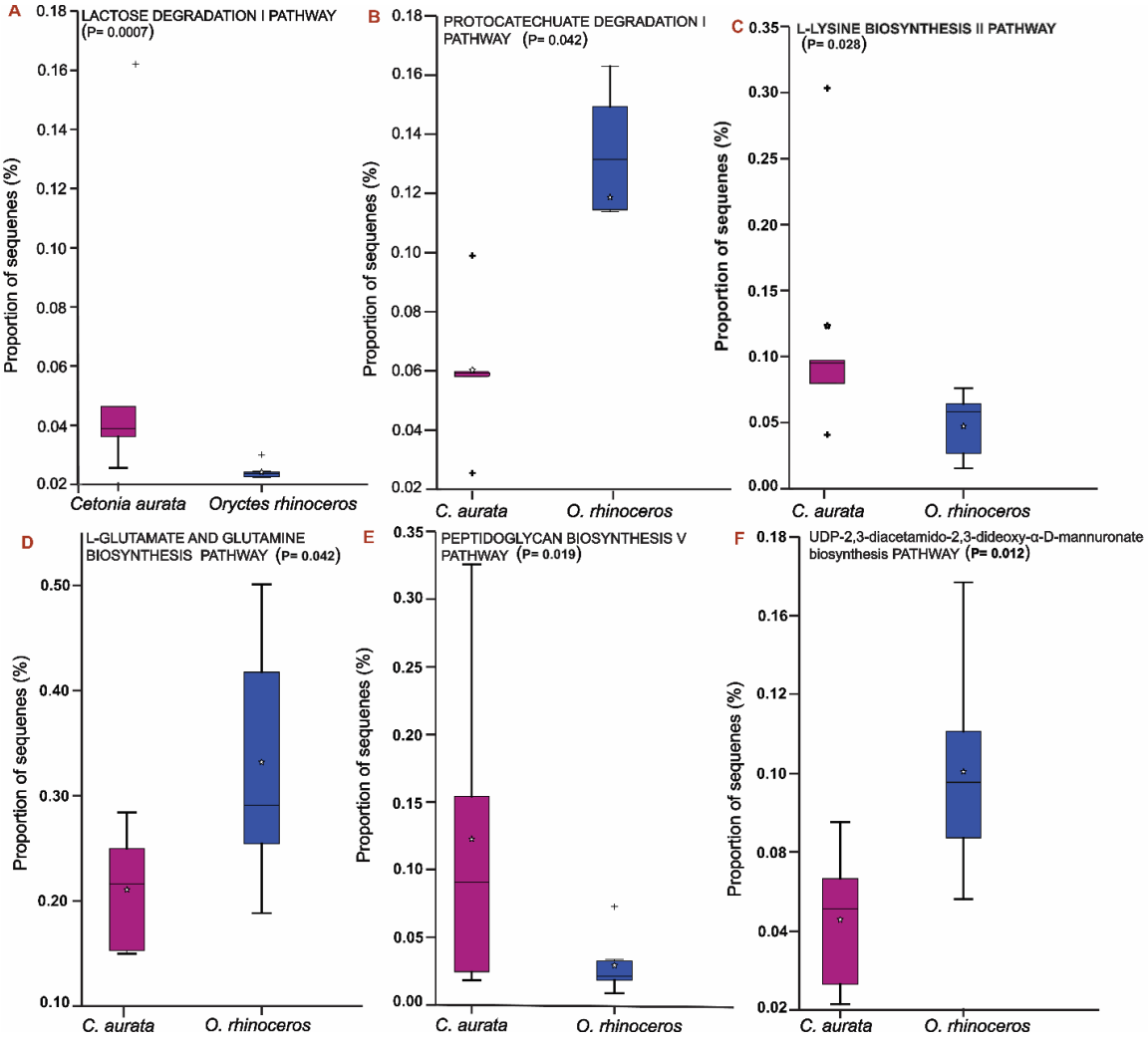

Figure 4:11: Box plots showing the significantly different KEGG pathways between *C. aurata* and *O. rhinoceros* larvae. *C. aurata* had a higher proportion of sequences in lactose degradation I (**Figure 4.11 A**), L-lysine biosynthesis II (**Figure 4.11 C**) and

peptidoglycan biosynthesis V (**Figure 4.11 E**); while *O. rhinoceros* had a higher proportion of sequences in protocatechuate degradation I (**Figure 4.11 B**), L-glutamate and L-glutamine biosynthesis (**Figure 4.11 D**) and UDP-2,3-diacetamido-2,3-dideoxy-α-D-mannuronate biosynthesis (**Figure 4.11 F**)

In nitrogen-limited environments, biological nitrogen fixation is performed by diazotrophs, while auxotrophic hydrocarbon-degrading bacteria rely on them to provide essential nutrients. This synergistic mechanism helps increase the degradation rate of pollutants (Chaudhary *et al.*, 2019). The presence of nitrogen-fixing pathways in both hydrocarbon-degrading bacteria (Gammaproteobacteria) and diazotrophs (Bacillus and Clostridium) is notable. This supports the use of larval microbiota in pollutant degradation in nitrogen-limited environments, such as farmland soil contaminated with persistent organic pollutants (POPs). Organochlorine pesticides like dichlorodiphenyltrichloroethane (DDT) and benzene hexachloride (BHC) use in agriculture have contributed significantly to increase in food production. Even though their use was banned over 45 years ago, they pose a threat to human healthiness and food security due to their lipophilicity, low degradation rates and ability to bioaccumulate in food chain (Burgos-Aceves *et al*., 2021). To reduce environmental pollution due to POPs, a biological and non-chemical approach like understanding the biochemical metabolic pathways in microbes in order to design bioremediation strategies can be exploited.

Under anaerobic conditions, denitrifying, Sulphur and carbonic degraders prevail against methanogens. Sulfate reducing microbes are versatile and can use wide electron acceptors such as metals, sulfates and organic compounds with halogen groups (Villemur *et al*., 2006). One the Desulfobacterota bacteria has been documented to be capable of de-halogenating benzene compounds in presence of a hybrid metallic catalyst (Baxter-Plant *et al*., 2004). Further, Pannu and Kumar (2017) and Tran *et al.* (2022) reported decomposition of dioxin, pentachloronitrobenzene and lindane in the presence of Bacillus, Gammaprotobacteria, Clostridia, Actinobacteria and Alphaprotobacteria. Microbial remediation is a green, sustainable and nature-based waste management process that leverages microbes' ability to degrade organic pollutants. Introducing specific microbes to polluted soils or environments could help reclaim them.

4.3.4.2 Functional Role of Gut Microbiota for Food/Feed and as Targets for Bio-Therapeutic Interventions

Presently, there is a growing consumer interest in healthier food options aimed at maintaining wellbeing of the population. By 2029, this shift towards wellness is anticipated to elevate the probiotics segment within functional foods, projecting an estimated market value increase to USD 105.7 billion (Market and Market, 2024). The incorporation of microorganisms into foods not only presents significant technological benefits but also offers therapeutic advantages, underscoring their holistic role in advancing food science and health. On the other hand, *Bacillus* species exhibit remarkable resilience by thriving under adverse conditions, including the gastrointestinal tracts of various organisms other than insects, due to their capacity to widely sporulate (Piewngam *et al*., 2018). This resilience positions them as fascinating targets for probiotic research in functional foods field.

Synergistic effects observed from combining diverse *Bacillus* strains enhance the production of functional metabolites leading to the conservation of gut homeostasis in hosts (Lu *et al*., 2024). These functional metabolites, when accumulated through *in vitro* fermentation and subsequently utilized *in vivo*, present enhanced benefits (Barros *et al*., 2020; Nataraj *et al*., 2020). Consequently, *C. aurata* larvae emerged as a promising reservoir of diverse *Bacillus* strains that could be advanced for probiotics research in nutrition. Furthermore, these larvae hold potential as prebiotics to supplement the nutritional profile of livestock such as pigs, chickens, and fish. The escalating unsustainability in the rearing of these animals, exacerbated by the pervasive use of medications and the looming threat of AMR, underscores the significance of exploring alternative nutritional strategies (Hoseinifar *et al*., 2024). Moreover, in the management of intestinal diseases, probiotics aid in regulating the intestinal microbiota and alleviating inflammation. Recent research involving the synergistic effect of probiotics containing *Lactococcus* and *Enterococcus* bacterial strains found that they had an inhibitory effect on intestinal colitis in mice induced by *Citrobacter* (Naveed *et al*., 2024). Leveraging *C. aurata* larvae as a prebiotic source could offer a sustainable solution, mitigating reliance on antimicrobials and enhancing the nutritional management of livestock.

A new generation probiotic organism, the Christensenellaceae group, also identified in this study was initially identified in healthy human feces and recently isolated from

Coconut rhinoceros beetle (*O. rhinoceros*) and Japanese beetles (*Popillia japonica*) (Chouaia *et al*., 2019; Han *et al*., 2024). The Christensenella family encompasses commensal bacteria with transmissible properties that exhibit shared interactions with other transmissible microbes. This group has been shown to help in the management of metabolic diseases, including obesity, and diabetes, by counteracting microbiome dysbiosis and altering the metabolism profile of the host. Microbial dysbiosis, characterized by a decrease in beneficial bacteria, is associated with metabolic disorders and contributes to higher mortality rates from these diseases (Ang *et al*., 2023). To preserve the balance of the host's gut microbiota, isolating the Christensenellaceae group from scarabaeoid larvae mighty present a promising option for novel biotherapeutic approaches either through oral administration as a probiotic or fecal microbiota transplantation.

Other microbes reported with probiotic activity are *Alistipes inops* and *Alistipes ssp* previously isolated from human microbiome/fecal matter not insects (Parker *et al*., 2020). Despite being reported in our present investigation, they may be facultative symbionts in insects since the dung from each county included mixed fiber dietary items such as legumes and whole grains, which are known sources of these bacteria.

4.4 Biomolecules Extraction and Characterization

4.4.1 Antibacterial Screening

The antibacterial evaluations of all the mixed crude culture extracts against the four strains of bacteria were assessed by checking diameters of inhibition around the seeded discs after one day of incubation. Endozoic fungi isolated from *O. rhinoceros* exhibited greater antibacterial activity compared to those from *C. aurata* (**Table 4.11**). The extracts of mixed fungal cultures (**Appendix 7.4**) from different sites demonstrated different antibacterial activities against all four tested strains. *B. subtills* and *E. coli* were found to be more susceptible as compared to the other strains whereas only one extract demonstrated activity against *p. aeruginosa* and *S. aureus* (**Table 4.11**). *Bacillus subtills,* being a gram-positive bacterium was more susceptible to the fungal extracts which agrees with study done by Wani *et al*. (2020).

The positive control; Streptomycin portrayed the highest activity as shown in **table 4.11** and **Appendix 7.5**. Scarab beetle larvae spend their whole lives in dung which contains pathogenic microbes released from indigestible material excreted by mammals'

gastrointestinal tract (Thiyonila *et al.,* 2018). Some colonies of microbiota obtained from the oral discharges of the bark beetle; *Dendroctonus rufipennis* were demonstrated to significantly inhibit the development of antagonistic fungi (Hernández-García *et al*., 2017). These symbiotic relationships could be key in safeguarding either the insect host or its nutritional supplies from predators and parasitoids by producing secondary metabolites.

Table 4.11: Comparing antibacterial activity of standard streptomycin with mixed fungal crude extracts obtained from Embu, Murang'a and Nairobi

Fungal crude extracts (20 mg/µl)		**Zones of inhibition (mm) Bacterial strains**			
		E. coli	***B. subtilis***	***P. aeruginosa***	***S. aureus***
Nairobi	*O. rhinoceros*	-	9.74±0.34^{bc}	-	-
Murang'a	*O. rhinoceros*	-	10.37±0.45^{b}	-	-
Embu	*O. rhinoceros*	-	7.67±1.09^{a}	-	-
Embu	*O. rhinoceros*	11.86± 0.48^{a}	8.21±0.70^{a}	-	7.68±0.49
Embu	*O. rhinoceros*	10.23±0.69^{b}	-	-	-
Nairobi	*O. rhinoceros*		9.82±0.72^{bc}	-	-
Murang'a	*O. rhinoceros*	9.64±0.56^{b}	-	8.82±0.15^{a}	-
Nairobi	*C. aurata*	8.54±0.47^{c}	20.61±1.57^{d}	-	-
Murang'a	*C. aurata*	-	20.26±1.01^{d}	-	-
Embu	*C. aurata*	-	11.14±0.17^{b}	-	-
Nairobi	*C. aurata*	8.78± 0.29^{c}	19.79±0.49^{d}	-	-
Streptomycin (1 mg/µl)		24.55±1.17^{d}	24.34±1.34^{e}	29.45±1.98^{b}	20.94±0.85

20 µL of extract, 24 hours of incubation, and 37°C are the parameters used. The dash (-) denotes the absence of activity

The mixed fungal culture of *O. rhinoceros* from Kairi-Murang'a, exhibited activity against gram-negative bacteria and was selected for sub-culturing. Fifteen pure fungal (**Appendix 7.6**) cultures were obtained from this process and were subjected to preliminary antibacterial screening. From the screening results, the means of the zones of inhibition across the extracts did not vary significantly ($p>0.05$) except for fungal culture 12, which showed significantly higher activity against *P. aeruginosa* (**Figure 4.12 C**) compared to the others ($p<0.05$). Streptomycin demonstrated significantly different activity than all the extracts ($p<0.05$) (**Figure 4.12**). Fungus 12 was chosen for mass cultivation because the extract demonstrated rapid growth and showed better susceptibility results against the tested bacteria.

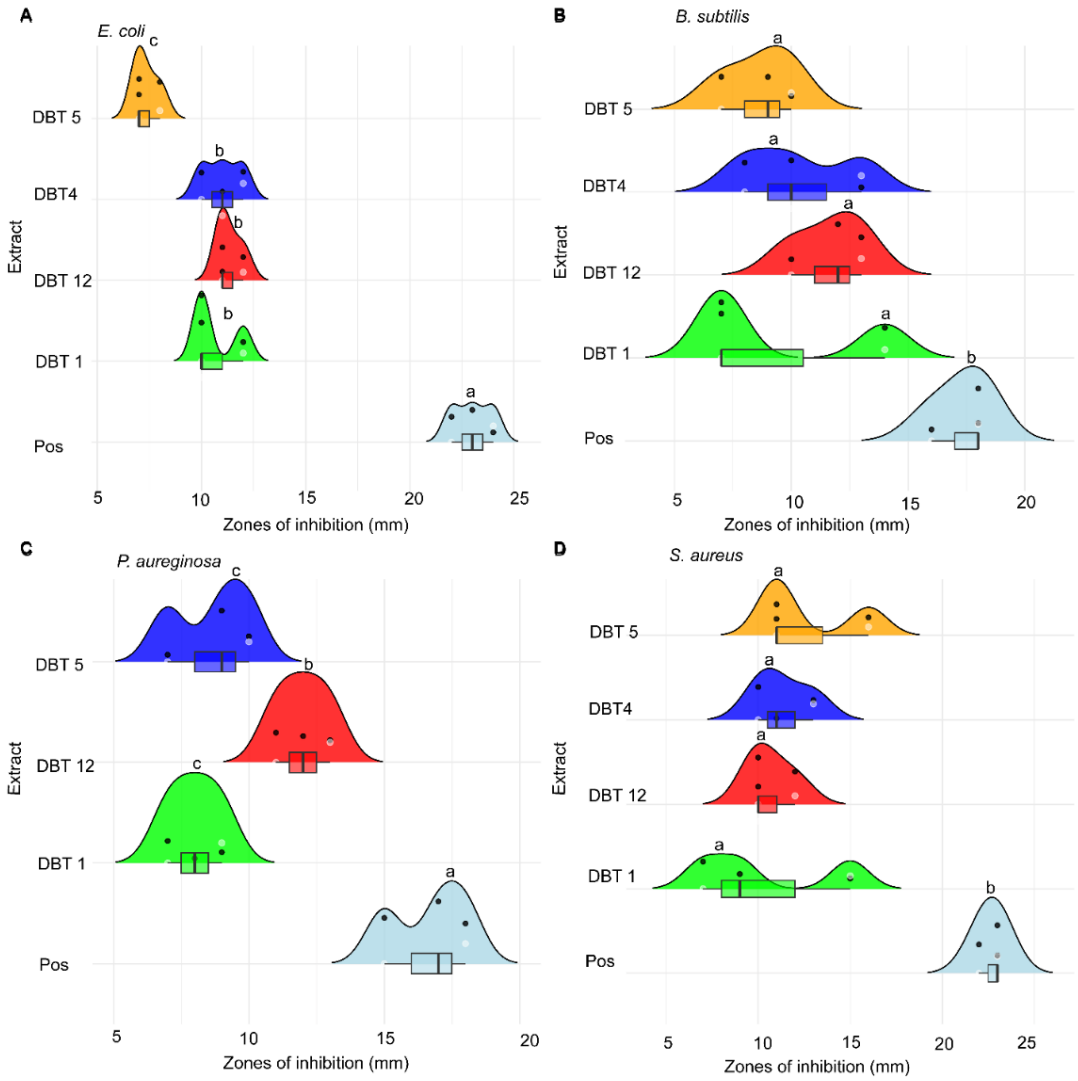

Figure 4:12: Raincloud plots displaying the zones of inhibition for four selected endophytic fungal extracts from *O. rhinoceros* against *E. coli* (**Figure 4.12 A**), *B. subtilis* (**Figure 4.12 B**), *P. aeruginosa* (**Figure 4.12 C**), and *S. aureus* (**Figure 4.12 D**). Rainclouds marked with the similar letters at the top designate no variations ($p > 0.05$)

4.4.2 Fungal Identification

The fungus grew rapidly in clumps on modified PDA media initially appearing white with light yellow mycelia during the first four days, then shifting to brown, and finally black when fully developed. The spores or conidia were produced in chains and formed a powdery layer on the surface of mature colonies making them appear as if suspended above the fungus (**Figure 4.12 B**). The bioactive fungus was identified at the species level using ITS1-5.8S rRNA gene as *Aspergillus welwitschia*. The nucleotide sequence

obtained after sanger sequencing was deposited at NCBI GenBank with the accession number PP738978.1.

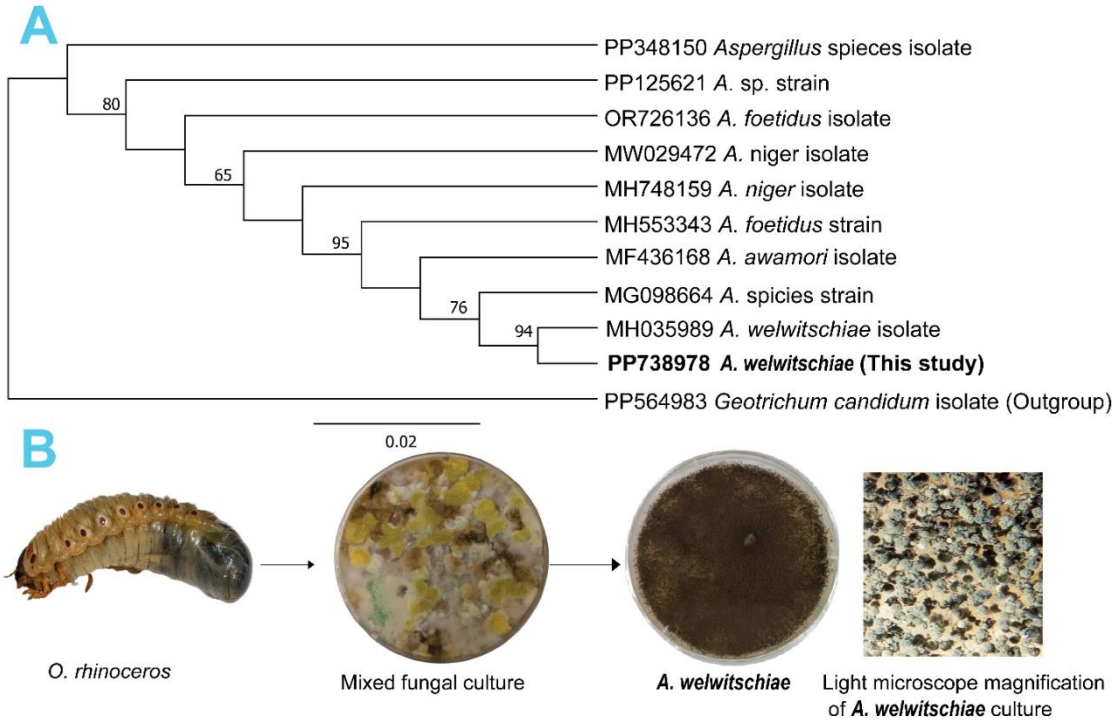

Figure 4:13: Utilizing the maximum likelihood method, a phylogenetic tree (A) was created utilizing the sequences of the ITS gene. Beside each branch is the percent fraction of trees in which the related species grouped together during the bootstrap analysis (1000 repetitions). The branch lengths in the scaled representation of the tree indicate how many substitutions there are at each place. An outline (B) showing how the *A. welwitschia* fungus originated

4.4.3 Antibacterial Activity of *A. welwitschia* Fungus Extracts'

The antibacterial results revealed that the EtOAc extract from *A. welwitschia* showed noticeably different activity ($p<0.05$) compared to the crude and aqueous fractions

(**Figure 4.14**). *E. coli*, a gram-negative bacterium was more vulnerable to this extract as compared to the other strains (**Figure 4.14**).

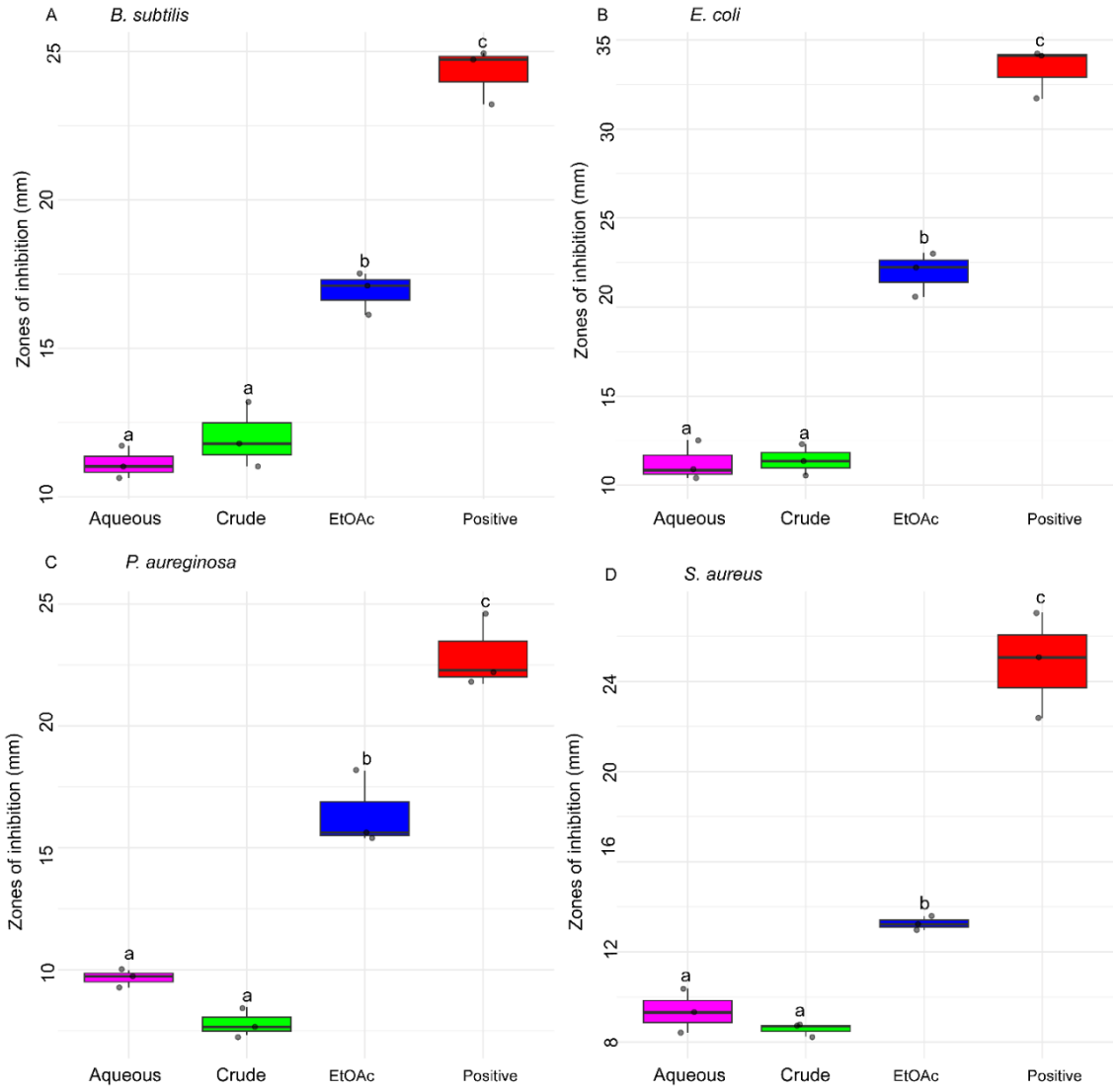

Figure 4:14: Boxplots showing antibacterial potency of crude extract, EtOAc, and aqueous fractions against *E. coli* (**Figure 4.14 A**), *B. subtilis* (**Figure 4.14 B**), *P. aeruginosa* (**Figure 4.14 C**), and *S. aureus* (**Figure 4.14 D**). Boxplots with distinct letters on top are significantly varied at ($p<0.05$)

From the dose-dependent assay, it was evident that 13 mg/mL was not the lowest inhibitory amount for the extract as it still demonstrated activity against all four strains (**Figure 4.15**). The 100 mg/mL dose of the EtOAc fraction exhibited similar activity to the streptomycin positive control (**Figure 4.15 D**).

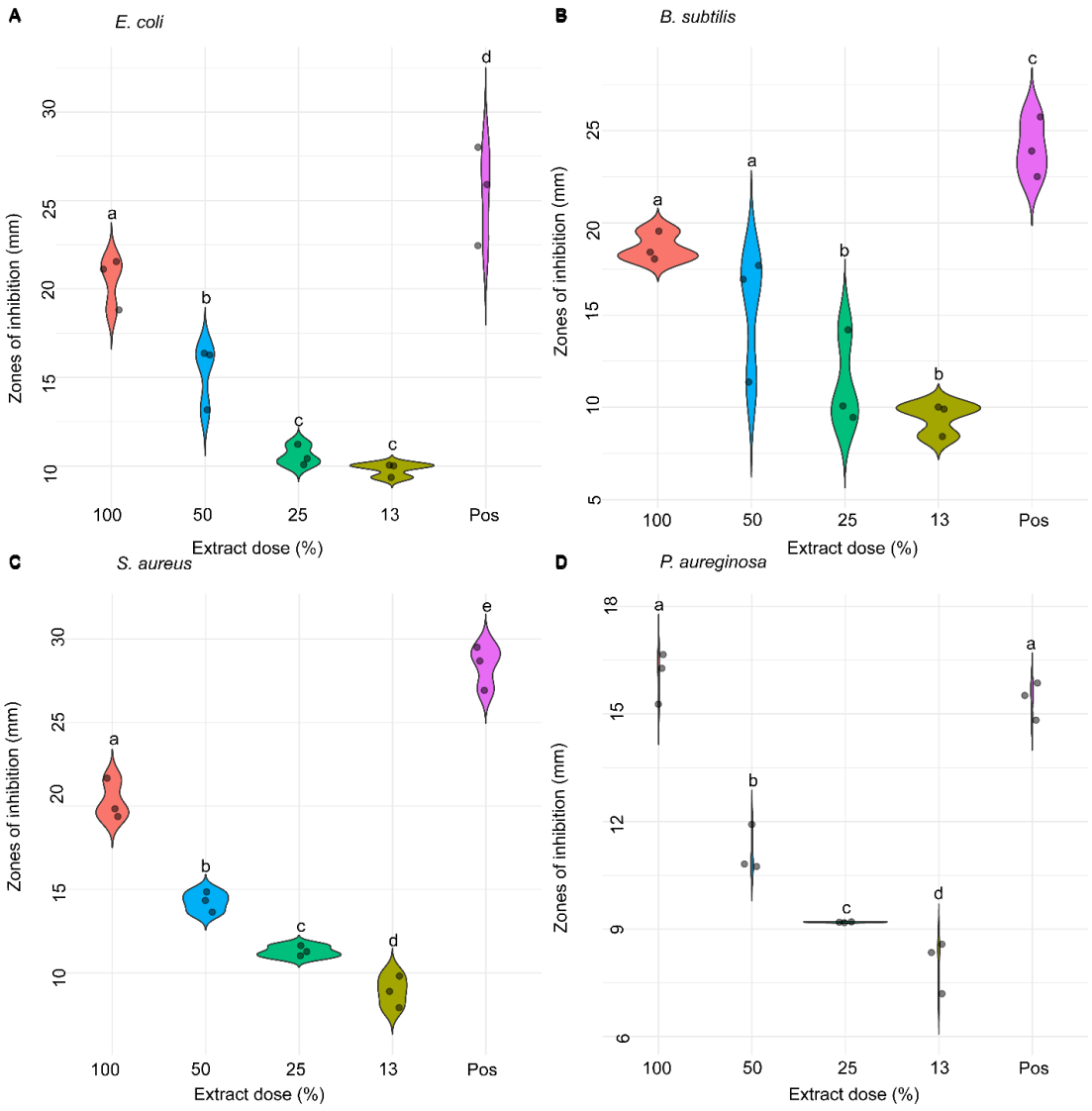

Figure 4:15: Jittered violin plots displaying antibacterial activity of EtOAc fraction against *E. coli* (**Figure 4.15 A**), *B. subtilis* (**Figure 4.15 B**), *P. aeruginosa* (**Figure 4.15 C**), and *S. aureus* (**Figure 4.15 D**). Violin plots with disparate letters on top were considerably varying at $p<0.05$. The highest dose applied was 100 mg/mL and the lowest was 13 mg/mL

4.4.4 Spectroscopic Analysis

Compounds **1- 4** were obtained as brown -yellow amorphous powder from ethyl acetate extract PDA extracts of *A. welwitschia* through semi-preparative HPLC. The LC-MS profile of the EtOAc extract from *A. welwitschia* revealed four major peaks eluting between the 15th and 21st min. The peak eluting at 15.27 min had an [M+H] of 287.1; the one at 17.97 min had $[M+H]^+$ of 358.2; and the peaks at 19.28 and 20.99 min both had an [M+H] *m/z* of 571.2 (**Appendix 7.7**). The molecules exhibited longer UV maximum wavelength due to presence of auxochromes (hydroxyls, methyls) conjugated with a π - electron system (**Appendix 7.8 C and Appendix 7.9 C**).

Compound **1** was obtained as a brown-yellow powder with ESI-MS at *m/z* = 287.1 $[M+H]^+$ (calcd. 287.09) with the molecular formula as $C_{16}H_{14}O_5$. The ^1H and ^{13}C NMR chemical shifts, as displayed in **Table 4.12**, reveal features such as meta-coupling of benzene protons located at H-7 (δ_H = 6.40, dd, J = 2.2 Hertz) and H-9 (δ_H = 6.59, dd, J = 2.2 Hz) (**Appendix 7.10**). These spectra also indicated the presence of one methyl and two methoxy groups. The analysis of the ^{13}C NMR spectrum showed 13 sp^2 hybridized carbon signals, including one at a carbonyl carbon (δ_C = 182.8) (**Appendix 7.11**). The correlations of HMBC demonstrate interactions from H-7 with carbons; 6 (δ_C = 159.0), 8 (δ_C = 161.4), and 9 (δ_C = 97.9); proton 9 with carbons; 7 (δ_C = 97.0), 8, 10 (δ_C = 105.8), and 13 (δ_C = 104.8); and proton 3 (δ_H = 6.26) with carbons; 2 (δ_C = 161.4), 2-Me (δ_C = 20.4), and 12 (δ_C = 108.7). Additionally, the two methoxy groups (δ_H = 3.97 at 6-OMe; δ_H = 3.92 at 8-OMe) were linked to carbons 6 and 8, respectively, as evidenced by HMBC interactions. A methyl group at carbon 2 (δ_H = 2.03, 2-Me) was also identified and verified through HMBC correlations with carbons 2 and 3 (**Appendix 7.14**). Compound 1 NMR correlations were equivalent to those reported by (Priestap, 1986; He *et al*., 2016) hence the compound was identified as rubrofusarin B (**Figure 4.16 A**).

Table 4.12: ^1H- and ^{13}C-NMR data for rubrofusarin B (600/150 MHz, in $CDCl_3$) and the reference data for carbon and proton ($CDCl_3$, 600/100 MHz) (He *et al*., 2016; Priestap, 1986)

Position	δ_C	Reference δC	δ_H (M, *J* (Hz))	Reference δ_H (M, *J* (Hz)	HMBC
2	161.4	167.1			
3	110.2	107.2	6.26 (S)	6.98 (s)	2, 4a, 2-Me
4	182.8	184.0			
5-OH	156.4	162.5			
6	159.0	160.6			
7	97.0	97.2	6.40 (d, 2.2)	6.56 (d, 2.2)	6, 8, 9
8	161.4	160.2			
9	97.9	97.8	6.59 (d, 2.2)	6.38 (d, 2.2)	8, 7, 10, 5a,
10	105.8	100.9	6.87 (s)	5.98 (s)	8,9,5a
10a	158.2	153.2			
4a	108.7	104.2			
5a	104.8	108.3			
9a	141.1	141.0			
2-Me	20.4	20.4	2.50	2.35	2, 3
6-Ome	55.8	55.9	3.97 (s)	3.91 (s)	6
8-Ome	55.4	55.2	3.92 (s)	3.99 (s)	8

Compound **3** had the molecular formula of $C_{32}H_{26}O_{10}$ based on the ESI-MS peak at *m/z* 571.2 $[M+H]^+$ (calcd. For $C_{32}H_{26}O_{10}^+$ 571.16), requiring 20 double bond equivalents. The ^1H- and ^{13}C-NMR chemical shifts (refer to **Table 4.13**) exhibited characteristics

including two benzyl protons at H-7′ (δ_H = 6.03, doublet, J = 2.30 Hz) and H-9′ (δ_H = 6.42, doublet, J = 2.8 Hz) positioned at meta positions to each other (**Appendix 7.16**). These spectra also revealed the presence of two phenolic hydroxy groups, two methyl groups, and three methoxy groups. The analysis of the ^{13}C-NMR spectrum identified 26 sp2 hybridized carbon signals, including two carbonyl carbons (δ_C = 184.8 and 184.4) (**Appendix 7.17**), which were arranged in pairs, suggesting the compound's dimeric nature. Additionally, chemical shifts for two carbon atoms bonded to phenolic hydroxy protons (δ_C = 163.5 and 162.9) indicate that the dimer is composed of two linear 5-hydroxynaphthopyrone units.

The HMBC correlations (**Appendix 7.20**) include interactions from H-7′ with carbons;8′ (δ_C = 161.8), 9′ (δ_C = 96.5), and 13′ (δ_C = 104.6); proton 9′ with carbons; 7′ (δ_C = 97.2), 8′, 13′, and 14′ (δ_C = 140.2); and proton 3′ (δ_H = 5.97) with carbons; 2′ (δ_C = 167.8), 2′-Me (δ_C = 20.7), and 12′ (δ_C = 108.8). These correlations support the structure of a 2',5',6',8',10'-pentasubstituted naphtho-γ-pyrone. Furthermore, two methoxy groups (δ_H = 4.03 at 6′-OMe; δ_H = 3.50 at 8′-OMe) were connected to carbons 6′ and 8′ respectively, as revealed by their HMBC interactions. A methyl group (δ_H = 2.03, 2′-Me) was identified at carbon 2′, confirmed by HMBC correlations with carbos 2′ and 3′. Therefore, one half of the molecule was identified as rubrofusarin B, linked to the other monomeric unit at C-10′. Further, the NOESY correlations (**Appendix 7.21**) of proton 7′ with 8′-OMe and 6′-OMe and of proton 9′ with 8′-OMe (**Figure 4.16 B**) indicated that the rubrofusarin B was connected to the other naphtho-γ-pyrone unit at C-10′. The other part of the molecule was identical to the first one. These correlations were comparable to that reported by (Huang *et al*., 2010), hence compound **3** was identified as rubasperone B.

Table 4.13: ^{1}H- and ^{13}C-NMR data for rubasperone B (600/150 MHz, in $CDCl_3$) and compared reference (Huang *et al*., 2010) reported in literature using 400/100 MHz, in DMSO-d6

Position	δ C	δ H (M, *J* (Hz))	HMBC	Reference δC	Reference δ H (M, *J* (Hz))
2	167.9			169.2	
3	107.4	5.94 (d, 0.74)	2, 4a, 2-Me	107.0	6.11 (s)
4	184.8			184.1	
5	163.5			163.5	
6	161.7			161.7	
7	92.8	6.70 (s)	6, 8, 9	93.9	6.95 (s)
8	159.5			160.1	
9	108.7		10, 10a, 4a	107.6	
10	99.2	6.33 (s)		98.3	6.19 (s)
10a	153.5			153.1	
4a	107.0			103.7	

5a	104.3			108.0	
9a	141.0			140.3	
2-Me	20.8	2.22 (d, 0.75)	2, 3	204.4	2.21 (s)
6-Ome	56.3	4.17 (s)	6	56.6	4.08 (s)
8-Ome	56.5	3.81 (s)	8	56.8	3.84 (s)
2’	167.8			169.0	
3’	107.3	5.97 (d, 0.82)	2’, 4a’, 2’-Me	107.2	
4’	184.4			184.5	
5’	162.9			162.7	
6’	161.3			161.5	
7’	97.2	6.42 (d, 2.8)	8’, 9’, 5a’	97.0	6.53 (d, 22)
8’	161.8			161.9	
9’	96.5	6.03 (d, 2.30)	7’, 8’, 5a’, 9a’	96.9	5.95 (d, 22)
10a’	108.9			106.9	
10a’	151.3			151.0	
4a’	108.8			104.0	
5a’	104.6			108.3	
9a’	140.2			140.7	
2’-Me	20.7	2.03 (d, 0.75)	2’, 3’	20.5	2.04 (s)
6’-Ome	56.4	4.03 (s)	6’	56.6	3.93 (s)
8’-Ome	55.3	3.50 (s)	8’	55.5	3.48 (s)

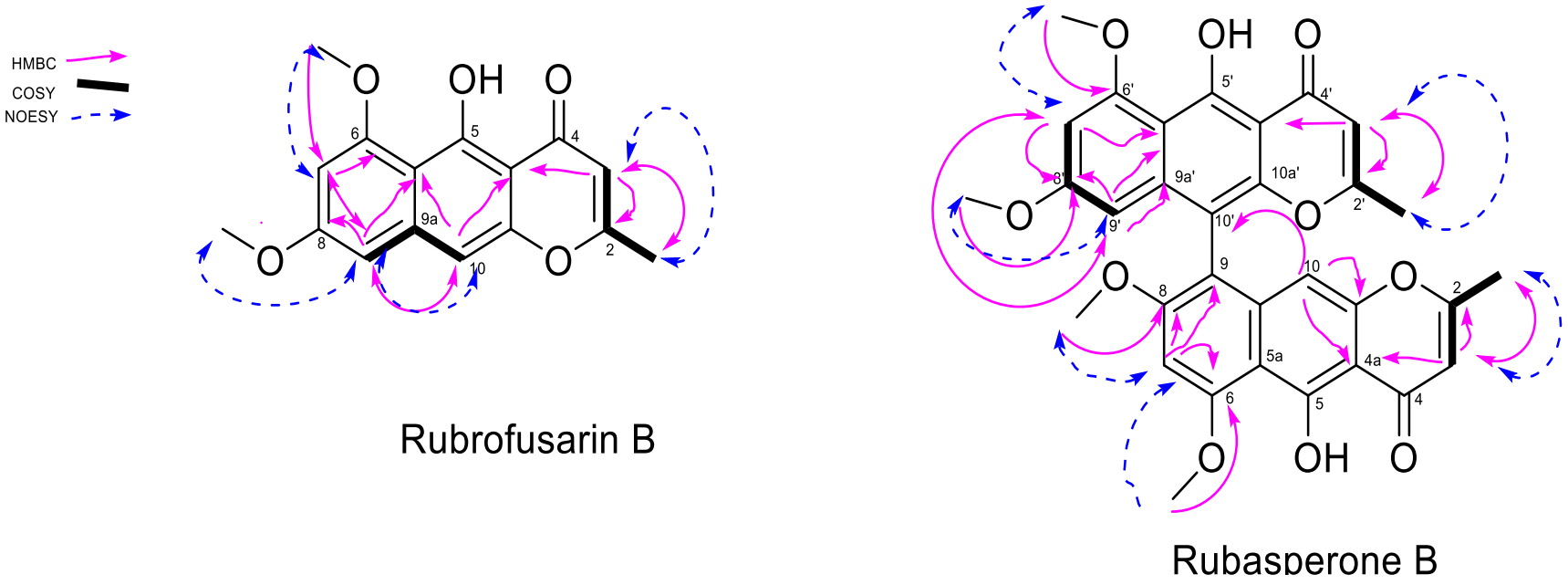

Figure 4:16: Structures of rubrofusarin B and rubasperone B isolated from *A. welwitschia*

4.4.5 Physiochemical Parameters, Pharmacokinetics, Drug lead-likeness and Antibacterial Efficacy

Molecular weight of the isolated compounds influence how they would diffuse across the cell membrane, which is crucial in drug discovery (Lipinski *et al*., 2012). Lipinski and Ghose argue that for an ideal drug candidate, the molecular weight should be below 500 g/mol and 480 g/mol, respectively (Lipinski *et al*., 2012). Although both rubasperone B and streptomycin exceed these thresholds, they demonstrate good bioavailability scores, suggesting that various parameters influence the diffusion of drug molecules. Moreover, rubasperone B and rubrofusarin B exhibited lipophilicity values below the threshold of 5 (Kathuria *et al*., 2021), potentially facilitating their passage through the lipid layers of both the inner and outer membranes of bacteria, thereby enhancing their bioactivity.

The threshold value for the total count of heavy atoms in approved drugs typically falls around 20-70 non-hydrogen atoms. Heavy atoms include the total count of non-hydrogen atoms in a molecule. These atoms affect the binding efficiency of a ligand (drug) to receptor proteins; therefore, a high binding efficiency suggests increased drug potency (Veber *et al*., 2002). Rubasperone B contained 42 heavy atoms, rubrofusarin B had 21, and streptomycin had 40, all within the range approved for preclinical drugs. Streptomycin contained zero aromatic heavy atoms, while rubasperone B and rubrofusarin B had 28 and 14, respectively. All compounds had a high count of heavy atoms, implying that they might be better ligands if targeted towards medication development. Another physiological parameter assessed was the hydrogen bond donors' and acceptors' number which affects the oral bioavailability of a drug. According to Lipinski and Veber, the ideal hydrogen donors' number should be less than five (Veber *et al*., 2002; Lipinski *et al*., 2012). Rubasperone B and rubrofusarin B were predicted to have 2 and 1 hydrogen donors, respectively, which contributed to their commendable bioavailability scores. Good bioavailability scores enhance their membrane permeability and partitioning and thus making them more plausible drug candidates. Additionally, these two molecules exhibited rotatable bonds below the recommended threshold of nine (Bojarska *et al*., 2020), which positively influences their ligand binding efficiency and bioavailability thereby enhancing their drug-likeness.

Another parameter assessed was fraction Csp3 ratio determines the carbon capacity of a molecule by correlating the number of saturated carbons to the total number of carbon atoms. For a molecule to be effectively processed and eradicated from the body, the fraction Csp3 ratio should be at least 0.42 (Wei *et al*., 2020). The fraction Csp3 value observed for rubasperone B and rubrofusarin B was 0.19, while for streptomycin it was 0.86. Streptomycin exhibited a Fraction Csp3 greater than this stipulated criterion and demonstrated superior solubility compared to rubasperone B and rubrofusarin B, which had lower values. The recorded Topological Polar Surface Area (TPSA) values were 68.9 for rubrofusarin B, 158.92 for rubasperone B and 133.78 for streptomycin. Rubasperone B and rubrofusarin B exhibited TPSA values less than 140 $Å^2$ which positively correlates with their ability to permeate cell membranes (Veber *et al*., 2002), thereby enhancing their bioavailability scores. Rubrofusarin B had a much lower value, leading to its classification as a blood-brain barrier penetrator. Remarkably, streptomycin displayed a value greater than 140 $Å^2$, indicating that relying solely on TPSA values might not be definitive for assessing the potential of therapeutic agents. Other factors should also be considered.

In terms of pharmacokinetic properties, rubrofusarin B had high GI absorption implying high oral bioavailability of this molecule via the intestines whereas streptomycin and rubasperone B showed low GI absorption. Rubrofusarin B was predicted as a BBB permeant indicating that it is largely bioavailable to the central nervous system and might be a potential drug candidate for neurological conditions such as antidepressants, antiepileptics or neuroprotective agents. Streptomycin was flagged as a substrate of P-glycoprotein (P-gp), which leads to reduced drug absorption and enhanced efflux; however, the drug encounters resistance in cells where this protein is highly expressed *(Elmeliegy et al*., 2020). Rubasperone B and rubrofusarin B were not identified as substrates of P-gp, meaning they are not easily excreted from the system, resulting in increased drug exposure and potentially increasing their therapeutic efficacy. Further, their drug-drug interactions mediated through P-gp inhibition will be minimal; therefore, combining therapy with scaffolds that are P-gp substrates is recommended.

The interaction of molecules with cytochrome P450 (CYP) enzymes is crucial during the co-administration of drugs because inhibition of one isoform can lead to alterations in drug metabolism, resulting in the buildup of the drug in the body or the production of toxic byproducts (Kirchmair *et al*., 2015). Rubasperone B inhibits only a few CYP

isoforms, indicating a lower probability of affecting metabolism when administered with other drugs, which could potentially reduce toxicity.

The synthetic accessibility scores ranged from 2.99 to 4.38. The synthetic accessibility of both rubasperone B and rubrofusarin B was low, suggesting that their synthesis process is easier due to their less complex structures. The compounds were never flagged as PAINS; therefore, utilizing them in computational chemistry assays provides potent responses across various protein targets without generating false alerts. Nevertheless, rubasperone B and rubrofusarin B triggered BRENK alerts because they contain polycyclic aromatic hydrocarbons, which suggest potential toxicity or metabolic instability (Brenk *et al*., 2008). Rubrofusarin B did not violate any rules of drug lead-likeness, whereas Rubasperone B, with a molecular weight exceeding the recommended 500 g/mol, violated one rule. This indicates potential challenges in the drug optimization process for Rubasperone B. The pKCSM predictions revealed that all three compounds were hERG II inhibitors, and only streptomycin was flagged as AMES toxic. None of the compounds were hepatotoxic, skin sensitizers, or hERG I inhibitors.

Rubasperone B and rubrofusarin B (10 µg/mL) did not exhibit antibacterial activities against the tested bacterial strains. Similar compounds extracted from *Aspergillus* species demonstrated significant different biological activities linked with their structures. It has been reported that asperpyrone naphtho-gamma-pyrones with C-10’ to C-7 linkages exhibit the highest antibacterial activity, as demonstrated by these compounds. Furthermore, the absence of electron-donating groups at C2/C2’, such as hydroxyl groups, has also been associated with high antibacterial activity. For monomers, rubrofusarin B exhibited moderate antibacterial activity due to its linear shape compared to angular naphtho-gamma-pyrones (He *et al*., 2016). Research suggests that naphtho-γ-pyrone compounds act as inhibitors of fatty acid biosynthesis in bacteria (Zheng *et al*., 2007). This pathway is crucial for bacterial cell membrane synthesis, making the enzymes involved in fatty acid biosynthesis prime targets for the development of new antibacterial agents.

CHAPTER FIVE

CONCLUSIONS AND RECOMMENDATIONS

5.1 Conclusions

I. Some of the nutraceutical properties of the larvae varied considerably between the species (radical scavenging activity, micronutrients composition, protein content, ash content) with no discernible effects across the sampling locations. The geographical site of the beetle species had a huge influence on the fatty acid composition.

II. Unlike the sharing of specific microbes, differences in relative abundances between the species and across the sampling locations were witnessed. The Alphaproteobacteria (29.60 %) and Actinobacteria (8.60 %) emerged as the predominant bacterial classes in *O. rhinoceros* larvae contrasting sharply with *C. aurata*, which exhibited a notable dominance of Bacteroidia (32.50 %), Bacilli (22.40 %) and Clostridia (19.20 %).

III. Two compounds were successfully isolated from the EtOAc fraction and characterized as rubasperone B and rubrofusarin B.

IV. By use of *in vitro* assays rubasperone B and rubrofusarin B did not possess antibacterial activities at 10µg/mL, however, SwissADME and pKCSM techniques identified as potent molecules for drug development.

5.2 Recommendations

I. The larvae of the two beetle species have the probability of serving as nutritious food and therapeutic sources. This is because larvae could substantially contribute to the daily protein requirements for adults and children. Further, the presence of phenolic compounds would boost the capacity to prevent oxidation of body molecules like lipids thereby fostering good health.

II. Metagenomics and functional predictions uncovered the mechanisms underlying cellulose and nitrogen degradation in scarabaeoids. The results suggest that the degradation of cellulose and nitrogen waste could be successfully driven by the bacterial families present in the larvae gut microbiome.

III. The compounds did not show considerable antibacterial activity, highlighting the necessity for further investigation into their biological features.

5.3 Further Studies

1. Further studies are required on protein digestibility, vitamin profile and potential allergenicity aspects of the beetle species.
2. Clearly, various factors influence the microbiome composition hence future investigations are needed to contribute to an improved understanding of variations in beetles.
3. Further isolation of the minor constituents of the EtOAc extracts should be done. Moreover, studies involving computational chemistry such as molecular docking of the compounds against enzymes like FabI involved in fatty acid membrane synthesis are recommended. This is because naphtho-γ-pyrones are known to hinder fatty acid synthesis.

REFERENCES

Ademola, O. A., Omolara, A. H., & Olatoye, R. A. (2017). Amino Acids Profile of Bee Brood, Soldier Termite, Snout Beetle Larva, Silkworm Larva and Pupa: Nutritional Implications. *Advances in Analytical Chemistry*, scientific reports, *7*(2), 31–38. https://doi.org/10.5923/j.aac.20170702.02

Akpossan, R., Digbeu, Y., Koffi, M., Kouadio, J., Dué, E., & Kouamé, P. (2015). Protein Fractions and Functional Properties of Dried *Imbrasia oyemensis* Larvae Full-Fat and Defatted Flours. *International Journal of Biochemistry Research & Review*, *5*(2), 116–126. https://doi.org/10.9734/IJBCRR/2015/12178

Ali, S. S., Jiao, H., El-Sapagh, S., & Sun, J. (2023). Biodegradation of willow sawdust by novel cellulase-producing bacterial consortium from wood-feeding termites for enhancing methane production. *Bioresource Technology*, *383*, 129232.

Alvarez-Uria, G., Gandra, S., & Laxminarayan, R. (2016). Poverty and prevalence of antimicrobial resistance in invasive isolates. *International Journal of Infectious Diseases*, *52*, 59–61.

An, J. S., Hong, S.-H., Somers, E., Lee, J., Kim, B.-Y., Woo, D., Kim, S. W., Hong, H.-J., Jo, S.-I., & Shin, J. (2020). Lenzimycins A and B, Metabolites With Antibacterial Properties From *Brevibacillus* sp. Associated With the Dung Beetle *Onthophagus lenzii*. *Frontiers in Microbiology*, *11*, 2705.

Ang, W.-S., Law, J. W.-F., Letchumanan, V., Hong, K. W., Wong, S. H., Ab Mutalib, N. S., Chan, K.-G., Lee, L.-H., & Tan, L. T.-H. (2023). A Keystone Gut Bacterium *Christensenella minuta*—A Potential Biotherapeutic Agent for Obesity and Associated Metabolic Diseases. *Foods*, *12*(13), 2485.

Ara, B., Urmi, U. L., Haque, T. A., Nahar, S., Rumnaz, A., Ali, T., Alam, M. S., Mosaddek, A. S. M., Rahman, N. A. A., & Haque, M. (2021). Detection of mobile colistin-resistance gene variants (mcr-1 and mcr-2) in urinary tract pathogens in Bangladesh: the last resort of infectious disease management colistin efficacy is under threat. *Expert Review of Clinical Pharmacology*, *14*(4), 513–522.

Atanasov, A. G., Zotchev, S. B., Dirsch, V. M., & Supuran, C. T. (2021). Natural products in drug discovery: Advances and opportunities. *Nature Reviews Drug Discovery*, *20*(3), 200–216.

Ateshim, Y., Bereket, B., Major, F., Emun, Y., Woldai, B., Pasha, I., Habte, E., & Russom, M. (2019). Prevalence of self-medication with antibiotics and associated factors in the community of Asmara, Eritrea: a descriptive cross sectional survey. *BMC Public Health*, *19*(1), 1–7.

Atowa, C. O., Okoro, B. C., Umego, E. C., Atowa, A. O., Emmanuel, O., Ude, V. C., & Ugbogu, E. A. (2021). Nutritional values of *Zonocerus variegatus*, *Macrotermes bellicosus* and *Cirina forda* insects: Mineral composition, fatty acids and amino acid profiles. *Scientific African*, *12*, e00798. https://doi.org/10.1016/j.sciaf.2021.e00798

Ausubel, F. M., Brent, R., Kingston, R. E., Moore, D. D., Seidman, J. G., Smith, J. A., & Struhl, K. (1992). Short protocols in molecular biology. *New York*, *275*, 28764–28773.

Badwaik, H. R., Nakhate, K., Kumari, L., & Sakure, K. (2018). Oral Delivery of Proteins and Polypeptides through Polysaccharide Nanocarriers. In *Polysaccharide-based Nano-Biocarrier in Drug Delivery* (pp. 1–24). CRC Press.

Banjo, A. D., Lawal, O. A., & Songonuga, E. A. (2006). The nutritional value of fourteen species of edible insects in southwestern Nigeria. *African Journal of Biotechnology*, *5*(3), 298–301.

Barcoto, M. O., Carlos-Shanley, C., Fan, H., Ferro, M., Nagamoto, N. S., Bacci, M., Currie, C. R., & Rodrigues, A. (2020). Fungus-growing insects host a distinctive microbiota apparently adapted to the fungiculture environment. *Scientific Reports*, *10*(1), 1–13.

Barros, C. P., Guimarães, J. T., Esmerino, E. A., Duarte, M. C. K. H., Silva, M. C., Silva, R., Ferreira, B. M., Sant'Ana, A. S., Freitas, M. Q., & Cruz, A. G. (2020). Paraprobiotics and postbiotics: concepts and potential applications in dairy products. *Current Opinion in Food Science*, *32*, 1–8.

Baxter-Plant, V. S., Mikheenko, I. P., Robson, M., Harrad, S. J., & Macaskie, L. E. (2004). Dehalogenation of chlorinated aromatic compounds using a hybrid bioinorganic catalyst on cells of *Desulfovibrio desulfuricans*. *Biotechnology Letters*, *26*(24), 1885–1890. https://doi.org/10.1007/s10529-004-6039-x

Bedford, G. O. (1974). Descriptions of the larvae of some rhinoceros beetles (Col., Scarabaeidae, Dynastinae) associated with coconut palms in New Guinea. *Bulletin of Entomological Research*, *63*(3), 445–472.

Bhowmick, S. (2021). *Exploiting traditional Chinese medicine for potential anti-microbial drug leads*. Aberystwyth University.

Blackwell, M., Suh, S. O., & Nardi, J. B. (2007). Fungi in the hidden environment: the gut of beetles. *Fungi in the Environment. British Mycological Society Symposia, Cambridge*, 357–370.

Bojarska, J., Remko, M., Breza, M., Madura, I. D., Kaczmarek, K., Zabrocki, J., & Wolf, W. M. (2020). A supramolecular approach to structure-based design with a focus on synthons hierarchy in ornithine-derived ligands: Review, synthesis, experimental and in silico studies. *Molecules*, *25*(5), 1135.

Bongaarts, J. (2009). Human population growth and the demographic transition. *Philosophical Transactions of the Royal Society B: Biological Sciences*, *364*(1532), 2985–2990. https://doi.org/10.1098/rstb.2009.0137

Bophimai, P., & Siri, S. (2010). Fatty acid composition of some edible dung beetles in Thailand. *International Food Research Journal*, *17*(4), 1025–1030.

Botella-Martínez, C., Lucas-González, R., Pérez-Álvarez, J. A., Fernández-López, J., & Viuda-Martos, M. (2021). Assessment of chemical composition and antioxidant properties of defatted flours food fortification obtained from several edible insects. *Food Science and Technology International research journal*, *27*(5), 383–391. https://doi.org/10.1177/1082013220958854

Brenk, R., Schipani, A., James, D., Krasowski, A., Gilbert, I. H., Frearson, J., & Wyatt, P. G. (2008). Lessons learnt from assembling screening libraries for drug discovery for neglected diseases. *ChemMedChem: Chemistry Enabling Drug*

Discovery, *3*(3), 435–444.

Brown, J., Scholtz, C. H., Janeau, J.-L., Grellier, S., & Podwojewski, P. (2010). Dung beetles (Coleoptera: Scarabaeidae) can improve soil hydrological properties. *Applied Soil Ecology*, *46*(1), 9–16.

Bukkens, S. G. F. (1997). The nutritional value of edible insects. *Ecology of Food and Nutrition*, *36*(2–4), 287–319. https://doi.org/10.1080/03670244.1997.9991521

Buonocore, F., Fausto, A. M., Pelle, G. Della, Roncevic, T., Gerdol, M., & Picchietti, S. (2021). Attacins: A Promising Class of Insect Antimicrobial Peptides. *Antibiotics*, *10*(2), 212.

Burgos-Aceves, M. A., Migliaccio, V., Di Gregorio, I., Paolella, G., Lepretti, M., Faggio, C., & Lionetti, L. (2021). 1,1,1-trichloro-2,2-bis (p-chlorophenyl)-ethane (DDT) and 1,1-Dichloro-2,2-bis (p, p'-chlorophenyl) ethylene (DDE) as endocrine disruptors in human and wildlife: A possible implication of mitochondria. *Environmental Toxicology and Pharmacology science research*, volume; *87*, 103684. https://doi.org/https://doi.org/10.1016/j.etap.2021.103684

CABI. (2023). *Cetonia aurata* (flower, beetle). In *CABI Compendium*. CABI Compendium. https://doi.org/10.1079/cabicompendium.16834

Callahan, B. J., McMurdie, P. J., Rosen, M. J., Han, A. W., Johnson, A. J. A., & Holmes, S. P. (2016). DADA2: High-resolution sample inference from Illumina amplicon data. *Nature Methods*, *13*(7), 581–583.

Casadevall, A., Dadachova, E., & Pirofski, L. (2004). Passive antibody therapy for infectious diseases. *Nature Reviews Microbiology*, *2*(9), 695–703.

Chakraborti, S., Chakraborti, T., Chattopadhyay, D., & Shaha, C. (2019). *Oxidative stress in microbial diseases*. Springer.

Chakravorty, J., Ghosh, S., & Meyer-Rochow, V. B. (2011). Practices of entomophagy and entomotherapy by members of the Nyishi and Galo tribes, two ethnic groups of the state of Arunachal Pradesh (North-East India). *Journal of Ethnobiology and Ethnomedicine*, *7*(1), 1–14.

Challinor, V. L., & Bode, H. B. (2015). Bioactive natural products from novel microbial sources. *Annals of the New York Academy of Sciences*, *1354*(1), 82–97.

Chandler, C. I. R. (2019). Current accounts of antimicrobial resistance: stabilisation, individualisation and antibiotics as infrastructure. *Palgrave Communications*, *5*(1), 1–13.

Chaudhary, D. K., Bajagain, R., Jeong, S.-W., & Kim, J. (2019). Development of a bacterial consortium comprising oil-degraders and diazotrophic bacteria for elimination of exogenous nitrogen requirement in bioremediation of diesel-contaminated soil. *World Journal of Microbiology and Biotechnology*, *35*, 1–11.

Chen, H., & Boutros, P. C. (2011). VennDiagram: a package for the generation of highly-customizable Venn and Euler diagrams in R. *BMC Bioinformatics*, *12*(1), 35. https://doi.org/10.1186/1471-2105-12-35

Chouaia, B., Goda, N., Mazza, G., Alali, S., Florian, F., Gionechetti, F., Callegari, M., Gonella, E., Magoga, G., & Fusi, M. (2019). Developmental stages and gut

microenvironments influence gut microbiota dynamics in the invasive beetle *Popillia japonica* Newman (Coleoptera: Scarabaeidae). *Environmental Microbiology*, *21*(11), 4343–4359.

Church, N. A., & McKillip, J. L. (2021). Antibiotic resistance crisis: challenges and imperatives. *Biologia*, 1–16.

Comeau, A. M., Vincent, W. F., Bernier, L., & Lovejoy, C. (2016). Novel chytrid lineages dominate fungal sequences in diverse marine and freshwater habitats. *Scientific Reports*, *6*(1), 30120. https://doi.org/10.1038/srep30120

Correa, Y., Cabanillas, B., Jullian, V., Álvarez, D., Castillo, D., Dufloer, C., Bustamante, B., Roncal, E., Neyra, E., & Sheen, P. (2019). Identification and characterization of compounds from *Chrysosporium multifidum*, a fungus with moderate antimicrobial activity isolated from Hermetia illucens gut microbiota. *PloS One*, *14*(12), e0218837.

Cortez, K. J., Roilides, E., Quiroz-Telles, F., Meletiadis, J., Antachopoulos, C., Knudsen, T., Buchanan, W., Milanovich, J., Sutton, D. A., & Fothergill, A. (2008). Infections caused by *Scedosporium* spp. *Clinical Microbiology Reviews*, *21*(1), 157–197.

Da Silva Lucas, A. J., de Oliveira, L. M., Da Rocha, M., & Prentice, C. (2020). Edible insects: An alternative of nutritional, functional and bioactive compounds. *Food Chemistry*, *311*, 126022.

Del Carmen Villegas-Aguilar, M., de la Luz Cádiz-Gurrea, M., Arráez-Román, D., & Segura-Carretero, A. (2023). Anti-aging effects of phenolic compounds. In *Anti-Aging Pharmacology* (pp. 119–152). Elsevier.

Dhingra, S., Rahman, N. A. A., Peile, E., Rahman, M., Sartelli, M., Hassali, M. A., Islam, T., Islam, S., & Haque, M. (2020). Microbial resistance movements: an overview of global public health threats posed by antimicrobial resistance, and how best to counter. *Frontiers in Public Health*, *8*, 531.

Di Mattia, C., Battista, N., Sacchetti, G., & Serafini, M. (2019). Antioxidant Activities in vitro of Water and Liposoluble Extracts Obtained by Different Species of Edible Insects and Invertebrates. *Frontiers in Nutrition*, volume (pages) ;*6*, 106. https://doi.org/10.3389/fnut.2019.00106

Douglas, G. M., Maffei, V. J., Zaneveld, J., Yurgel, S. N., Brown, J. R., Taylor, C. M., Huttenhower, C., & Langille, M. G. I. (2019). PICRUSt2: An improved and extensible approach for metagenome inference. *BioRxiv*, 672295.

Duraipandiyan, V., & Ignacimuthu, S. (2009). Antibacterial and antifungal activity of Flindersine isolated from the traditional medicinal plant, Toddalia asiatica (L.) Lam. *Journal of Ethnopharmacology*, *123*(3), 494–498.

Ebert, K. M., Arnold, W. G., Ebert, P. R., & Merritt, D. J. (2021). Hindgut microbiota reflects different digestive strategies in dung beetles (Coleoptera: Scarabaeidae: Scarabaeinae). *Applied and Environmental Microbiology*, *87*(5), e02100-20.

Eggleton, P. (2020). *Annual Review of Environment and Resources The State of the World's Insects*. https://doi.org/10.1146/annurev-environ-012420

El-Sayed, W. S., & Ibrahim, R. A. (2015). Diversity and phylogenetic analysis of

endosymbiotic bacteria of the date palm root borer *Oryctes agamemnon* (Coleoptera: Scarabaeidae). *BMC Microbiology*, *15*, 1–10.

Elmeliegy, M., Vourvahis, M., Guo, C., & Wang, D. D. (2020). Effect of P-glycoprotein (P-gp) inducers on exposure of P-gp substrates: review of clinical drug–drug interaction studies. *Clinical Pharmacokinetics*, *59*, 699–714.

Engel, P., & Moran, N. A. (2013). The gut microbiota of insects–diversity in structure and function. *FEMS Microbiology Reviews*, *37*(5), 699–735.

Estes, A. M., Hearn, D. J., Snell-Rood, E. C., Feindler, M., Feeser, K., Abebe, T., Dunning Hotopp, J. C., & Moczek, A. P. (2013). Brood ball-mediated transmission of microbiome members in the dung beetle, *Onthophagus taurus* (Coleoptera: Scarabaeidae: Scarabaeinae). *PLoS ONE*, Insect scientific reports, *8*(11), 1–15. https://doi.org/10.1371/journal.pone.0079061

Fatima, H., Goel, N., Sinha, R., & Khare, S. K. (2021). Recent strategies for inhibiting multidrug-resistant and β-lactamase producing bacteria: A review. *Colloids and Surfaces B: Biointerfaces*, 111901.

Feikin, D. R., Olack, B., Bigogo, G. M., Audi, A., Cosmas, L., Aura, B., Burke, H., Njenga, M. K., Williamson, J., & Breiman, R. F. (2011). The burden of common infectious disease syndromes at the clinic and household level from population-based surveillance in rural and urban Kenya. *PloS One*, *6*(1), e16085.

Ferronato, N., & Torretta, V. (2019). Waste mismanagement in developing countries: A review of global issues. *International Journal of Environmental Research and Public Health*, *16*(6), 1060.

Fiebelkorn, F., Puchert, N., & Dossey, A. T. (2020). An exercise on data-based decision making: Comparing the sustainability of meat & edible insects. *The American Biology Teacher*, *82*(8), 522–528.

Firke, S. (2021). *Simple tools for examining and cleaning dirty data*.

Fogang Mba, A. R., Kansci, G., Viau, M., Hafnaoui, N., Meynier, A., Demmano, G., & Genot, C. (2017). Lipid and amino acid profiles support the potential of *Rhynchophorus phoenicis* larvae for human nutrition. *Journal of Food Composition and Analysis*, *60*, 64–73. https://doi.org/10.1016/j.jfca.2017.03.016

Franzini, P. Z. N. (2017). The gut microbiomes of desert *Pachysoma* spp. MacLeay (Coleoptera: Scarabaeidae). University of Pretoria.

Franzini, P. Z. N., Ramond, J.-B., Scholtz, C. H., Sole, C. L., Ronca, S., & Cowan, D. A. (2016). The Gut Microbiomes of Two *Pachysoma* MacLeay Desert Dung Beetle Species (Coleoptera: Scarabaeidae: Scarabaeinae) Feeding on Different Diets. https://doi.org/10.1371/journal.pone.0161118

Friedman, N., Shriker, E., Gold, B., Durman, T., Zarecki, R., Ruppin, E., & Mizrahi, I. (2017). Diet-induced changes of redox potential underlie compositional shifts in the rumen archaeal community. *Environmental Microbiology*, *19*(1), 174–184.

Fuzi, M., Rodriguez Baño, J., & Toth, A. (2020). Global evolution of pathogenic bacteria with extensive use of fluoroquinolone agents. *Frontiers in Microbiology*, *11*, 271.

Gajdács, M., Urbán, E., Stájer, A., & Baráth, Z. (2021). Antimicrobial Resistance in the Context of the Sustainable Development Goals: A Brief Review. *European Journal of Investigation in Health, Psychology and Education*, *11*(1), 71–82.

Ghosh, S., Lee, S.-M., Jung, C., & Meyer-Rochow, V. B. (2017). Nutritional composition of five commercial edible insects in South Korea. *Journal of Asia-Pacific Entomology*, *20*(2), 686–694. https://doi.org/10.1016/j.aspen.2017.04.003

Guillou, L., Bachar, D., Audic, S., Bass, D., Berney, C., Bittner, L., Boutte, C., Burgaud, G., de Vargas, C., & Decelle, J. (2012). The Protist Ribosomal Reference database (PR2): a catalog of unicellular eukaryote small sub-unit rRNA sequences with curated taxonomy. *Nucleic Acids Research*, *41*(D1), D597–D604.

Guindon, S., Dufayard, J.-F., Lefort, V., Anisimova, M., Hordijk, W., & Gascuel, O. (2010). New Algorithms and Methods to Estimate Maximum-Likelihood Phylogenies: Assessing the Performance of PhyML 3.0. *Systematic Biology*, *59*(3), 307–321. https://doi.org/10.1093/sysbio/syq010

Hallali, E., Kokou, F., Chourasia, T. K., Nitzan, T., Con, P., Harpaz, S., Mizrahi, I., & Cnaani, A. (2018). Dietary salt levels affect digestibility, intestinal gene expression, and the microbiome, in Nile tilapia (*Oreochromis niloticus*). *PloS One*, *13*(8), e0202351.

Hammer, T. J., McMillan, W. O., & Fierer, N. (2014). Metamorphosis of a butterfly-associated bacterial community. *PloS One*, *9*(1), e86995.

Hammer, T. J., & Moran, N. A. (2019). Links between metamorphosis and symbiosis in holometabolous insects. *Philosophical Transactions of the Royal Society B*, *374*(1783), 20190068.

Han, C.-J., Cheng, C.-H., Yeh, T.-F., Pauchet, Y., & Shelomi, M. (2024). Coconut rhinoceros beetle digestive symbiosis with potential plant cell wall degrading microbes. *Npj Biofilms and Microbiomes*, *10*(1), 34. https://doi.org/10.1038/s41522-024-00505-9

Harrison, M.-C., LaBella, A. L., Hittinger, C. T., & Rokas, A. (2022). The evolution of the Galactose utilization pathway in budding yeasts. *Trends in Genetics*, *38*(1), 97–106.

He, Y., Tian, J., Chen, X., Sun, W., Zhu, H., Li, Q., Lei, L., Yao, G., Xue, Y., & Wang, J. (2016). Fungal naphtho-γ-pyrones: Potent antibiotics for drug-resistant microbial pathogens. *Scientific Reports*, *6*(1), 24291.

Helrich, K. (1990). *Official methods of analysis of the Association of Official Analytical Chemists* (Issue Book). Association of official analytical chemists.

Hernández-García, J. A., Briones-Roblero, C. I., Rivera-Orduña, F. N., & Zúñiga, G. (2017). Revealing the gut bacteriome of *Dendroctonus* bark beetles (Curculionidae: Scolytinae): diversity, core members and co-evolutionary patterns. *Scientific Reports*, *7*(1), 13864. https://doi.org/10.1038/s41598-017-14031-6

Hoseinifar, S. H., Ashouri, G., Marisaldi, L., Candelma, M., Basili, D., Zimbelli, A., Notarstefano, V., Salvini, L., Randazzo, B., & Zarantoniello, M. (2024). Reducing the Use of Antibiotics in European Aquaculture with Vaccines, Functional Feed

Additives and Optimization of the Gut Microbiota. *Journal of Marine Science and Engineering*, *12*(2), 204.

Hou, X. (2012). Anaerobic xylose fermentation by *Spathaspora passalidarum*. *Applied Microbiology and Biotechnology*, *94*(1), 205–214. https://doi.org/10.1007/s00253-011-3694-4

Huang, H.-B., Feng, X.-J., Liu, L., Chen, B., Lu, Y.-J., Ma, L., She, Z.-G., & Lin, Y.-C. (2010). Three dimeric naphtho-γ-pyrones from the mangrove endophytic fungus Aspergillus tubingensis isolated from *Pongamia pinnata*. *Planta Medica*, *76*(16), 1888–1891.

Human, Z. R., Slippers, B., Wilhelm de Beer, Z., Wingfield, M. J., & Venter, S. N. (2017). Antifungal actinomycetes associated with the pine bark beetle, *Orthotomicus erosus*, in South Africa. *South African Journal of Science*, *113*(1–2), 1–7.

Hunter, P. (2020). A war of attrition against antibiotic resistance: current strategies try to keep antibiotic resistance at bay and further encourage research to produce genuinely novel antibacterials. *EMBO Reports*, *21*(6), e50807.

Hutchings, M. I., Truman, A. W., & Wilkinson, B. (2019). Antibiotics: past, present and future. *Current Opinion in Microbiology*, *51*, 72–80.

Jácome-Hernández, A., Lamelas, A., Desgarennes, D., Huerta, C., Cruz-Rosales, M., & Favila, M. E. (2023). Influence of phylogenetic, environmental, and behavioral factors on the gut bacterial community structure of dung beetles (Scarabaeidae: Scarabaeinae) in a Neotropical Biosphere Reserve. *Frontiers in Microbiology*, *14*.

Janssen, R. H., Vincken, J.-P., van den Broek, L. A. M., Fogliano, V., & Lakemond, C. M. M. (2017). Nitrogen-to-protein conversion factors for three edible insects: *Tenebrio molitor*, *Alphitobius diaperinus*, and *Hermetia illucens*. *Journal of Agricultural and Food Chemistry*, *65*(11), 2275–2278.

Jantzen da Silva Lucas, A., Menegon de Oliveira, L., da Rocha, M., & Prentice, C. (2020). Edible insects: An alternative of nutritional, functional and bioactive compounds. *Food Chemistry*, *311*, 126022. https://doi.org/10.1016/j.foodchem.2019.126022

Jasovský, D., Littmann, J., Zorzet, A., & Cars, O. (2016). Antimicrobial resistance—a threat to the world's sustainable development. *Upsala Journal of Medical Sciences*, *121*(3), 159–164.

Joint, F. A. O., & WHO, G. (2002). *Human vitamin and mineral requirements*.

Jonathan, H. G. E., & Stoltenberg, R. H. J. (2012). UN commission on life-saving commodities for women and children. *New York: United Nations*.

Joosten, L., Lecocq, A., Jensen, A. B., Haenen, O., Schmitt, E., & Eilenberg, J. (2020). Review of insect pathogen risks for the black soldier fly (*Hermetia illucens*) and guidelines for reliable production. *Entomologia Experimentalis et Applicata*, *168*(6–7), 432–447.

Kassambara, A. (2018). ggpubr:"ggplot2" based publication ready plots (Version 0.1. 7). *Obtido Desde Https://CRAN. R-Project. Org/Package= Ggpubr*.

Kathuria, H., Handral, H. K., Cha, S., Nguyen, D. T. P., Cai, J., Cao, T., Wu, C., & Kang, L. (2021). Enhancement of skin delivery of drugs using proposome depends on drug lipophilicity. *Pharmaceutics*, *13*(9), 1457.

Kearse, M., Moir, R., Wilson, A., Stones-Havas, S., Cheung, M., Sturrock, S., Buxton, S., Cooper, A., Markowitz, S., Duran, C., Thierer, T., Ashton, B., Meintjes, P., & Drummond, A. (2012). Geneious Basic: An integrated and extendable desktop software platform for the organization and analysis of sequence data. *Bioinformatics*, *28*(12), 1647–1649. https://doi.org/10.1093/bioinformatics/bts199

Kibet, S., Kimani, N. M., Mwanza, S. S., Mudalungu, C. M., Santos, C. B. R., & Tanga, C. M. (2024). Unveiling the Potential of Ent-Kaurane Diterpenoids: Multifaceted Natural Products for Drug Discovery. *Pharmaceuticals*, *17*(4), 510.

Kim, T.-K., Yong, H. I., Kim, Y.-B., Kim, H.-W., & Choi, Y.-S. (2019). Edible Insects as a Protein Source: A Review of Public Perception, Processing Technology, and Research Trends. *Food Science of Animal Resources*, *39*(4), 521–540. https://doi.org/10.5851/kosfa.2019.e53

Kirchmair, J., Göller, A. H., Lang, D., Kunze, J., Testa, B., Wilson, I. D., Glen, R. C., & Schneider, G. (2015). Predicting drug metabolism: experiment and/or computation? *Nature Reviews Drug Discovery*, *14*(6), 387–404.

Kyritsi, M., Tsoureki, A., Koukaras, K., Kamidis, N., Krey, G., Michailidou, S., & Argiriou, A. (2023). Seasonal Dynamics of Marine Bacterial Communities in Aquaculture Farms: The Case of the Northern Ionian Coastal Ecosystem (Mediterranean Sea). *Journal of Marine Science and Engineering*, *11*(7), 1332.

Lange, K. W., & Nakamura, Y. (2021). Edible insects as future food: chances and challenges. *Journal of Future Foods*, Insect science research *1*(1), 38–46. https://doi.org/10.1016/j.jfutfo.2021.10.001

Lee, S. R., Lee, D., Yu, J. S., Benndorf, R., Lee, S., Lee, D.-S., Huh, J., De Beer, Z. W., Kim, Y. H., & Beemelmanns, C. (2018). Natalenamides A–C, cyclic tripeptides from the termite-associated *Actinomadura* sp. RB99. *Molecules*, *23*(11), 3003.

Lei, J., Sun, L., Huang, S., Zhu, C., Li, P., He, J., Mackey, V., Coy, D. H., & He, Q. (2019). The antimicrobial peptides and their potential clinical applications. *American Journal of Translational Research*, *11*(7), 3919.

Li, H., Young, S. E., Poulsen, M., & Currie, C. R. (2021). Symbiont-mediated digestion of plant biomass in fungus-farming insects. *Annual Review of Entomology*, *66*, 297–316.

Lipinski, C. A., Lombardo, F., Dominy, B. W., & Feeney, P. J. (2012). Experimental and computational approaches to estimate solubility and permeability in drug discovery and development settings. *Advanced Drug Delivery Reviews*, *64*, 4–17.

Lombardi, L., Falanga, A., Del Genio, V., & Galdiero, S. (2019). A new hope: self-assembling peptides with antimicrobial activity. *Pharmaceutics*, *11*(4), 166.

Lu, S., Na, K., Li, Y., Zhang, L., Fang, Y., & Guo, X. (2024). Bacillus-derived probiotics: metabolites and mechanisms involved in bacteria–host interactions. *Critical Reviews in Food Science and Nutrition*, *64*(6), 1701–1714.

Mabhegedhe, M. (2017a). Cellulolytic activities of the dung beetle, *Euoniticellus intermedius*, larva gut micro-flora. *The Open Biotechnology Journal*, *11*(1).

Mabhegedhe, M. (2017b). Cellulolytic Activities of the Dung Beetle, Larva Gut Micro-Flora. *The Open Biotechnology Journal*, *11*(1).

Mabhegedhe, M., Rumbold, K., & Ntwasa, M. (2016). Cellulose degradation capabilities of dung beetle, *Euoniticellus intermedius*, larva gut consortia. *African Journal of Biotechnology*, *15*(9), 315–319.

Maglangit, F., Yu, Y., & Deng, H. (2021). Bacterial pathogens: threat or treat (a review on bioactive natural products from bacterial pathogens). *Natural Product Reports*, *38*(4), 782–821.

Manditsera, F. A., Luning, P. A., Fogliano, V., & Lakemond, C. M. M. (2019). The contribution of wild harvested edible insects (*Eulepida mashona* and *Henicus whellani*) to nutrition security in Zimbabwe. *Journal of Food Composition and Analysis*, *75*, 17–25. https://doi.org/10.1016/j.jfca.2018.09.013

Manniello, M. D., Moretta, A., Salvia, R., Scieuzo, C., Lucchetti, D., Vogel, H., Sgambato, A., & Falabella, P. (2021). Insect antimicrobial peptides: potential weapons to counteract the antibiotic resistance. *Cellular and Molecular Life Sciences*, 1–24.

Market and Market. (2024). Probiotics market by product type (Functional food and Beverages(FnB) dietary supplements and feed), Ingredient (Bacteria and yeast), End user (Human and Animal), Distribution Channel and Region-global Forecast to 2029. https://www.marketsandmarkets.com/Market-Reports/probiotics-market-69.html

Marshall, B. M., & Levy, S. B. (2011). Food animals and antimicrobials: impacts on human health. *Clinical Microbiology Reviews*, *24*(4), 718–733.

Marshall, S. D. G., Moore, A., Vaqalo, M., Noble, A., & Jackson, T. A. (2017). A new haplotype of the coconut rhinoceros beetle, *Oryctes rhinoceros*, has escaped biological control by *Oryctes rhinoceros* nudivirus and is invading Pacific Islands. *Journal of Invertebrate Pathology*, *149*, 127–134.

Martens, E., & Demain, A. L. (2017). The antibiotic resistance crisis, with a focus on the United States. *The Journal of Antibiotics*, *70*(5), 520–526.

Martin, M. (2011). Cutadapt removes adapter sequences from high-throughput sequencing reads. *EMBnet. Journal*, *17*(1), 10–12.

Mckenna, D. D., Farrell, B. D., Caterino, M. S., Farnum, C. W., Hawks, D. C., Maddison, D. R., Seago, A. E., Short, A. E. Z., Newton, A. F., & Thayer, M. K. (2015). Phylogeny and evolution of *S. taphyliniformia* and *S. carabaeiformia*: forest litter as a stepping stone for diversification of nonphytophagous beetles. *Systematic Entomology*, *40*(1), 35–60.

McMurdie, P. J., & Holmes, S. (2013). phyloseq: an R package for reproducible interactive analysis and graphics of microbiome census data. *PloS One*, *8*(4), e61217.

Memarpoor-Yazdi, M., Mahaki, H., & Zare-Zardini, H. (2013). Antioxidant activity of protein hydrolysates and purified peptides from *Zizyphus jujuba* fruits. *Journal of*

Functional Foods, *5*(1), 62–70.

Menegatti, C., Fukuda, T. T. H., & Pupo, M. T. (2020). Chemical ecology in Insect-microbe interactions in the neotropics. *Planta Medica*.

Merrikh, H., & Kohli, R. M. (2020). Targeting evolution to inhibit antibiotic resistance. *The FEBS Journal*, *287*(20), 4341–4353.

Mishyna, M., Chen, J., & Benjamin, O. (2020). Sensory attributes of edible insects and insect-based foods–Future outlooks for enhancing consumer appeal. *Trends in Food Science & Technology*, *95*, 141–148.

Mokaya, H. O., Ndunda, R. M., Kegode, T. M., Koech, S. J., Tanga, C. M., Subramanian, S., & Ngoka, B. (2022). Silkmoth pupae: potential and less exploited alternative source of nutrients and natural antioxidants. *Journal of Insects as Food and Feed*, 1–12. https://doi.org/10.3920/JIFF2022.0134

Molloy, E. M., & Hertweck, C. (2017). Antimicrobial discovery inspired by ecological interactions. *Current Opinion in Microbiology*, *39*, 121–127.

Mudalungu, C. M., Mokaya, H. O., & Tanga, C. M. (2023). Beneficial sterols in selected edible insects and their associated antibacterial activities. *Scientific Reports*, *13*(1), 10786. https://doi.org/10.1038/s41598-023-37905-4

Mudalungu, C. M., Richter, C., Wittstein, K., Abdalla, M. A., Matasyoh, J. C., Stadler, M., & Süssmuth, R. D. (2016). Laxitextines A and B, cyathane xylosides from the tropical fungus Laxitextum incrustatum. *Journal of Natural Products*, *79*(4), 894–898.

Mudalungu, C. M., Tanga, C. M., Kelemu, S., & Torto, B. (2021). An Overview of Antimicrobial Compounds from African Edible Insects and Their Associated Microbiota. *Antibiotics*, *10*(6), 621.

Murugu, D. K., Onyango, A. N., Ndiritu, A. K., Osuga, I. M., Xavier, C., Nakimbugwe, D., & Tanga, C. M. (2021). From Farm to Fork: Crickets as Alternative Source of Protein, Minerals, and Vitamins. *Frontiers in Nutrition*, *8*, 704002. https://doi.org/10.3389/fnut.2021.704002

Mutungi, C., Irungu, F. G., Nduko, J., Mutua, F., Affognon, H., Nakimbugwe, D., Ekesi, S., & Fiaboe, K. K. M. (2019). Postharvest processes of edible insects in Africa: A review of processing methods, and the implications for nutrition, safety and new products development. *Critical Reviews in Food Science and Nutrition*, *59*(2), 276–298.

Mwangi, J., Hao, X., Lai, R., & Zhang, Z.-Y. (2019). Antimicrobial peptides: new hope in the war against multidrug resistance. *Zoological Research*, *40*(6), 488.

Nataraj, B. H., Ali, S. A., Behare, P. V, & Yadav, H. (2020). Postbiotics-parabiotics: The new horizons in microbial biotherapy and functional foods. *Microbial Cell Factories*, *19*, 1–22.

Naveed, U., Jiang, C., Yan, Q., Wu, Y., Zhao, J., Zhang, B., Xing, J., Niu, T., Shi, C., & Wang, C. (2024). Inhibitory Effect of *Lactococcus* and *Enterococcus faecalis* on *Citrobacter Colitis* in Mice. *Microorganisms*, *12*(4), 730.

Obakiro, S. B., Kiyimba, K., Paasi, G., Napyo, A., Anthierens, S., Waako, P., Van

Royen, P., Iramiot, J. S., Goossens, H., & Kostyanev, T. (2021). Prevalence of antibiotic-resistant bacteria among patients in two tertiary hospitals in Eastern Uganda. *Journal of Global Antimicrobial Resistance*, *25*, 82–86.

Ochieng, B. O., Anyango, J. O., Nduko, J. M., Cheseto, X., Mudalungu, C. M., Khamis, F. M., Ghemoh, C. J., Egonyu, P. J., Subramanian, S., Nakimbugwe, D., Ssepuuya, G., & Tanga, C. M. (2022). Dynamics in nutrients, sterols and total flavonoid content during processing of the edible Long-Horned grasshopper (*Ruspolia differens* Serville) for food. *Food Chemistry and nutrition research*, *383*, 132397. https://doi.org/10.1016/j.foodchem.2022.132397

Okaraonye, C. C., & Ikewuchi, J. C. (2008). Nutritional Potential of *Oryctes rhinoceros* larva. *Pakistan Journal of Nutrition*, food science research *8*(1), 35–38. https://doi.org/10.3923/pjn.2009.35.38

Oksanen, J., Blanchet, F. G., Kindt, R., Legendre, P., Minchin, P. R., O'hara, R. B., Simpson, G. L., Solymos, P., Stevens, M. H. H., & Wagner, H. (2018). Community ecology package. *R Package Version*, *2*, 2–5.

Oliveira, A. B., Dolabela, M. F., Braga, F. C., Jácome, R. L. R. P., Varotti, F. P., & Póvoa, M. M. (2009). Plant-derived antimalarial agents: new leads and efficient phythomedicines. Part I. Alkaloids. *Anais Da Academia Brasileira de Ciencias*, *81*, 715–740.

Omotoso, O. T., & Adedire, C. O. (2007). Nutrient composition, mineral content and the solubility of the proteins of palm weevil, *Rhynchophorus phoenicis* f. (Coleoptera: Curculionidae). *Journal of Zhejiang University SCIENCE B*, *8*(5), 318–322. https://doi.org/10.1631/jzus.2007.B0318

Organization, W. H. (2017). *Framing the health workforce agenda for the Sustainable Development Goals: biennium report 2016–2017: WHO health workforce*. World Health Organization.

Oriolowo, O. B., John, O. J., Mohammed, U. B., & Joshua, D. (2020). Amino acids profile of catfish, crayfish and larva of edible *dung* beetle. *Ife Journal of Science*, *22*(1), 9–16. https://doi.org/10.4314/ijs.v22i1.2

Ortega, H. E., Ferreira, L. L. G., Melo, W. G. P., Oliveira, A. L. L., Ramos Alvarenga, R. F., Lopes, N. P., Bugni, T. S., Andricopulo, A. D., & Pupo, M. T. (2019). Antifungal compounds from *Streptomyces* associated with attine ants also inhibit *Leishmania donovani*. *PLoS Neglected Tropical Diseases*, *13*(8), e0007643.

Orwa, P., Mugambi, G., Wekesa, V., & Mwirichia, R. (2020). Isolation of haloalkaliphilic fungi from Lake Magadi in Kenya. *Heliyon*, *6*(1), e02823.

Ozimek, L., Sauer, W. C., Kozikowski, V., Ryan, J. K., Jørgensen, H., & Jelen, P. (1985). Nutritive Value of Protein Extracted from Honey Bees. *Journal of Food Science*, *50*(5), 1327–1329. https://doi.org/10.1111/j.1365-2621.1985.tb10469.x

Pacheco, T. L., & Vaz-de-Mello, F. Z. (2019). New dung beetle genus and species from a cave in the Espinhaço mountain range, Brazil (Coleoptera: Scarabaeidae: Scarabaeinae). *Journal of Natural History*, *53*(19–20), 1247–1253.

Paiko, Y. B., Jacob, J. O., Salihu, S. O., Dauda, B. E. N., Suleiman, M. A. T., & Akanya, H. O. (2014). Fatty acid and amino acid profile of emperor moth caterpillar (*Cirina*

forda) in Paikoro Local Government Area of Niger State, Nigeria. *American Journal of Biochemistry*, *4*(2), 29–34.

Pannu, R., & Kumar, D. (2017). Process optimization of γ- Hexachlorocyclohexane degradation using three novel *Bacillus* sp. strains. *Biocatalysis and Agricultural Biotechnology*, *11*, 97–107.https://doi.org/https://doi.org/10.1016/j.bcab.2017.06.009

Parker, B. J., Wearsch, P. A., Veloo, A. C. M., & Rodriguez-Palacios, A. (2020). The genus *Alistipes*: gut bacteria with emerging implications to inflammation, cancer, and mental health. *Frontiers in Immunology*, *11*, 906.

Parks, D. H., & Beiko, R. G. (2010). Identifying biologically relevant differences between metagenomic communities. *Bioinformatics*, *26*(6), 715–721.

Peiman, K. S., & Robinson, B. W. (2012). Diversifying and correlational selection on behavior toward conspecific and heterospecific competitors in brook stickleback (C ulaea inconstans). *Ecology and Evolution*, *2*(9), 2141–2154.

Piewngam, P., Zheng, Y., Nguyen, T. H., Dickey, S. W., Joo, H.-S., Villaruz, A. E., Glose, K. A., Fisher, E. L., Hunt, R. L., & Li, B. (2018). Pathogen elimination by probiotic *Bacillus* via signalling interference. *Nature*, *562*(7728), 532–537.

Priestap, H. A. (1986). 13C NMR spectroscopy of naphtho-γ-pyrones. *Magnetic Resonance in Chemistry*, *24*(10), 875–878.

Provenzani, A., Hospodar, A. R., Meyer, A. L., Vinci, D. L., Hwang, E. Y., Butrus, C. M., & Polidori, P. (2020). Multidrug-resistant gram-negative organisms: a review of recently approved antibiotics and novel pipeline agents. *International Journal of Clinical Pharmacy*, 1–10.

Qiao-ru, H., YANG, L., Feng-jie, C., Peng-cheng, Z., Yan, L., & Feng-jie, Z. (2010). Analysis and Evaluation of the Nutritional Components in *Holitrichia parallela* Motschulsky. *Plant Diseases and Pests*, *1*(5), 7–9.

Quast, C., Pruesse, E., Yilmaz, P., Gerken, J., Schweer, T., Yarza, P., Peplies, J., & Glöckner, F. O. (2012). The SILVA ribosomal RNA gene database project: improved data processing and web-based tools. *Nucleic Acids Research*, *41*(D1), D590–D596.

Raja, H. A., Miller, A. N., Pearce, C. J., & Oberlies, N. H. (2017). Fungal identification using molecular tools: a primer for the natural products research community. *Journal of Natural Products*, *80*(3), 756–770.

Raper, K. B., & Fennell, D. I. (1965). The genus *Aspergillus*. *The Genus Aspergillus.*

Reátegui, R. C., Pawera, L., Panduro, P. P. V., & Polesny, Z. (2018). Beetles, ants, wasps, or flies? An ethnobiological study of edible insects among the Awajún Amerindians in Amazonas, Peru. *Journal of Ethnobiology and Ethnomedicine*, *14*(1), 1–11.

Rodríguez-Beltrán, J., DelaFuente, J., León-Sampedro, R., MacLean, R. C., & San Millán, Á. (2021). Beyond horizontal gene transfer: the role of plasmids in bacterial evolution. *Nature Reviews Microbiology*, 1–13.

Roohani, N., Hurrell, R., Kelishadi, R., & Schulin, R. (2013). Zinc and its importance

for human health: An integrative review. *Journal of Research in Medical Sciences : The Official Journal of Isfahan University of Medical Sciences*, *18*(2), 144–157. http://www.ncbi.nlm.nih.gov/pubmed/23914218

Ruess, L., & Müller-Navarra, D. C. (2019). Essential biomolecules in food webs. *Frontiers in Ecology and Evolution*, *7*, 269.

S˘ípek, P., Král, D., & Jahn, O. (2008). Description of the larvae of *Dicronocephalus wallichi* bourgoini Coleoptera: Scarabaeidae: Cetoniinae) with observations on nesting behavior and life cycle of two *Dicronocephalus* species under laboratory conditions. *Annales de La Société Entomologique de France*, *44*(4), 409–417.

Santoro, A., Franceschini, E., Meschiari, M., Menozzi, M., Zona, S., Venturelli, C., Digaetano, M., Rogati, C., Guaraldi, G., & Paul, M. (2020). Epidemiology and risk factors associated with mortality in consecutive patients with bacterial bloodstream infection: impact of MDR and XDR bacteria. *Open Forum Infectious Diseases*, *7*(11), ofaa461.

Sari, S. L. A., Pangastuti, A., Susilowati, A. R. I., Purwoko, T., Mahajoeno, E., Hidayat, W., Mardhena, I., Kurniawati, D., & Anitasari, R. (2016). Cellulolytic and hemicellulolytic bacteria from the gut of *Oryctes rhinoceros* larvae. *Biodiversitas Journal of Biological Diversity*, *17*(1).

Schwab, D. B., Riggs, H. E., Newton, I. L. G., & Moczek, A. P. (2016). Developmental and ecological benefits of the maternally transmitted microbiota in a dung beetle. *The American Naturalist*, *188*(6), 679–692.

Sharma, V. K. (2003). Adaptive significance of circadian clocks. *Chronobiology International*, *20*(6), 901–919.

Shelomi, M., & Chen, M.-J. (2020). Culturing-Enriched Metabarcoding Analysis of the *Oryctes rhinoceros* Gut Microbiome. In *Insects* (Vol. 11, Issue 11). https://doi.org/10.3390/insects11110782

Shelomi, M., Lin, S.-S., & Liu, L.-Y. (2019). Transcriptome and microbiome of coconut rhinoceros beetle (*Oryctes rhinoceros*) larvae. *BMC Genomics*, *20*(1), 957. https://doi.org/10.1186/s12864-019-6352-3

Shukla, S. P., Sanders, J. G., Byrne, M. J., & Pierce, N. E. (2016). Gut microbiota of dung beetles correspond to dietary specializations of adults and larvae. *Molecular Ecology*, *25*(24), 6092–6106. https://doi.org/10.1111/mec.13901

Sonnhammer, E. L. L., & Durbin, R. (1995). A dot-matrix program with dynamic threshold control suited for genomic DNA and protein sequence analysis. *Gene*, *167*(1–2), GC1–GC10. https://doi.org/10.1016/0378-1119(95)00714-8

Suárez-Moo, P., Cruz-Rosales, M., Ibarra-Laclette, E., Desgarennes, D., Huerta, C., & Lamelas, A. (2020). Diversity and Composition of the Gut Microbiota in the Developmental Stages of the Dung Beetle *Copris incertus* Say (Coleoptera, Scarabaeidae: Scarabaeinae). *Frontiers in Microbiology*, Available at: *11*. https://doi.org/10.3389/fmicb.2020.01698

Suh, H.-J., & Kang, S. C. (2012). Antioxidant activity of aqueous methanol extracts of *Protaetia brevitarsis* Lewis (Coleoptera: Scarabaedia: Scarabaenia) at different growth stages. *Natural Product chemistry Research*, *26*(6), 510–517.

https://doi.org/10.1080/14786419.2010.530267

Suh, H.-J., Kim, S.-R., Hwang, J.-S., Kim, M. J., & Kim, I. (2011). Antioxidant activity of aqueous methanol extracts from the lucanid beetle, *Serrognathus platymelus* castanicolor Motschulsky (Coleoptera: Lucanidae). *Journal of Asia-Pacific Entomology*, *14*(1), 95–98. https://doi.org/10.1016/j.aspen.2010.10.002

Suh, H.-J., Kim, S.-R., Lee, K.-S., Park, S., & Kang, S. C. (2010). Antioxidant activity of various solvent extracts from *Allomyrina dichotoma* (Arthropoda: Insecta) larvae. *Journal of Photochemistry and Photobiology B: Biology*, *99*(2), 67–73. https://doi.org/10.1016/j.jphotobiol.2010.02.005

Šustr, V., Chroňáková, A., Semanová, S., Tajovský, K., & Šimek, M. (2014). Methane production and methanogenic Archaea in the digestive tracts of millipedes (Diplopoda). *PloS One*, *9*(7), e102659.

Tafesh-Edwards, G., & Eleftherianos, I. (2023). The role of Drosophila microbiota in gut homeostasis and immunity. *Gut Microbes*, *15*(1), 2208503.

Tagliavia, M., Messina, E., Manachini, B., Cappello, S., & Quatrini, P. (2014). The gut microbiota of larvae of *Rhynchophorus ferrugineus* Oliver (Coleoptera: Curculionidae). *BMC MICROBIOLOGY*, *14*. https://doi.org/10.1186/1471-2180-14-136

Tanga, C. M., Mokaya, H. O., Kasiera, W., & Subramanian, S. (2023). Potential of Insect Life Stages as Functional Ingredients for Improved Nutrition and Health. *Insects*, *14*(2), 136. https://doi.org/10.3390/insects14020136

Teixeira, M. C., Carbone, C., Sousa, M. C., Espina, M., Garcia, M. L., Sanchez-Lopez, E., & Souto, E. B. (2020). Nanomedicines for the delivery of antimicrobial peptides (Amps). *Nanomaterials*, *10*(3), 560.

Thiyonila, B., Paulin Reneeta, N., Kannan, M., Shantkriti, S., & Krishnan, M. (2018). Dung beetle gut microbes: Diversity, metabolic and immunity related roles in host system. Insect research; *International Journal of Scientific Innovations*, *4*(03), 77–083. https://doi.org/10.32594/IJSI_20180403

Thomas, C. N. (2018). Nutritional Potentials of Edible Larvae of Longhorned Beetle (*A pomecyna p arumpunctata* Chev.) (Coleoptera : Cerambycidae) in Niger Delta , Nigeria. *International Journal of Agriculture and Earth Science*, *4*, 46–51.

Thomas, C. N., & Kiin-Kabari, D. B. (2022). Comparative Study on Fatty Acid Profiles of Selected Edible Insects and Animals in Africa : A Review. *Journal of Biology and Genetic Research*, *8*(1), 18–30.

Tinker, K. A., & Ottesen, E. A. (2016). The Core Gut Microbiome of the American Cockroach, *Periplaneta americana*, Is Stable and Resilient to Dietary Shifts, *82 (22), 6603–6610*.

Tran, H. T., Lin, C., Hoang, H. G., Bui, X. T., Le, V. G., & Vu, C. T. (2022). Soil washing for the remediation of dioxin-contaminated soil: A review. *Journal of Hazardous Material 421*, 126767. https://doi.org/https://doi.org/10.1016/j.jhazmat.2021.126767

Ukoroije, R. B., & Bobmanuel, R. B. (2019a). Biochemical Constituents of Larvae of the Rhinoceros Beetle *Oryctes Owariensis* Beauvois *(Coleoptera: Scarabaeidae)*

In Bayelsa State. https://doi.org/: 10.36344/ccijavs.2019.v01i06.001

Ukoroije, R. B., & Bobmanuel, R. B. (2019b). The acceptability of Oryctes owariensis beauvois (Coleoptera: Scarabaeidae) larva as food in Bayelsa State, Nigeria. *East African Scholars Journal of Agriculture and Life Sciences*, *2*(10), 509–515. https://doi.org/: 10.36344/ccijavs.2019.v01i06.001

Van Huis, A., Rumpold, B., Maya, C., & Roos, N. (2021). Nutritional Qualities and Enhancement of Edible Insects. *Annual Review of Nutrition*, *41*(1), 551–576. https://doi.org/10.1146/annurev-nutr-041520-010856

Van Moll, L., De Smet, J., Cos, P., & Van Campenhout, L. (2021). Microbial symbionts of insects as a source of new antimicrobials: a review. *Critical Reviews in Microbiology*, 1–18.

Veber, D. F., Johnson, S. R., Cheng, H.-Y., Smith, B. R., Ward, K. W., & Kopple, K. D. (2002). Molecular properties that influence the oral bioavailability of drug candidates. *Journal of Medicinal Chemistry*, *45*(12), 2615–2623.

Vega, F. E., & Blackwell, M. (2005). *Insect-fungal associations: ecology and evolution*. Oxford University Press.

Verkerk, M. C., Tramper, J., van Trijp, J. C. M., & Martens, D. E. (2007). Insect cells for human food. Insect research science, *Biotechnology Advances*, *25*(2), 198–202. https://doi.org/10.1016/j.biotechadv.2006.11.004

Villemur, R., Lanthier, M., Beaudet, R., & Lépine, F. (2006). The *Desulfitobacterium* genus . *FEMS Microbiology Reviews*, *30*(5), 706–733. https://doi.org/10.1111/j.1574-6976.2006.00029.x

Wang, S., Wang, L., Fan, X., Yu, C., Feng, L., & Yi, L. (2020). An insight into diversity and functionalities of gut microbiota in insects. *Current Microbiology*, *77*, 1976–1986.

Wani, N., Khanday, W., & Tirumale, S. (2020). Phytochemical analysis and evaluation of antibacterial activity of different extracts of soil-isolated fungus *Chaetomium cupreum*. *Journal of Natural Science, Biology and Medicine*, *11*(1), 72–80.

Wei, W., Cherukupalli, S., Jing, L., Liu, X., & Zhan, P. (2020). Fsp3: A new parameter for drug-likeness. *Drug Discovery Today*, *25*(10), 1839–1845.

Wickham, H., Averick, M., Bryan, J., Chang, W., McGowan, L., François, R., Grolemund, G., Hayes, A., Henry, L., Hester, J., Kuhn, M., Pedersen, T., Miller, E., Bache, S., Müller, K., Ooms, J., Robinson, D., Seidel, D., Spinu, V., … Yutani, H. (2019). Welcome to the Tidyverse. *Journal of Open Source Software*, *4*(43), 1686. https://doi.org/10.21105/joss.01686

Williams, P. (2007). Nutritional composition of red meat. *Nutrition & Dietetics*, *64*(s4 The Role of), S113–S119. https://doi.org/10.1111/j.1747-0080.2007.00197.x

Wilson, J. J. (2012). DNA Barcodes for Insects. In *Methods in Molecular Biology* (Vol. 858, pp. 17–46). https://doi.org/10.1007/978-1-61779-591-6_3

Winfrey, C. C., & Sheldon, K. S. (2021). Drivers of inter-population variation in the gut microbiomes of sister species of Phanaeus dung beetles. *BioRxiv*, 2002–2021.

Womeni, H. M., Linder, M., Tiencheu, B., Mbiapo, F. T., Villeneuve, P., Fanni, J., & Parmentier, M. (2009). Oils of insects and larvae consumed in Africa: potential sources of polyunsaturated fatty acids. *Oléagineux, Corps Gras, Lipides*, *16*(4-5–6), 230–235. https://doi.org/10.1051/ocl.2009.0279

Wright, E. S. (2016). Using DECIPHER v2. 0 to analyze big biological sequence data in R. *R Journal*, *8*(1).

Wu, Q., Jiang, N., Han, W. B., Mei, Y. N., Ge, H. M., Guo, Z. K., Weng, N. S., & Tan, R. X. (2014). Antibacterial epipolythiodioxopiperazine and unprecedented sesquiterpene from *Pseudallescheria boydii*, a beetle (coleoptera)-associated fungus. *Organic & Biomolecular Chemistry*, *12*(46), 9405–9412.

Yang, Q., Liu, S., Sun, J., Yu, L., Zhang, C., Bi, J., & Yang, Z. (2014). Nutritional composition and protein quality of the edible beetle *Holotrichia parallela*. *Journal of Insect Science*, *14*(1).

Yeo, H., Youn, K., Kim, M., Yun, E.-Y., Hwang, J.-S., Jeong, W.-S., & Jun, M. (2013). Fatty Acid Composition and Volatile Constituents of *Protaetia brevitarsis* Larvae. *Preventive Nutrition and Food Science*, volume (pages); *18*(2), 150–156. https://doi.org/10.3746/pnf.2013.18.2.150

Young, C. C., Burghoff, R. L., Keim, L. G., Minak-Bernero, V., Lute, J. R., & Hinton, S. M. (1993). Polyvinylpyrrolidone-agarose gel electrophoresis purification of polymerase chain reaction-amplifiable DNA from soils. *Applied and Environmental Microbiology*, *59*(6), 1972–1974.

Zhang, M., Haga, A., Sekiguchi, H., & Hirano, S. (2000). Structure of insect chitin isolated from beetle larva cuticle and silkworm (*Bombyx mori*) pupa exuvia. *International Journal of Biological Macromolecules*, *27*(1), 99–105.

Zhang, Z., Malik, M. Z., Khan, A., Ali, N., Malik, S., & Bilal, M. (2022). Environmental impacts of hazardous waste, and management strategies to reconcile circular economy and eco-sustainability. *Science of The Total Environment*, *807*, 150856.

Zheng, C. J., Sohn, M.-J., Lee, S., Hong, Y.-S., Kwak, J.-H., & Kim, W.-G. (2007). Cephalochromin, a FabI-directed antibacterial of microbial origin. *Biochemical and Biophysical Research Communications*, *362*(4), 1107–1112.

Zhou, L.-F., Wu, J., Li, S., Li, Q., Jin, L.-P., Yin, C.-P., & Zhang, Y.-L. (2021). Antibacterial Potential of Termite-Associated *Streptomyces* spp. *ACS Omega*, *6*(6), 4329–4334.

Ziganshina, E. E., Mohammed, W. S., Shagimardanova, E. I., Vankov, P. Y., Gogoleva, N. E., & Ziganshin, A. M. (2018). Fungal, bacterial, and archaeal diversity in the digestive tract of several beetle larvae (Coleoptera). *BioMed Research International*, *2018*.

ETHICAL APPROVAL

Institutional Review Board Statement: The Authority to conduct the experiment and collect data was in accordance with the animal welfare regulations and granted by National Commission for Science, Technology, and Innovation (NACOSTI); Research Permit License No: NACOSTI/P/23/27477. This research also received approval from the Institutional Animal Care and Use Committee (IACUC) of Kenya Agricultural and Livestock Research Organization (KALRO)-Veterinary Science Research Institute (VSRI); Muguga North upon compliance with all provisions vetted under and coded: KALRO-VSRI/IACUC028/31072024.

APPENDICES

Appendix 7:1: **Rarefactions curves showing gut microbial community richness of both *O. rhinoceros* and *C. aurata* individuals for bacterial 16S rRNA gene amplicon and metazoan 18S gene region data**

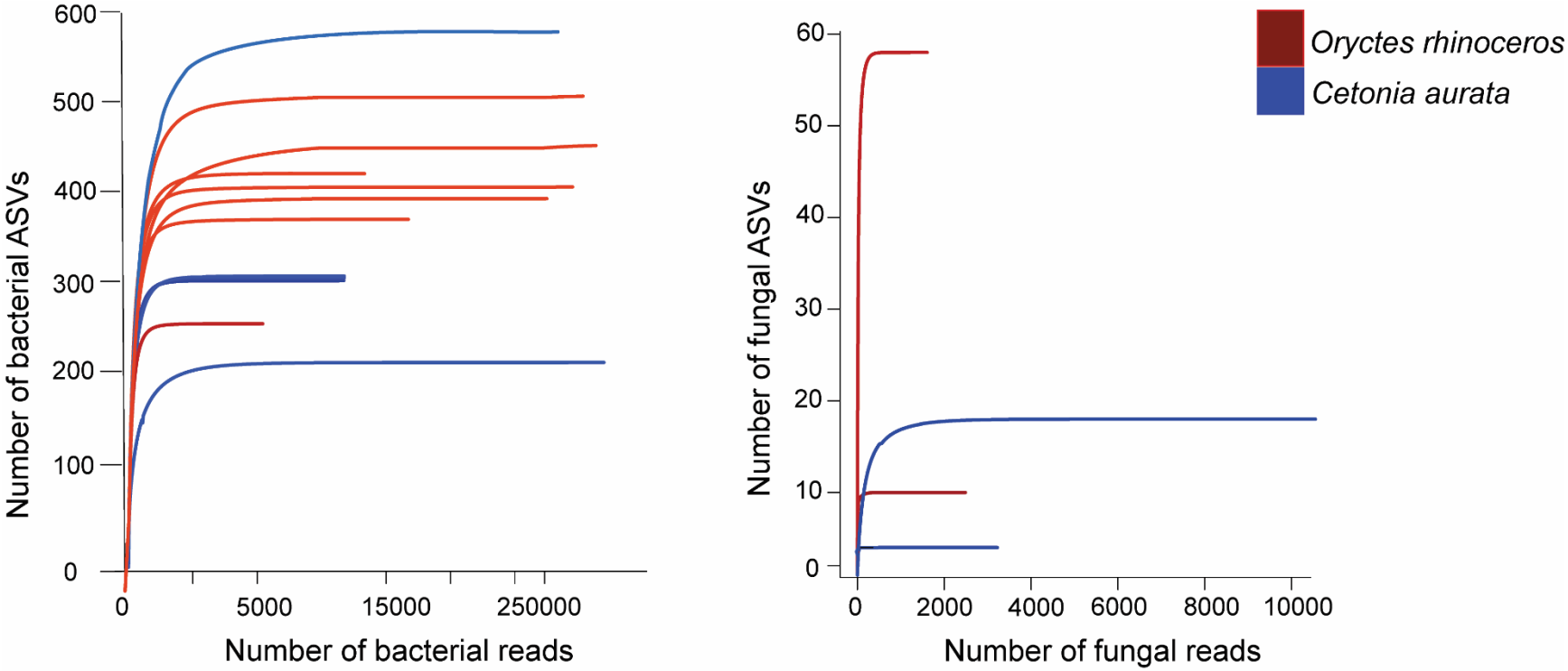

Appendix 7:2*:* A scatter dot graph showing the percentage relative abundances of the most abundant ASVs plotted at the species level for both samples of *O. rhinoceros* and *C. aurata*

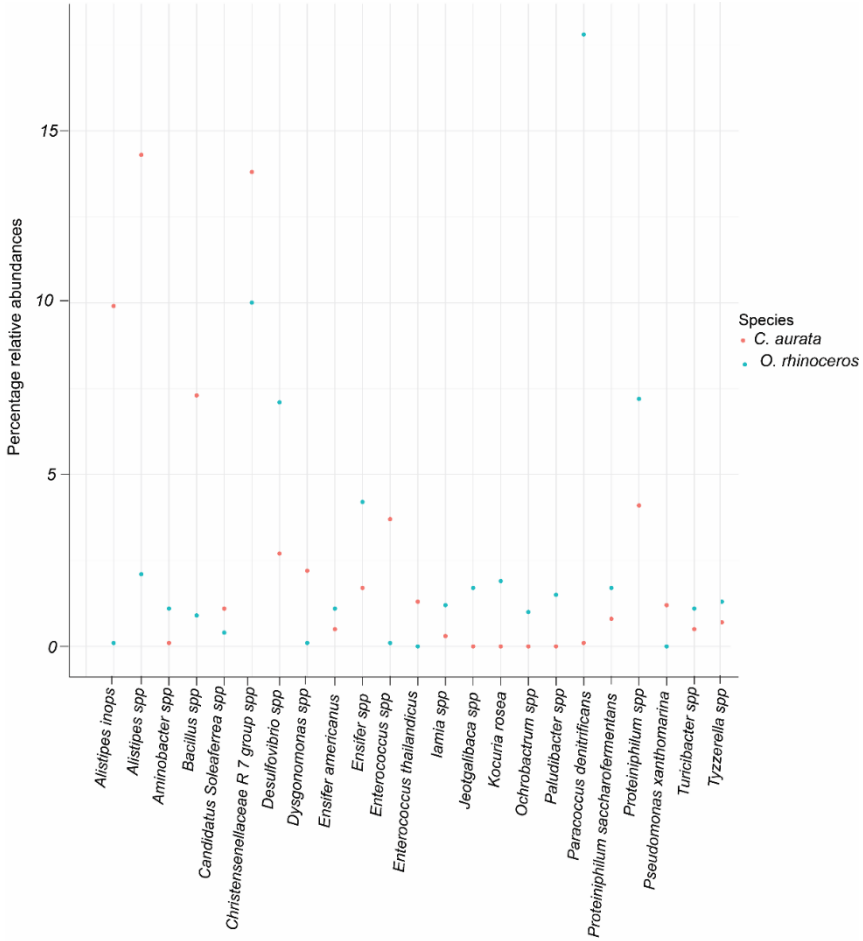

Appendix 7:3*:* Heat map of 71 categories at level 3 most abundant KOs, each column corresponds to a *C. aurata* and *O. rhinoceros* samples, and each row corresponds to a specific category

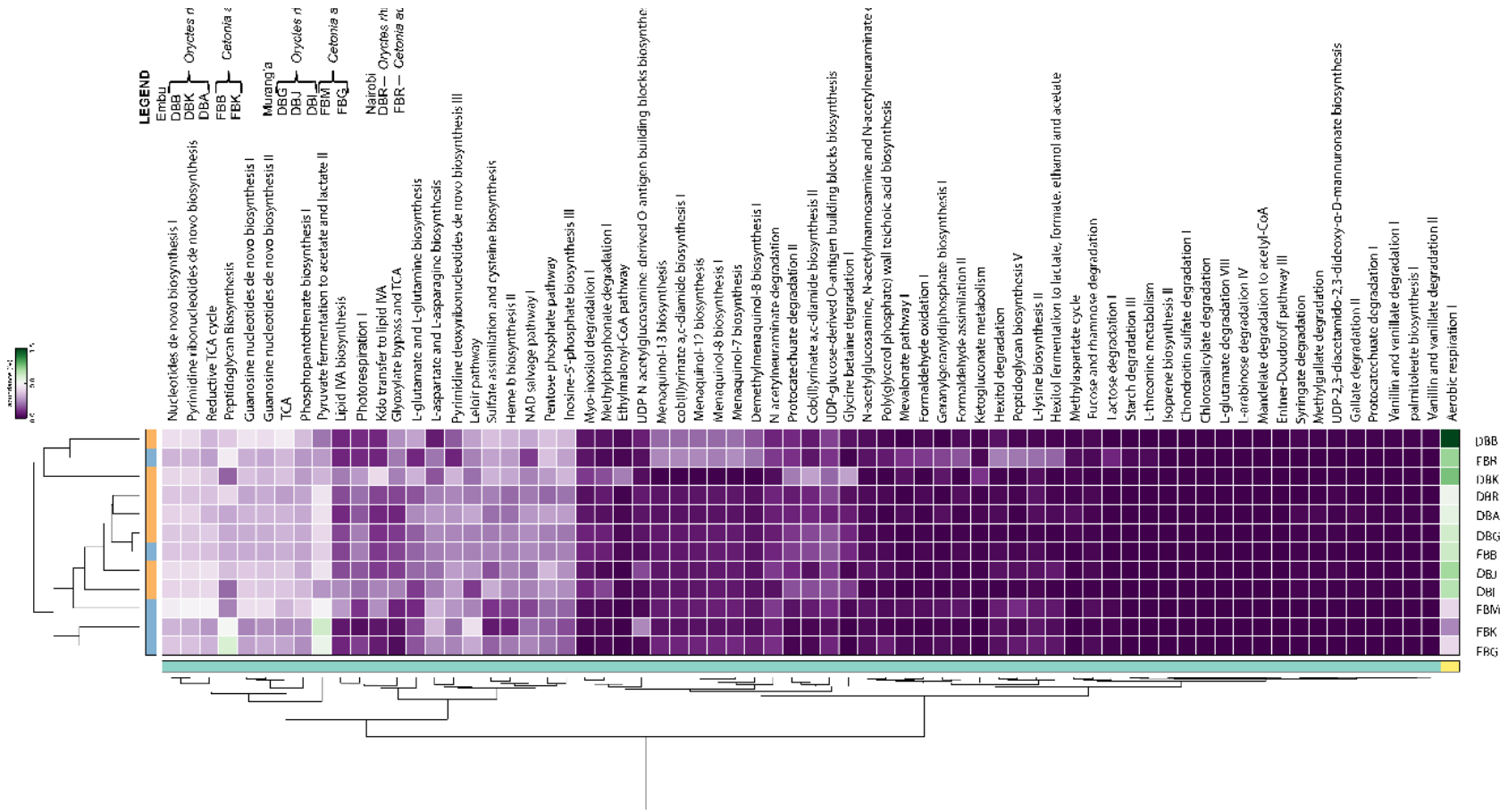

Appendix 7:4: Potato Dextrose Agar plates cultivated with mixed fungal cultures from gut homogenates obtained from *O. rhinoceros* and *C. aurata* larvae collected from three counties: Embu, Murang'a, and Nairobi.

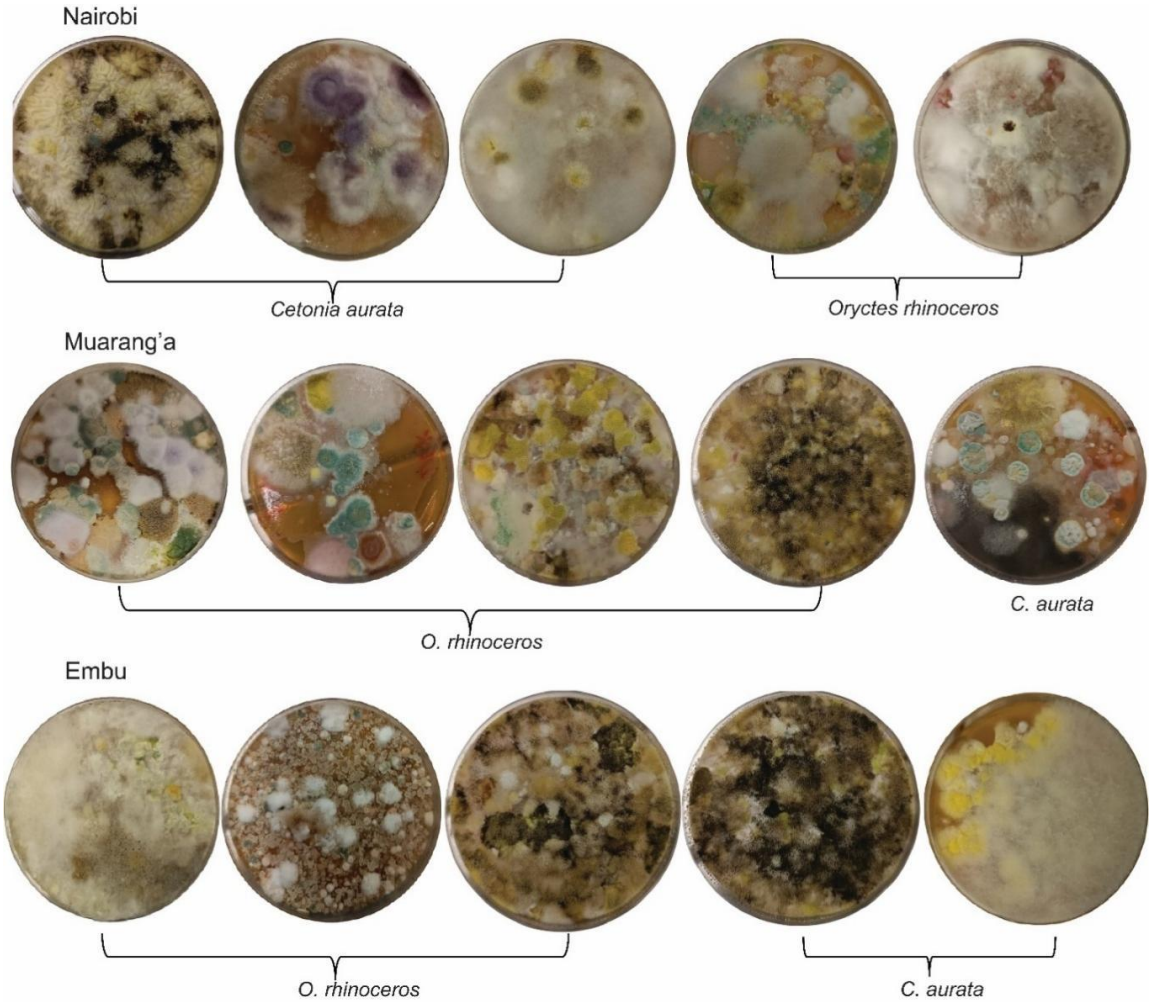

Appendix 7:5: An MHA plate showing zones of inhibition of positive control; P, DBK and DBK-- dung beetle larvae fungi extract, negative control; N - 10 % DMSO, FBM and FBA - fruit beetle fungi extract against *Bacillus subtilis* and *pseudomonas aeruginosa*

Appendix 7:6*:* PDA plates displaying pure cultures obtained from the mixed fungal culture of *O. rhinoceros* gut homogenate collected from Kairi in Murang'a County

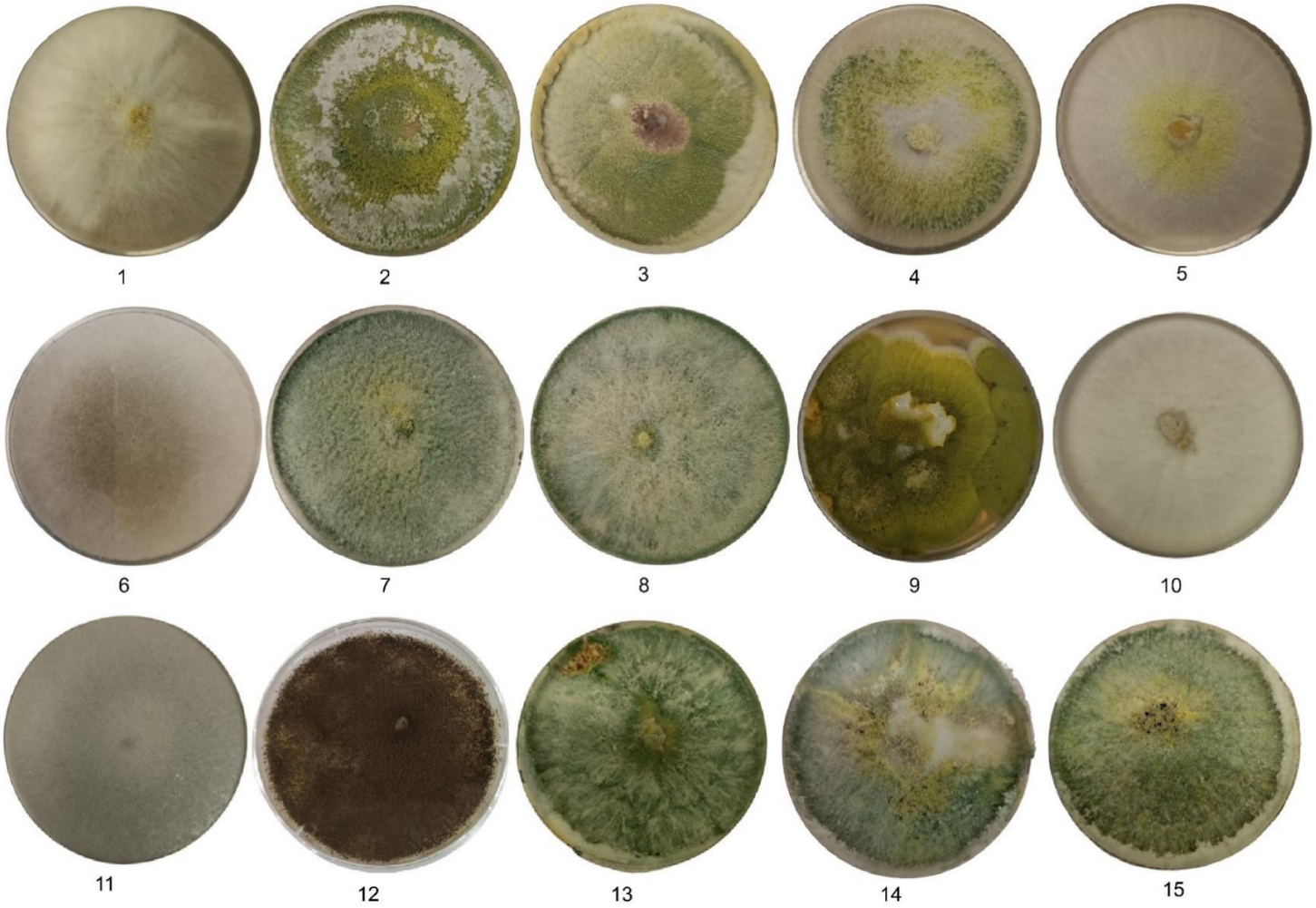

Appendix 7:7: LC-MS spectra for EtOAc extract from *A. welwitschia*

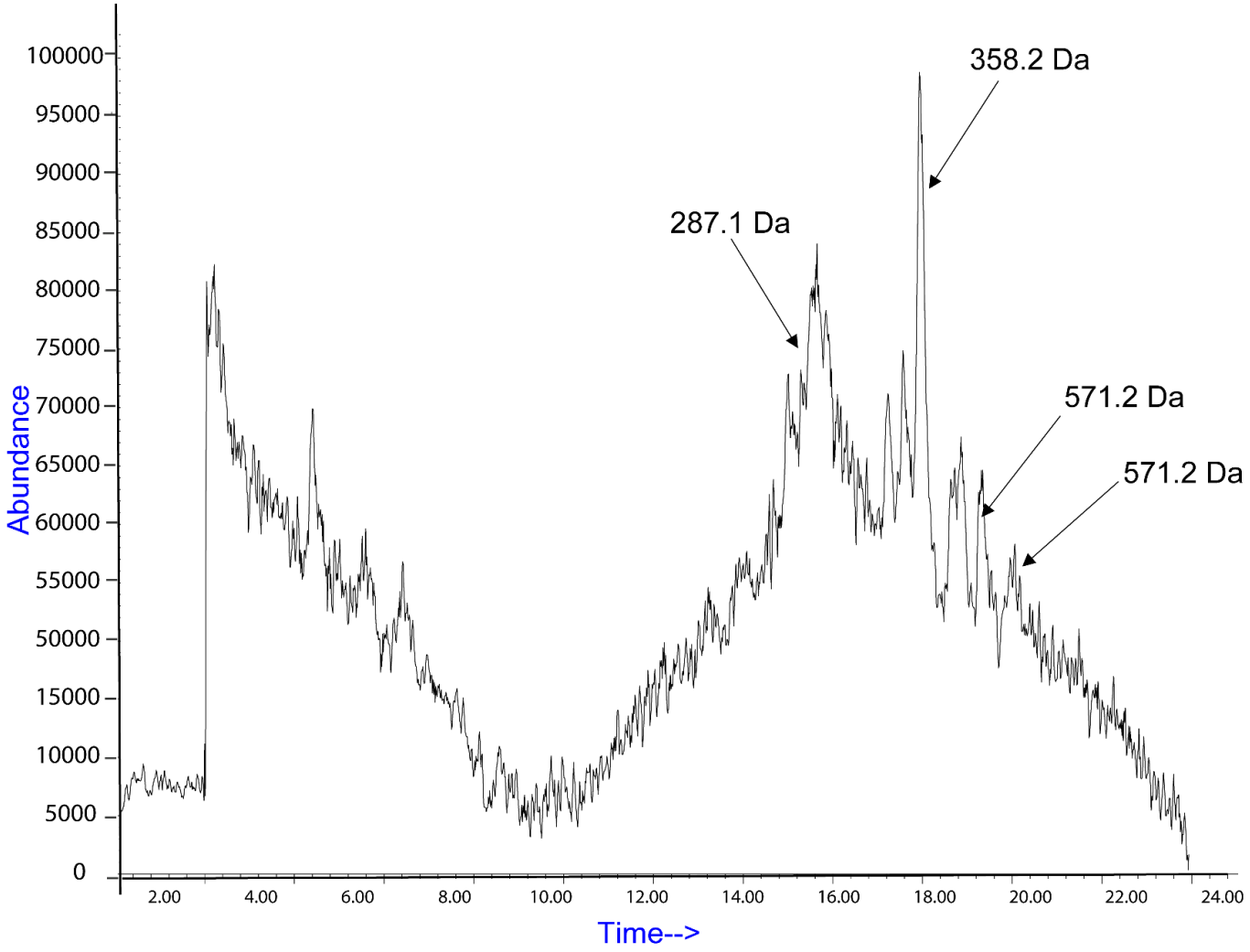

Appendix 7:8: Total ion count spectra (A), Mass spectrum (B) and HPLC-UV spectrum (C) of rubrofusarin B

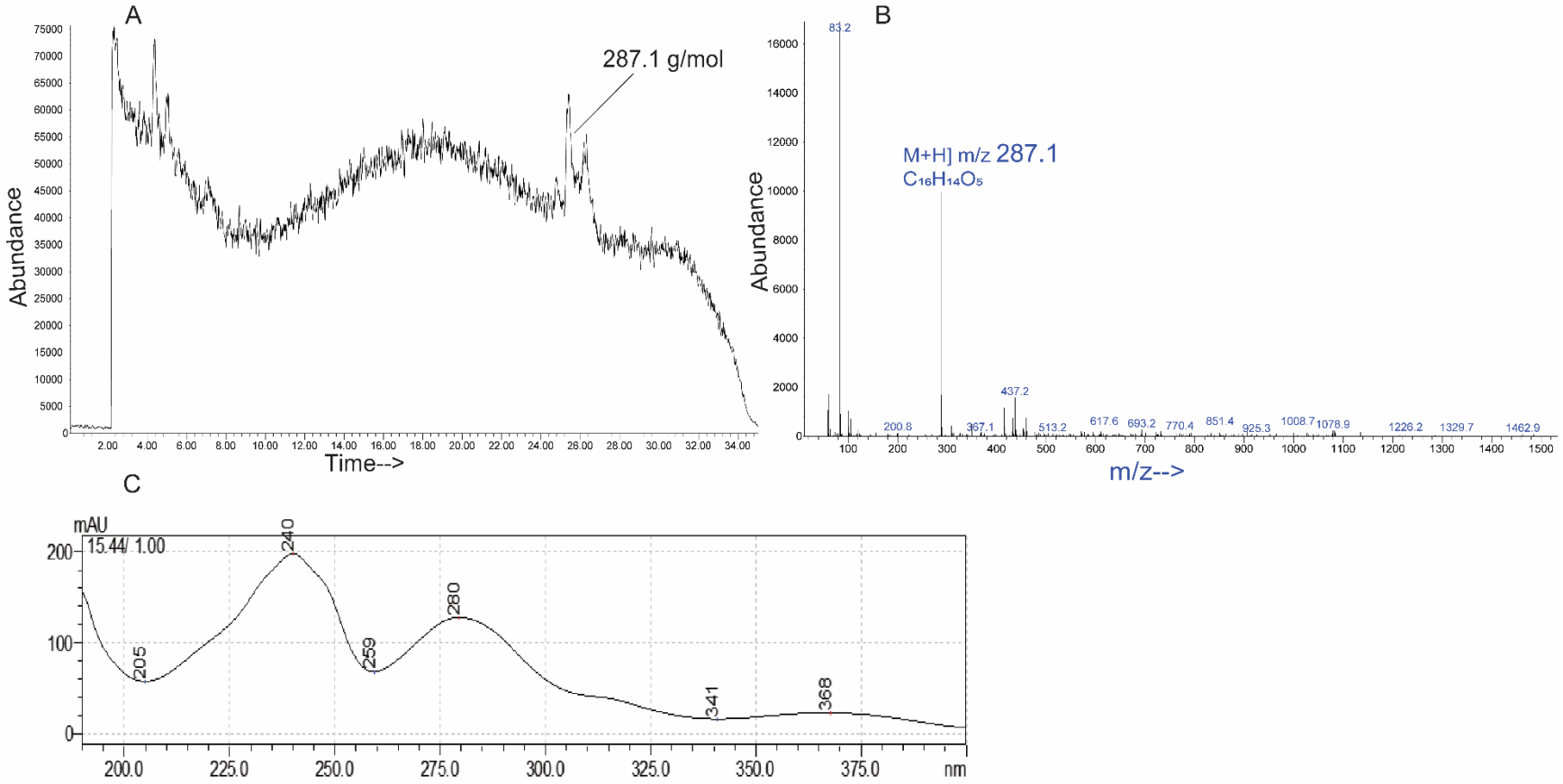

Appendix 7:9: Total ion count spectra (A), Mass spectrum (B) and HPLC-UV spectrum (C) of rubasperone B

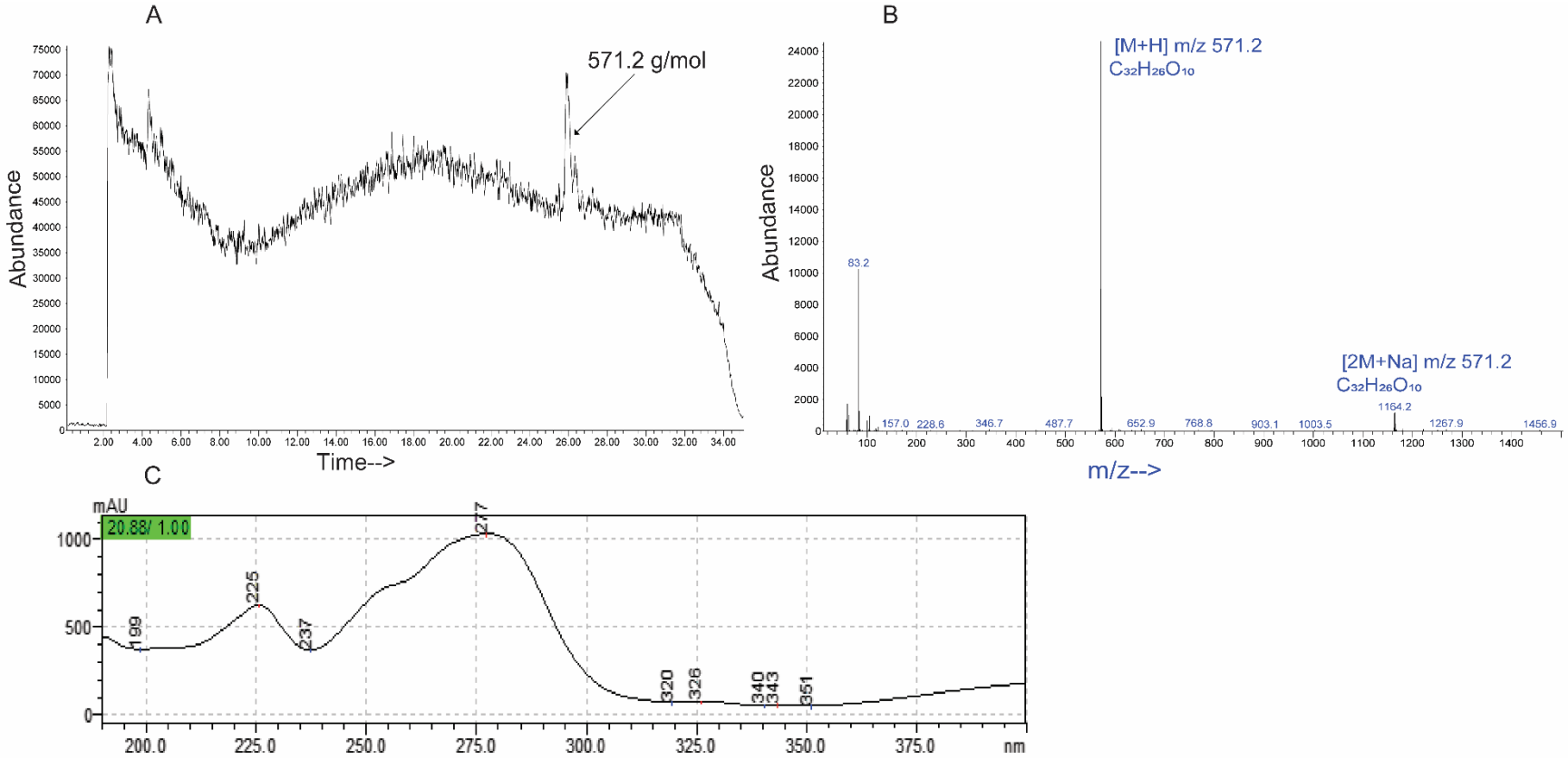

Appendix 7:10: ^{1}H NMR spectrum (600 MHz, $CDCl_3$) of rubrofusarin B with truncations

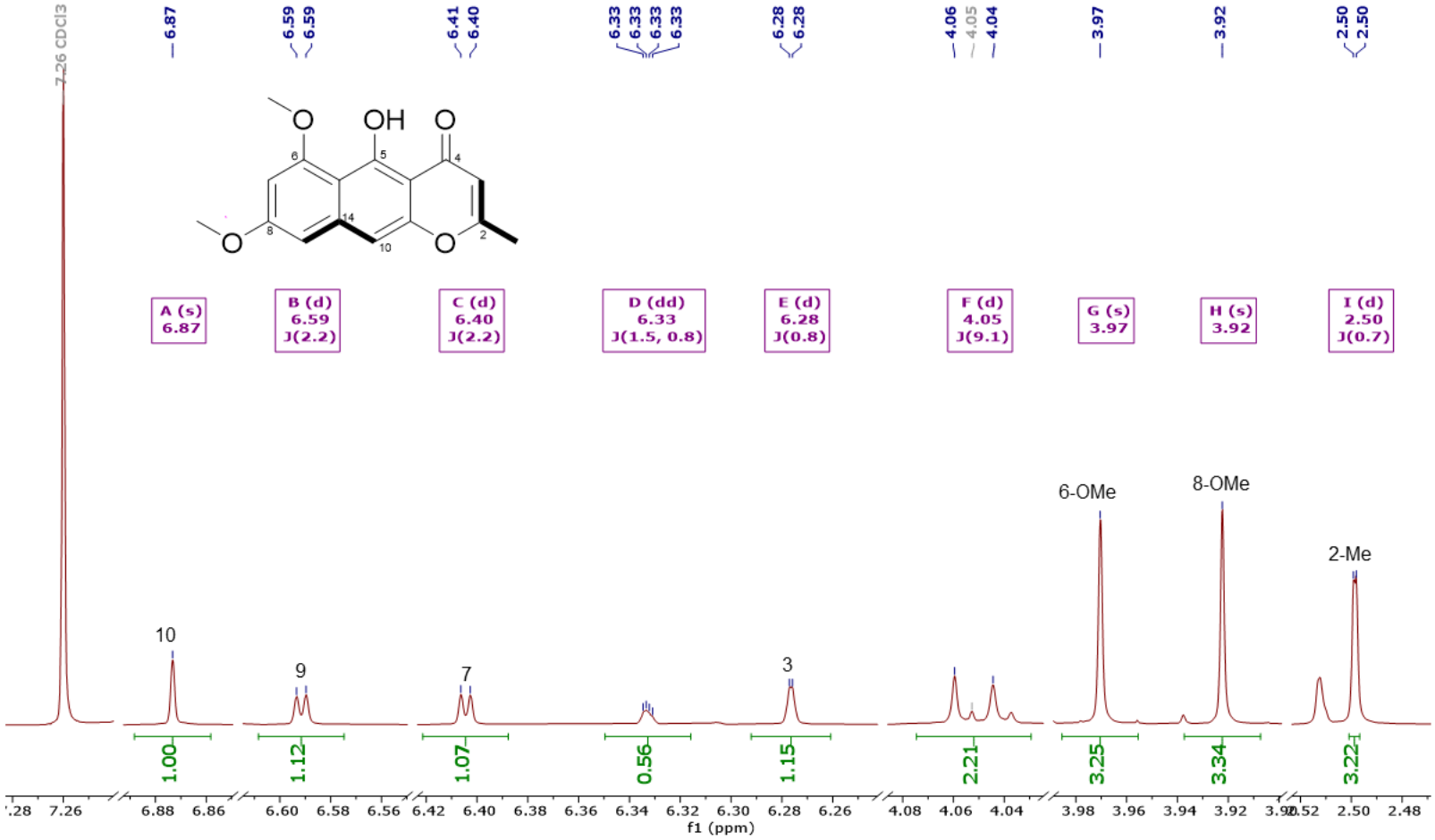

Appendix 7:11: ^{13}C NMR spectrum (150 MHz, $CDCl_3$) of rubrofusarin B with truncations

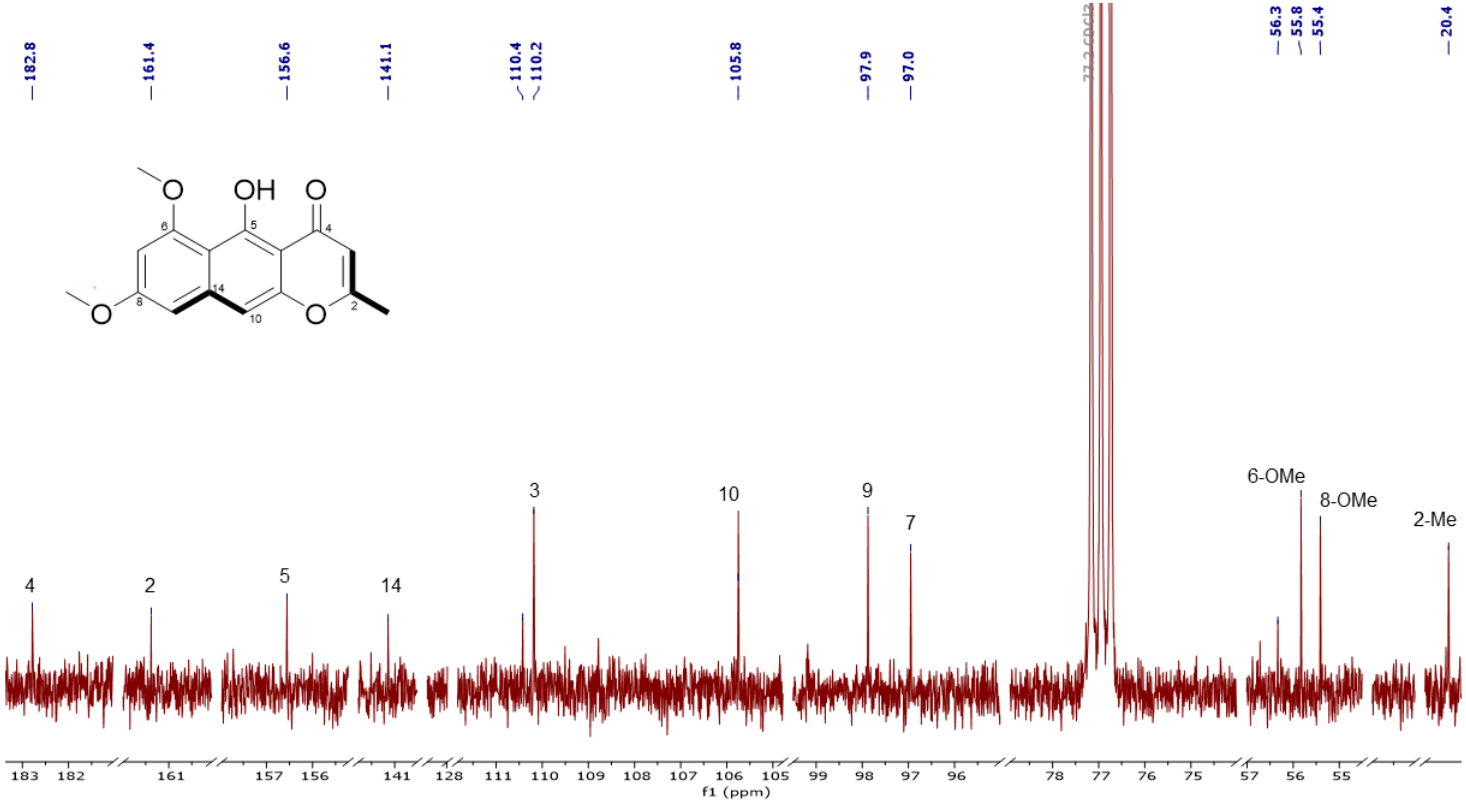

Appendix 7:12: $^{1}H/^{13}C$ NMR spectrum of rubrofusarin B

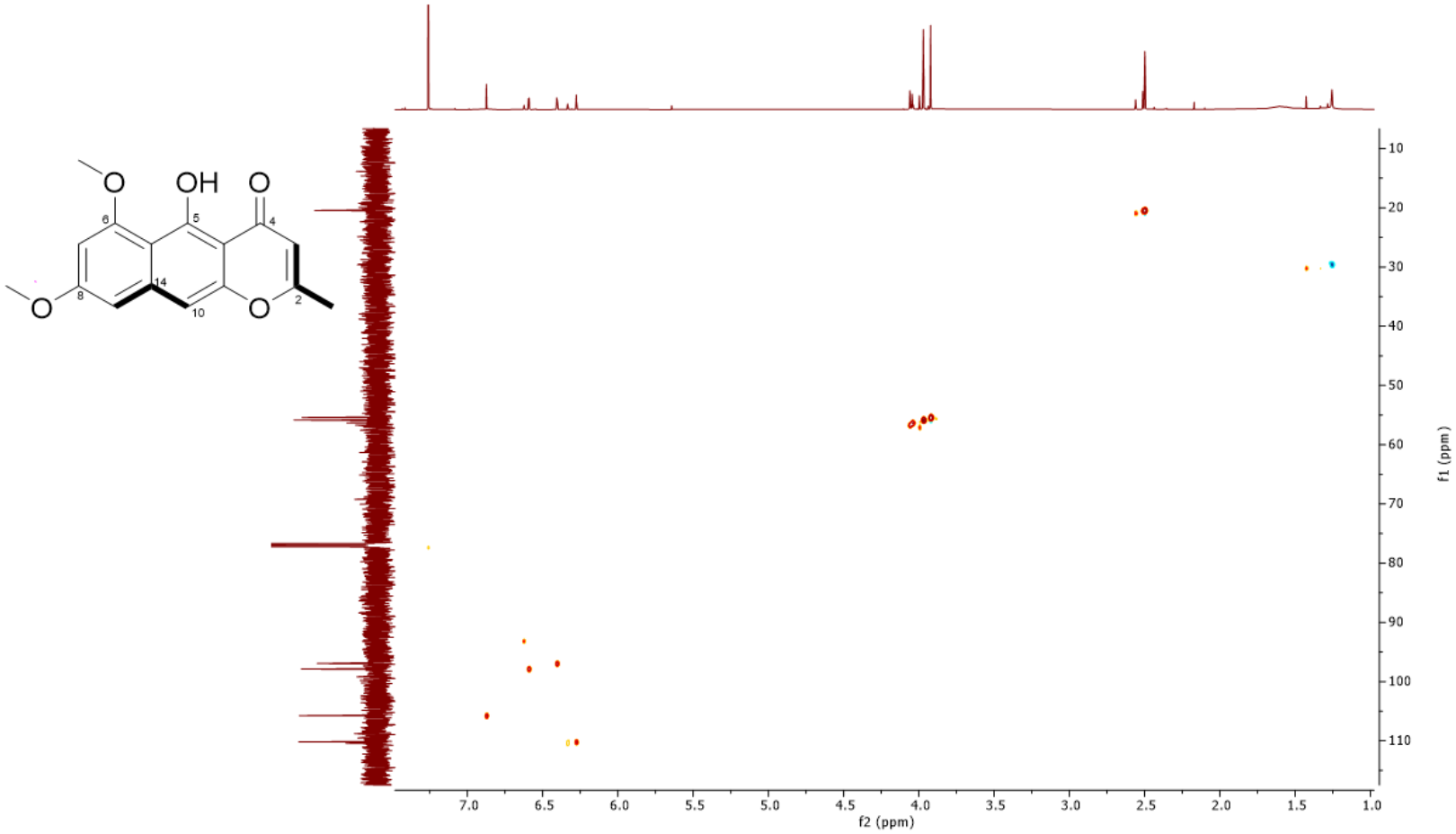

Appendix 7:13: $^{1}H/^{13}H$ NMR spectrum of rubrofusarin B

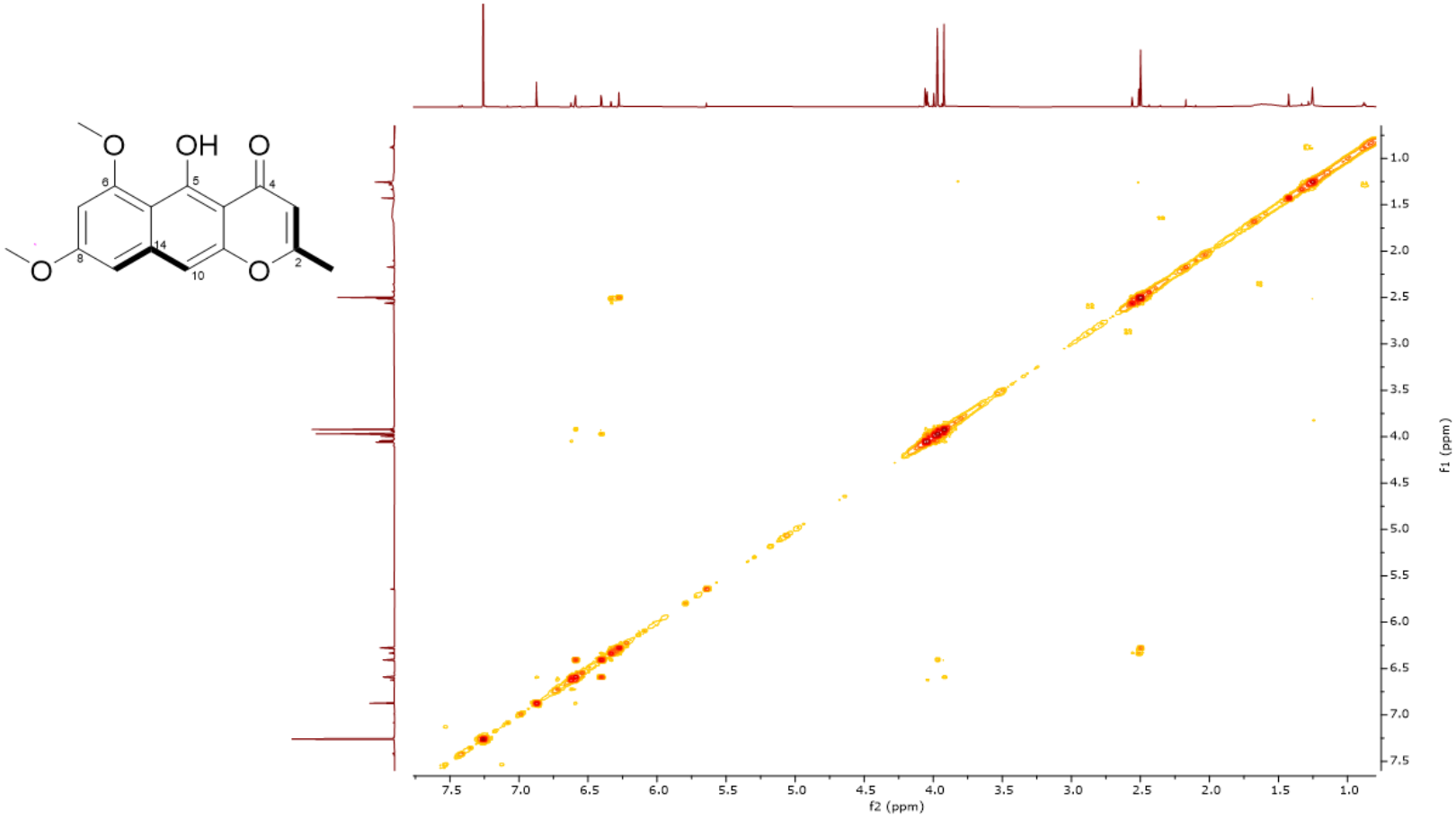

Appendix 7:14: HMBC spectrum of rubrofusarin B

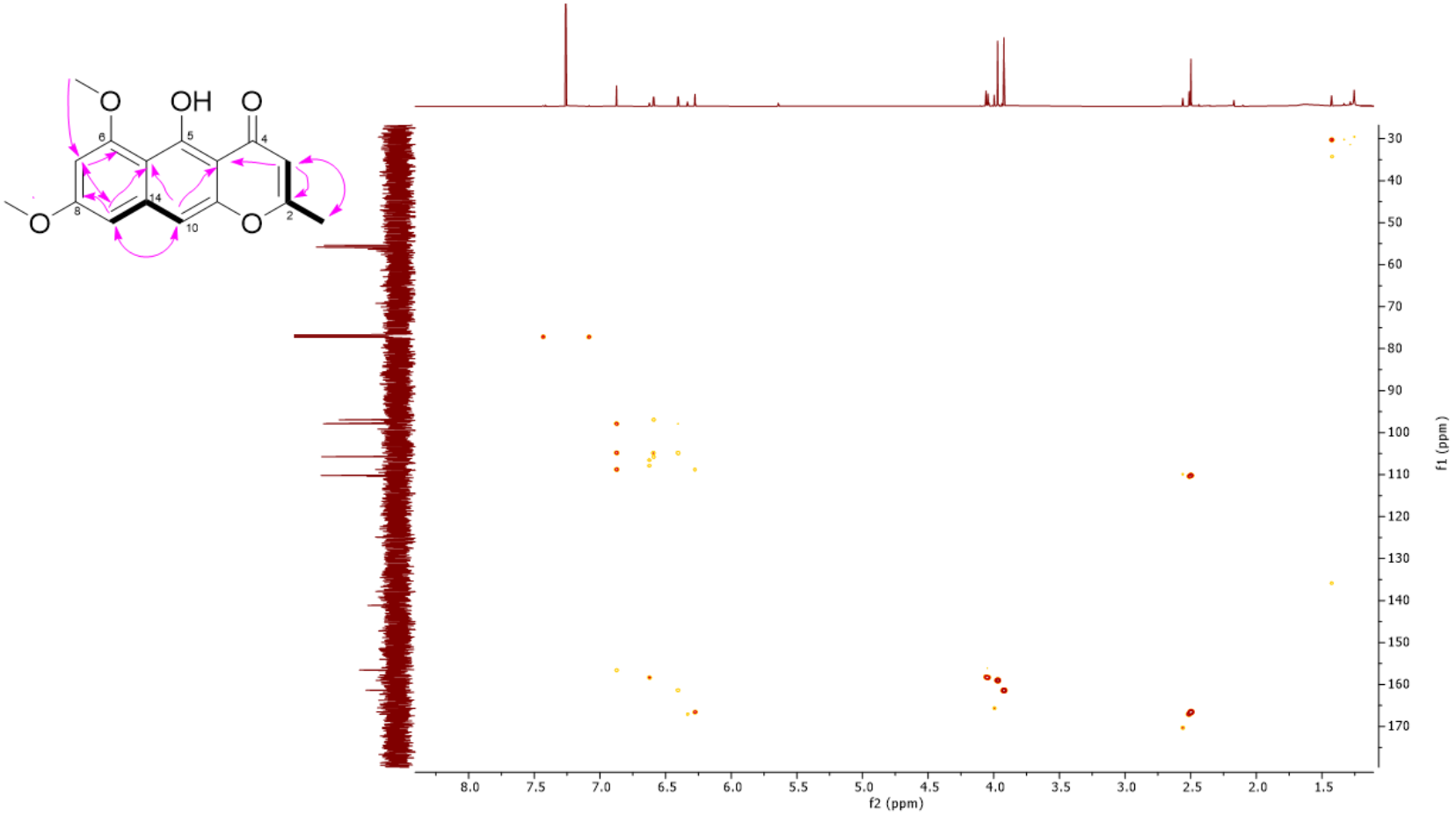

Appendix 7:15: NOESY spectrum of rubrofusarin B

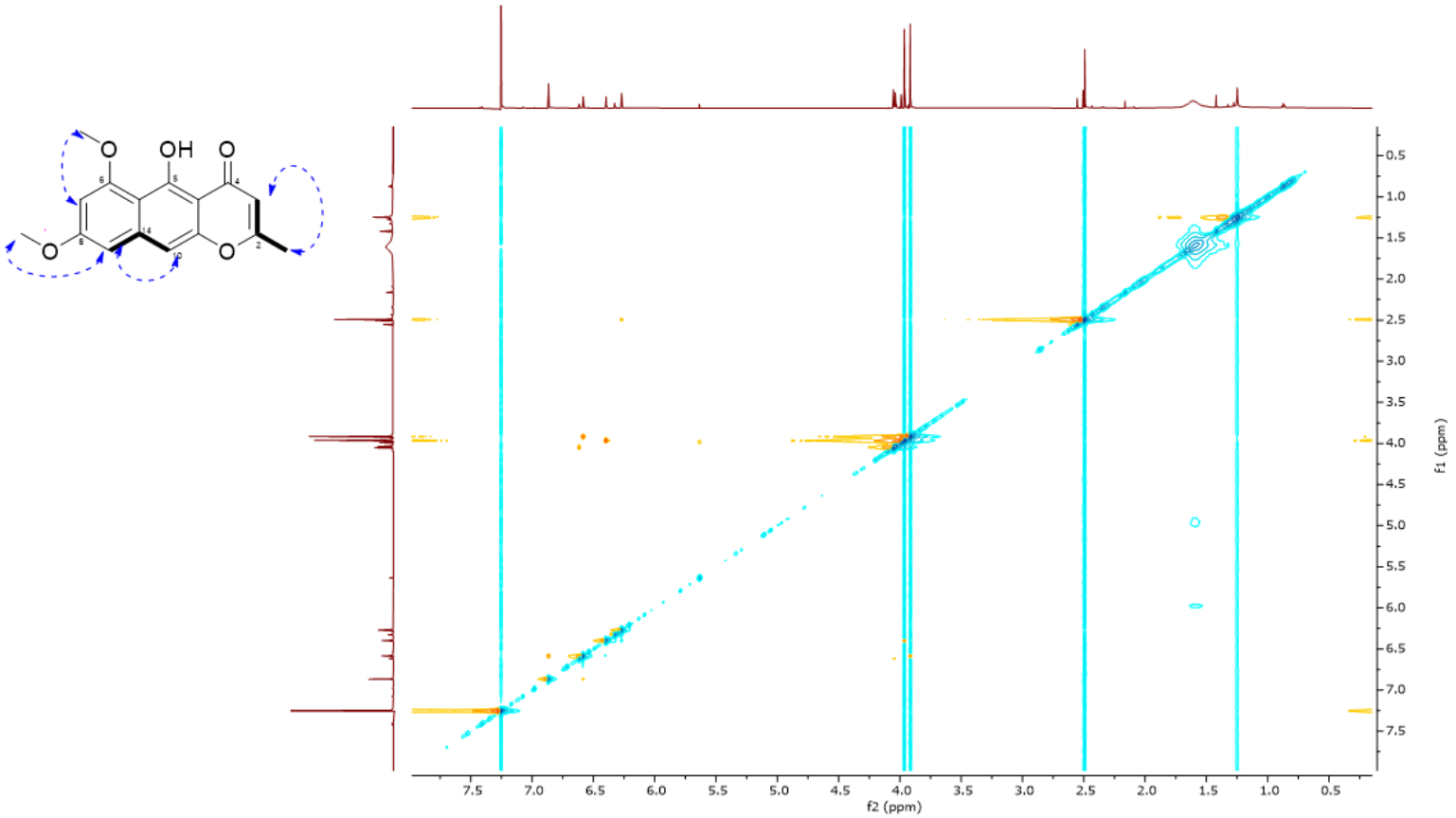

Appendix 7:16: ^{1}H NMR spectrum (600 MHz, $CDCl_3$) of rubasperone B with truncations

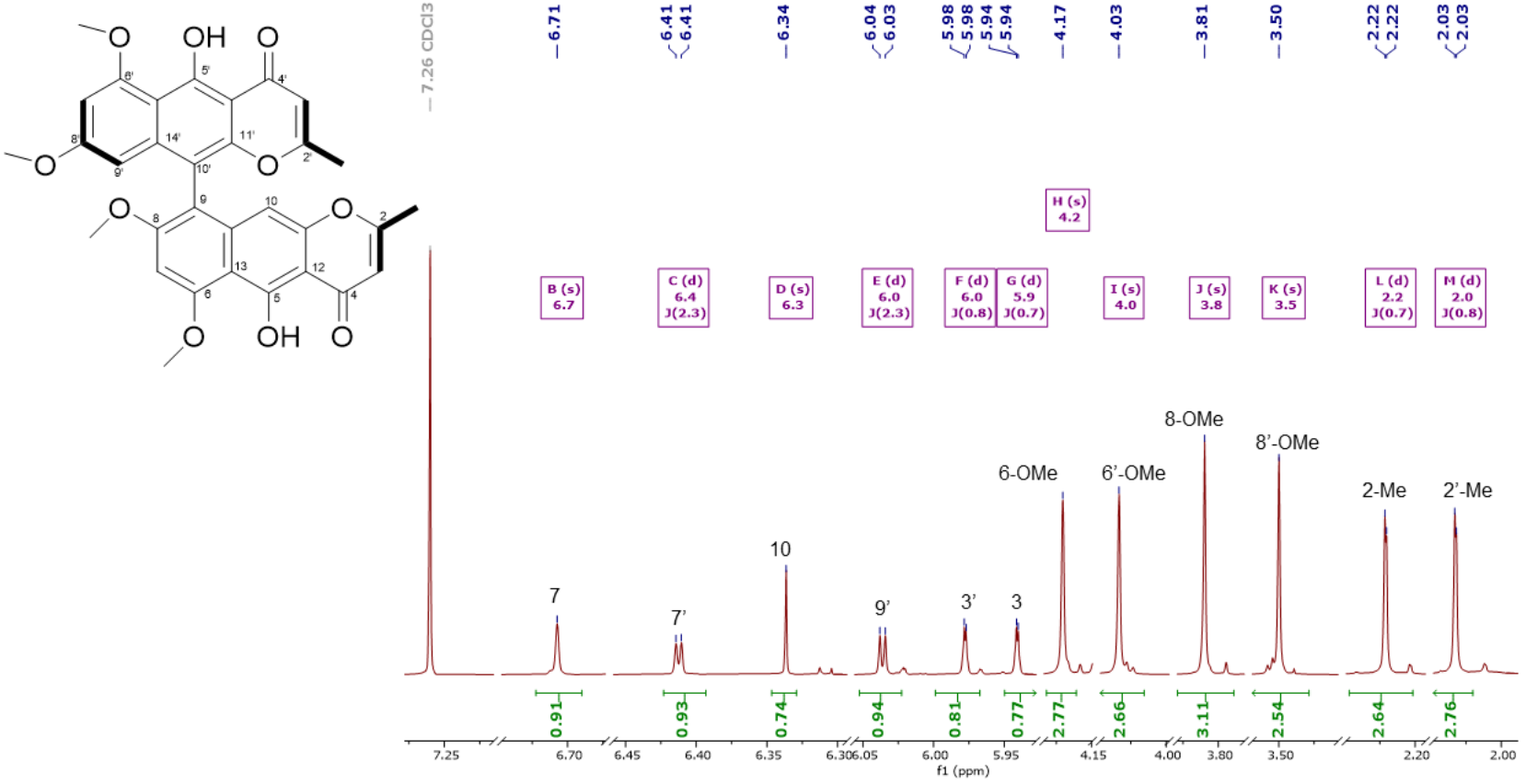

Appendix 7:17: ^{13}C NMR spectrum (150 MHz, $CDCl_3$) of rubasperone B with truncations

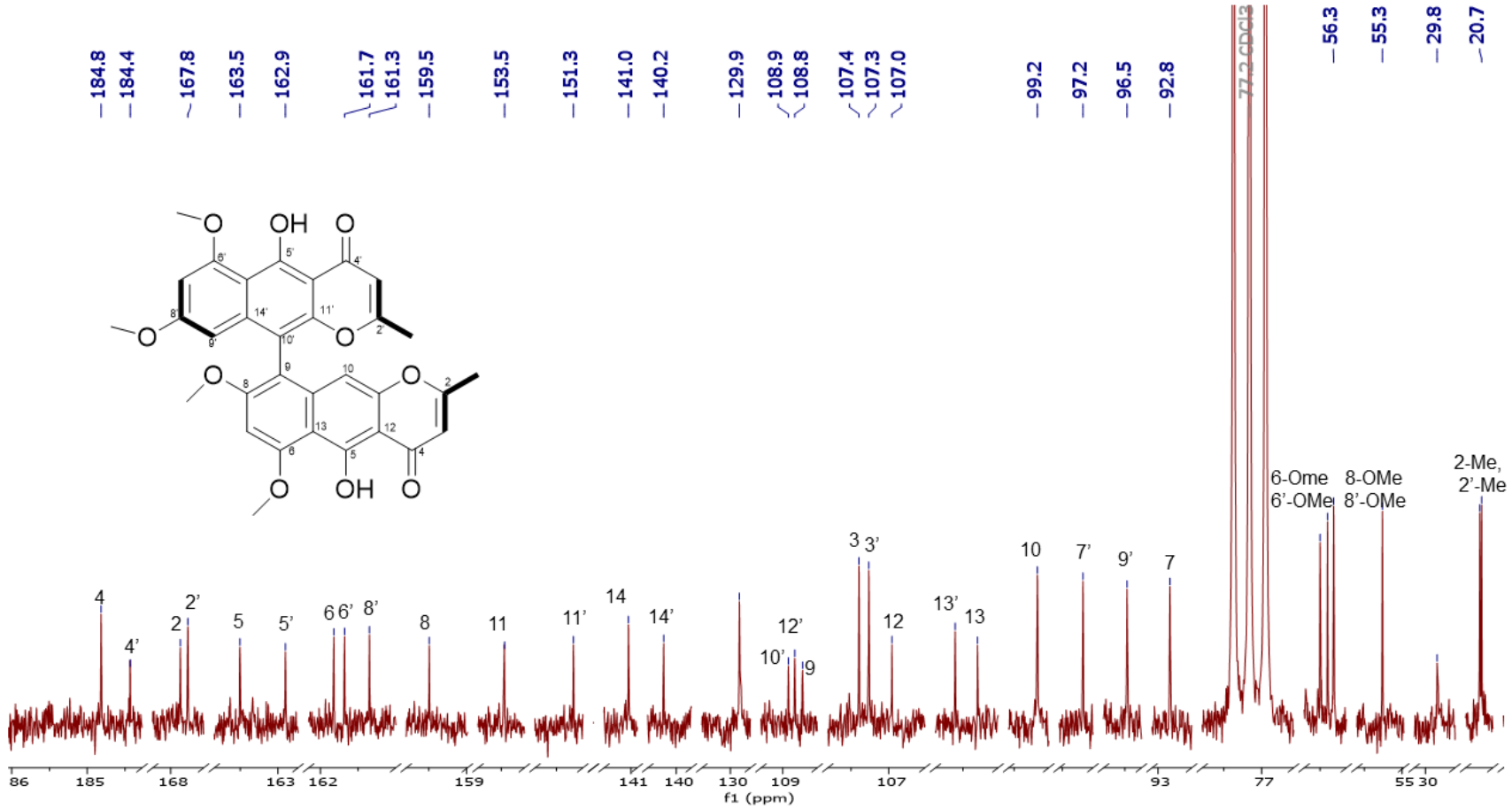

Appendix 7:18: HSQC spectrum of rubasperone B

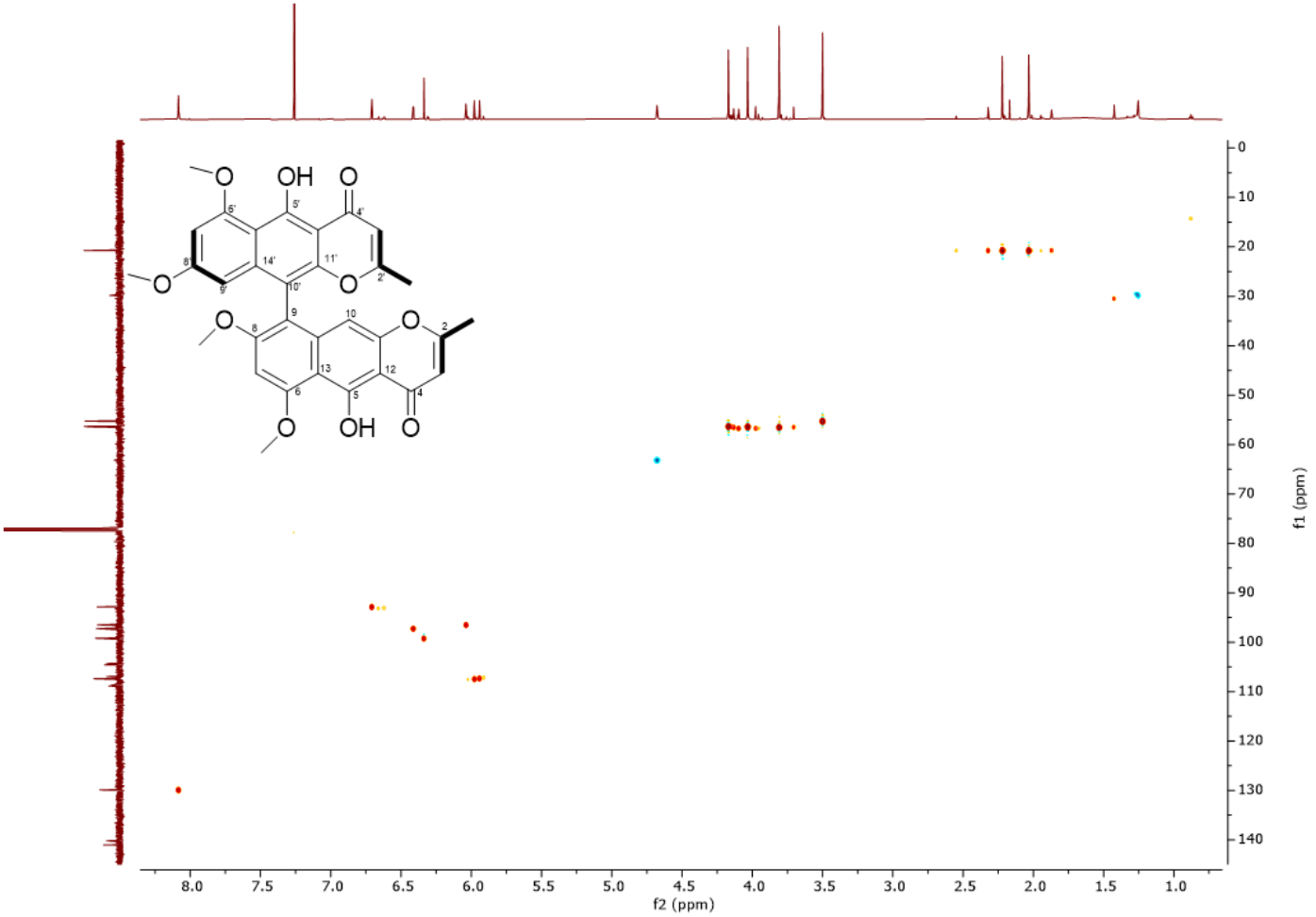

Appendix 7:19: COSY spectrum of ruasperone B

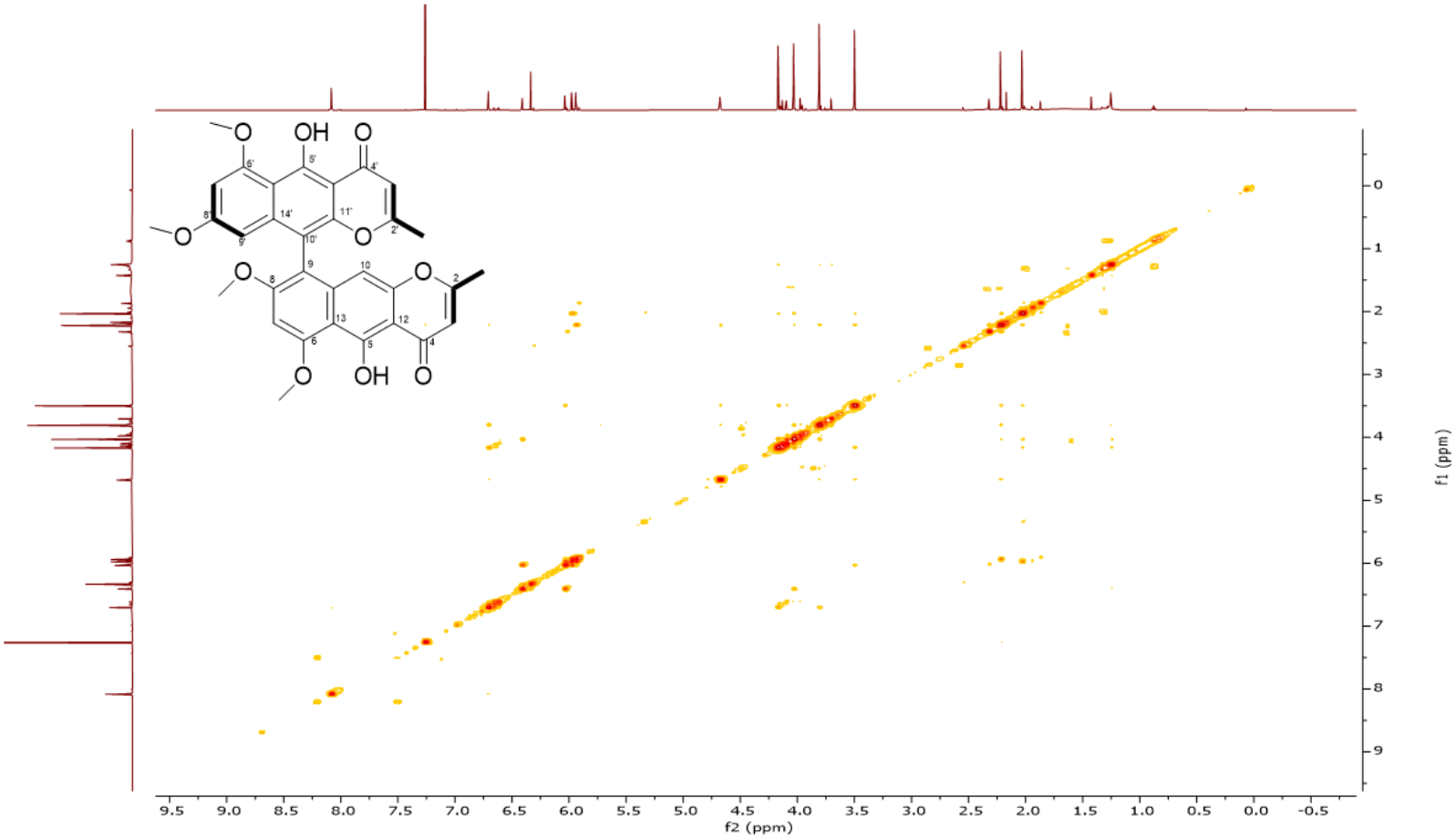

Appendix 7:20: HMBC spectrum of rubasperone B

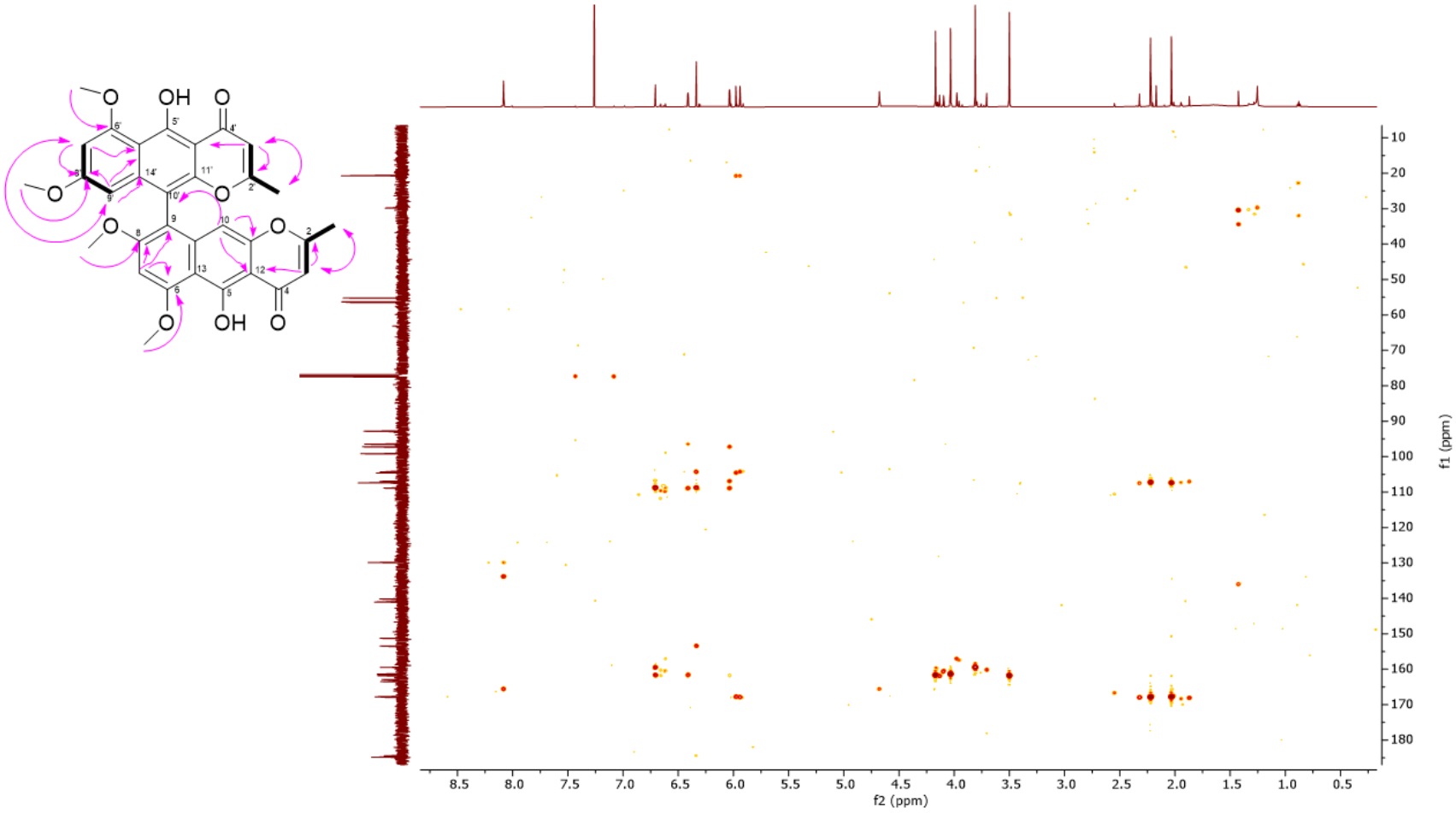

Appendix 7:21: NOESY spectrum of rubasperone B